2013

Geotechnical Technique To Strengthen Traditional I-Walls Through The Use Of Composite Material

Jimmy Irby Jackson
University of Mississippi

GEOTECHNICAL TECHNIQUE TO STRENGTHEN TRADITIONAL I-WALLS THROUGH THE USE OF COMPOSITE MATERIAL

The Thesis
presented is a partial fulfillment of the requirements required for the degree of Master of Engineering Science in the Department of Civil Engineering of
The University of Mississippi

by

JIMMY IRBY JACKSON II

May 2013

ABSTRACT

On Monday, August 29, 2005, Hurricane Katrina struck the southern gulf coast of the United States. Hurricane Katrina produced record high amounts of surge water along the coastal regions, that overtopped and eroded levees and floodwalls, inevitably flooding the entire city of New Orleans. After Hurricane Katrina, the Department of Homeland Security approved a research grant to The University of Mississippi to develop effective but economic technique of strengthening existing I-walls. Using composite materials, a new retrofitting technique was developed to increase the stability of existing I-walls by implementing composite caps. For economical and practical testing, scale models were tested for validation of results. Anisotropic scaling of materials dictated that each test become an independent case study. Each composite cap contains a principle fiber characteristic making each unique. The caps were denoted with a number to signify difference in mechanical properties. The cap denoted as Cap1 had a fiber orientation with a principle direction of X, Cap2 with a principle direction of Y, and Cap3 with a principle direction of X, with the difference being double the fibers and the addition of filler for Cap3. Therefore this study can state which cap exhibited superior structural integrity while sustaining high loading conditions and ultimately lowered the relative displacement of adjacent I-walls. The major findings were that the fiber orientation, thickness, and length, coupled with the application method of the material, played a major role in the structural integrity of the cap. Observations during testing showed that there was an effective height of the cap. When choosing the optimum geometrical properties of composite caps, one must consider the integrity of the concrete. If a cap is too small and extremely stiff, the cap can potentially damage the

concrete due to tension. If the cap is too large and thin, then it is economically not viable and may continue to produce high relative displacement. Through intensive testing, the University of Mississippi's Retrofitted Composite Cap System (UMRCCS) has been proven as a viable geotechnical technique for economically and structurally improving I-wall structures, susceptible to highly deviated soil types that are prone to catastrophic failure.

DEDICATION PAGE

This thesis is dedicated to the three matriarchs of my family James Jackson, Jimmy Hudgins, and Charles Marchbanks. To Pops I wish you could see what I have achieved. To Papaw I dedicate the completion and walk to you, and to Gramps I greatly appreciate the guidance and sound structured advice you've given me along the way.

LIST OF SYMBOLS/ABBREVIATIONS

IPET	Interagency Performance Evaluation Task-Force
GIWW	Gulf Intracoastal Waterway
IHNC	Inner Harbor Navigation Canal
MRGO	Mississippi River Gulf Outlet
ERDC	Engineering Research and Development Center -- US Army Corps of Engineers
HPS	Hurricane Protection System
CEC	Cooper Electrical Controls, Inc.
DMA	Dynamic Mechanical Analysis

ACKNOWLEDGEMENTS

I would like to acknowledge my committee members; Dr. Chung Song, Dr. Ahmed Al-Ostaz, Dr. Yacoub Najjar, and Dr. Hunain Alkhated; and thank them for all their support and guidance during this journey of my life. Without their guidance and support this would have been an impossible undertaking.

I would also like to thank and acknowledge the entire faculty in the Department of Civil Engineering; I always received such good advice and guidance from ever faculty member I went to with a specific technical issue during research.

It is also without saying how thankful I am for the tight nit group of graduate students we have here at the University, that help and support each other during times of struggle and frustration.

TABLE OF CONTENTS

LIST OF TABLES

LIST OF FIGURES

1. INTRODUCTION

Hurricane Katrina struck the southern gulf coast of the United States on August 29, 2005. The storm produced record high amounts of surge water, as high as 25 feet in places, that overtopped and eroded levees and floodwalls. The extreme weather conditions exceeded traditional design parameters causing massive failures of multiple engineering and safety systems. The massive flooding associated with Hurricane Katrina, was caused by overtopping, torrential rains, ranging from 6 to 13.9 inches within 24 hours (Graumann et al, 2005), and localized failure of floodwalls in New Orleans, LA region.

Affects of the storm surge were most prominent in Plaquemines Parish, St. Bernard Parish and New Orleans East. Storm surge also contributed to the elevation rise of Lake Pontchartrain. The rise in elevation of Lake Pontchartrain coupled with shifting storm winds, reaching speeds of 170 mph, forced massive amounts of lake water against the levees, floodwalls and New Orleans outfall canals. The elevation of Lake Pontchartrain directly resulted in the increase in water level in the IHNC to 15.7ft, the Mississippi River Gulf Outlet (MRGO) to 17.4ft, 17th St. Canal to 11.4ft, and London Avenue to 10.5ft. (LADOTD 2006)

Through collaborations of the University of Mississippi, Dutta Tech. Ltd. Inc., and ERDC, a new, innovative, and economical techniques to prevent localized failure or breaching of independent I-walls have been developed. This study reveals the effects and methodology of applying scaled models into retrofitting of I-walls for the New Orleans, LA floodwalls. This new development consists of retrofitting existing I-Walls with composite caps. The application

of composite caps, at connection point of two I-walls, structurally connects the existing I-walls. This as a result creates a global system, alleviating the probability of the localized failure. The logic behind using composite caps to join I-wall sections together is that of the floodwalls being constructed on poor soil conditions. The logic predicts that the I-walls may receive extra support from the floodwall constructed on strong soil condition when needed. Results found in IPET (2006) and (Brandon et al, 2008) have shown a relatively high deviation of shear strengths of subsoil's along the HPS (Hurricane Protection System). The deviation of soil strength parameters was in part a major factor in the localized breaching of certain regions of the HPS.

The use of composite caps is based on the concept that the global factor of safety, of the system, is higher than that of one independent I-wall. Otherwise, the use of composite caps may spread the local failure to global failure, which is not an ideal condition. The floodwalls in the New Orleans area were tested by two full scale hurricanes after Hurricane Katrina, namely Hurricane Gustav (2008) and Hurricane Isaac (2012), in which the floodwall system withheld its integrity. These events prove that the global factor of safety of the system is greater than one, validating the concept of composite cap as being a safe alternative technique.

The main objective for this research is to quantitatively design composite caps. Testing this concept would be economically prohibitive for a full scale scenario; therefore scaled model testing and numerical simulations are used.

This work tested an approximate $1/7^{th}$ scaled model of the existing New Orleans I-wall. The apparatus consisted of three mock levee I-walls one fixed; one representing an I-wall

constructed on strong soil conditions and lastly one constructed on weak soil conditions. A retrofitted composite cap was placed at the union point between the strong and weak simulated walls and force was applied using hydraulic pistons to represent increasing hydrostatic pressure.

The three choices of Composite Caps were tested in this study to see which would yield optimum results. Each Cap was denoted with a number to signify difference in fiber orientation. The axial directions are as follows: X representing the longitudinal direction along the levee, Y representing the vertical direction perpendicular to the levee. The Cap denoted as Cap1 had a fiber orientation with a principle direction of X, Cap2 with a principle direction of Y, and Cap3 with a principle direction of X with the difference being double the fibers. Therefore this study can state which cap exhibited superior structural integrity while sustaining high load conditions with above fiber orientations.

Accompanied with $1/7^{th}$ scaled model testing, $1/64^{th}$ scaled model tests were conducted by ERDC-USACE to evaluate he scale effect. The $1/64^{th}$ model was tested using ERDC's centrifuge in which achieved a peak acceleration of 150g's. One to one comparisons between the $1/64^{th}$ and the $1/7^{th}$ were deemed unfavorable due to anisotropic scaling, but test results gave much insight into the composite caps abilities.

Properties and dimensions of the full scale composite cap can be determined using dimensional analysis of the scaled model results. A full-scale composite cap with the dimensions of 2 feet in length, 1 foot in width, and 0.25 inches in thickness was found to costs in a range from $40 to $60 per cap to manufacture, according to the unofficial quote. Note this cap

is not the official final design; it was merely a gage to determine cost estimates when comparing composite caps vs. replacing all I-wall in New Orleans with T-walls. The total cost of replacing I-walls with T-walls could be as high as 9 billion dollars where as the cost for manufacturing and implementing composite caps is roughly 1 million dollars.

2. BACKGROUND

2.1 History of New Orleans Hurricane Protection System

London Avenue and 17th Street Canals first appeared on the map in 1878 and a significant levee protection system was not seriously proposed until the mid 1950's (Nelson 2012). In 1993 congress and all the related committees agreed on a design plan for the new flood protection system. This lengthy delay could be in part due to the city not experiencing a major storm during this 40 year span (Sills 2008). Today's current Hurricane Protection System (HPS) includes approximately 350 miles of protective structures, 56 miles of which are I-walls (IPET 2006), as shown in Figure 1.

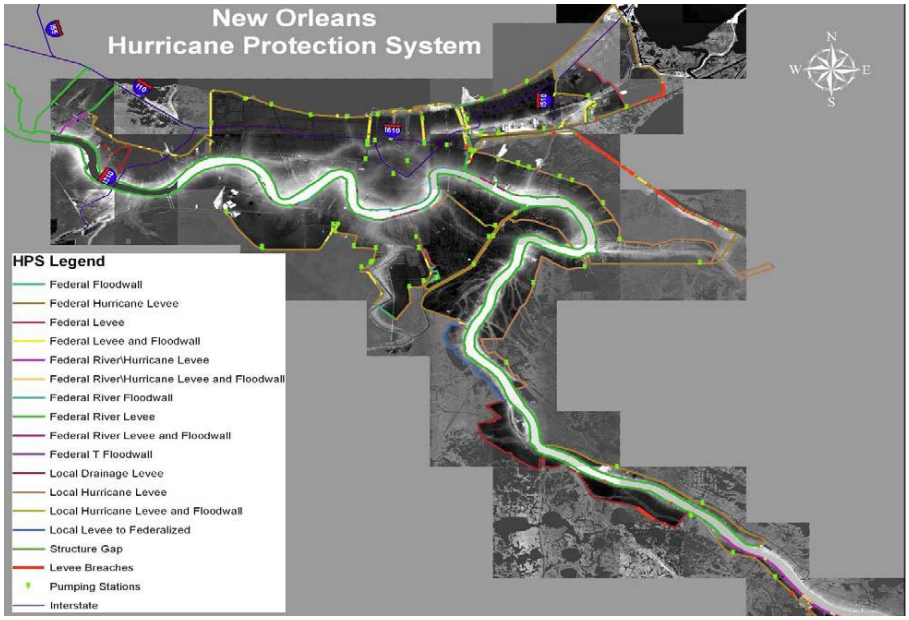

Figure 1. Outline of the New Orleans and Southeast Louisiana Hurricane Protection System (IPET 2006)

The system in question was that of adding I-Walls and or T-walls to the crowns of existing earthen levees. A majority of the floodwalls were designed as I-walls due to their lower expense of construction, but there was a small portion of T-walls and L-walls constructed. In the cases of London Avenue and 17th Street Canals the system of choice was that of the I-Wall.

In addition, the following is a basic summary of IPET (2006) findings of the geological history of New Orleans. The geological history of New Orleans plays a significant role in engineered structures. Through combined field tests and examinations of levee failure sites, data collected revealed a complex geomorphic structure that originated from the Holocene sea level rise (IPET, Volume 1, 2006). This complex geomorphic structure assisted in the development of a multitude of Mississippi River delta lobes and the distribution of channels related to the development of a delta (IPET 2006). The city of New Orleans is surrounded by waterways with most of the cities geologic structures sitting below sea level, some to a depth of 10 feet below sea level. The HPS is made up not just of levee walls but a series of complex systems all working in unison during turbulent weather conditions. The HPS consists of earthen levees, I-wall, inverted T-wall, floodgates, and pump stations (Vipulanandan 2006). According to Vipulanandan (2006), roughly 75% of the municipal areas of New Orleans are lower than the sea level. To date Hurricane Katrina has been the most destructive and economically devastating in United States history.

2.2 Hurricane Protection System Failure Modes

2.2.1 Soil Type—Distribution along the 17th Street Canal Breach

The breach area along the 17th Street Canal was categorized into six subsurface soil types shown in Table 1. The embankment is classified as compacted CL and/or CH soil, with a liquid limit averaging 45% (IPET 2006) and a total unit weight of 109 pcf (Duncan et al. 2008). To an average depth of 11.5 ft is the marsh layer, composed of highly organic clay and silt materials. The marsh has an average unit weight of approximately 80pcf. Beneath the marsh layer is the lacustrine layer, it is classified as a CH with a unit weight of 100 pcf, liquid limit of 95% and a plasticity index of 65 (Duncan et al 2008). The lacustrine layer is considered to be normally consolidated throughout the depth (IPET 2006). The shear strength of the area contained a high variance. The shear strength recorded varied from 120 psf upwards of 5,000 psf, Duncan et al. (2008). Therefore a s_u = 900psf was determined to be a reasonable value of the levee fill taken from multiple UU test on 5 in diameter samples Duncan et al. (2008). All laboratory data collected for this breach site can be found in Appendix 1 of IPET 2007 (Duncan et al. 2008).

Table 1. Major Soil Groups at the 17th Street Outfall Canal Breach Site (IPET 2006)

Layer	Approximate Elevation of Top of Layer, ft (NAVD88)	Approximate Elevation of Bottom of Layer, ft (NAVD88)	Soil Type	Consistency
Embankment	5	-11.5	Clayey (CL's and CH)	Stiff
Marsh	-11.5	-16.5	Organic/Peat	Very Soft
Lacustrine	-16.5	-36.5	Clays (CH)	Very Soft
Beach Sand	-36.5	-45	Sand	
Bay Sound/Estuarine	-45	-75	Clayey (CH)	Stiff to Very Stiff
Pleistocene (Undifferentiated) Prairie Formation	-75		Clays – Generally CH with some sand	Stiff

A longitudinal cross section of the 17th Street Canal breach, along the centerline of the levee, depicts the soil stratification in detail; this is shown in Figure 2. A latitudinal cross section was also taken from this region, depicting subsurface strata from the East Bank to the West Bank, shown in Figure 3.

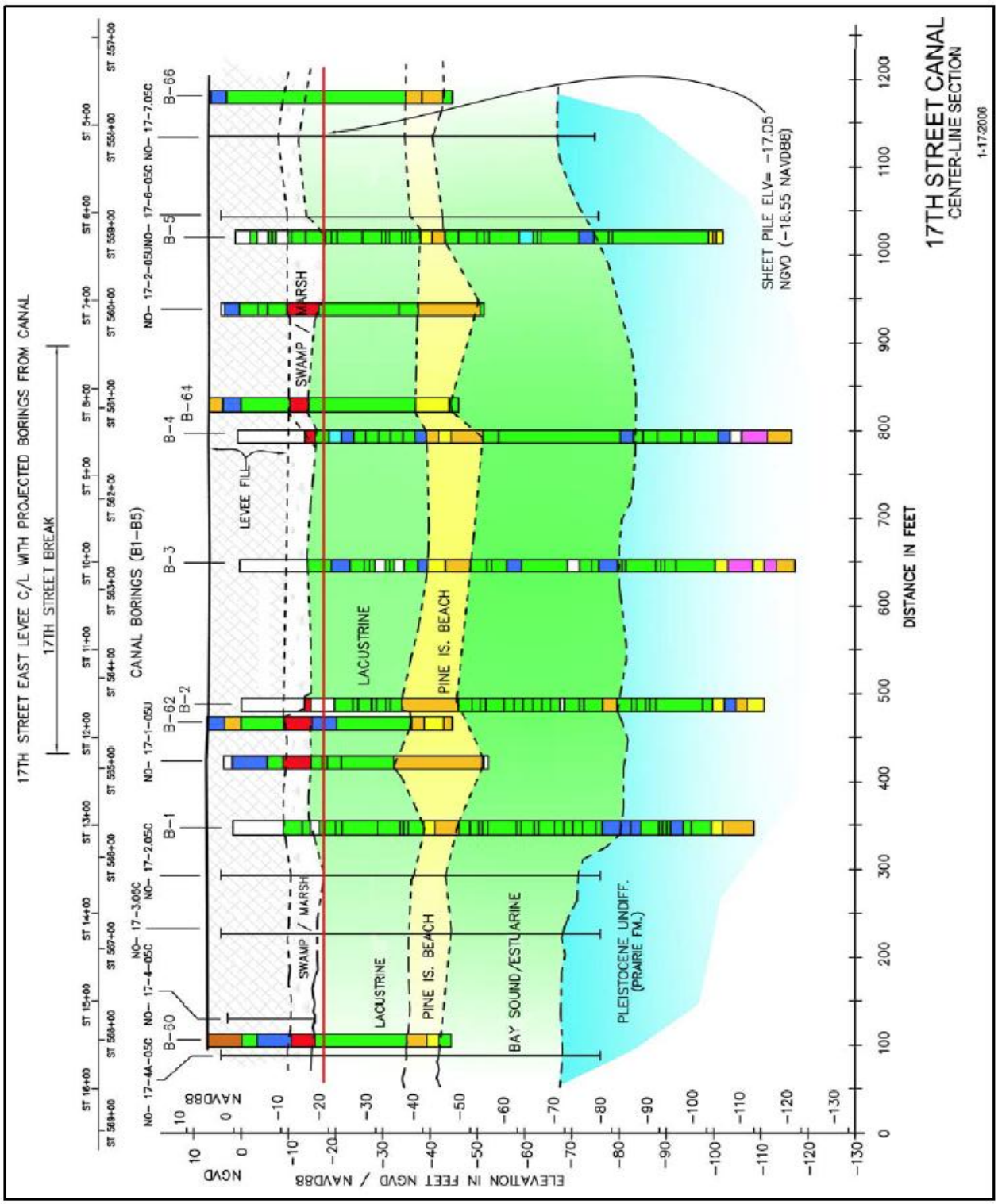

Figure 2. Centerline longitudinal section of 17th Street Canal breach (IPET 2006)

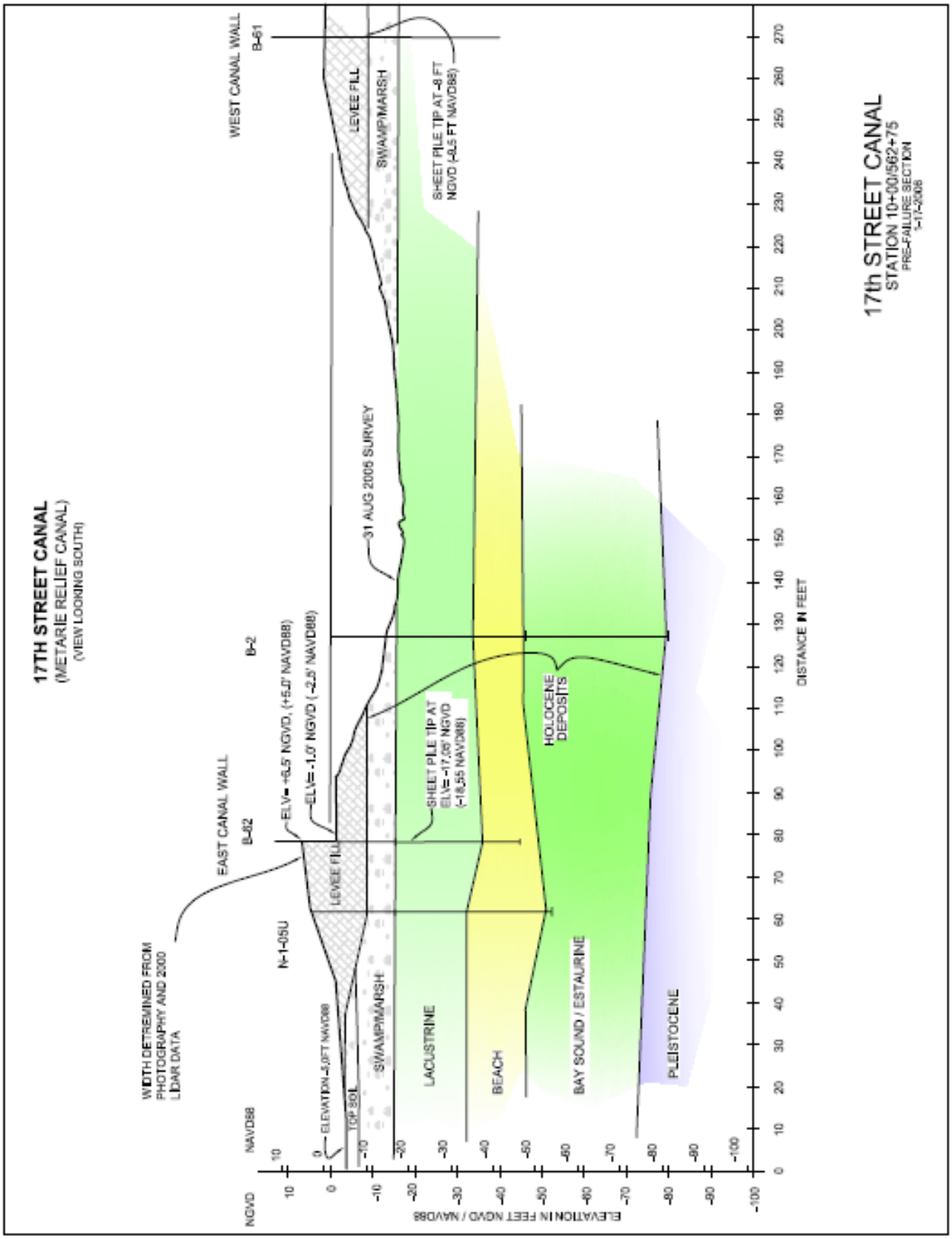

Figure 3. Pre-failure cross section 17th Street Canal breach (IPET 2006)

2.2.2 Overtopping and Scouring

According to IPET (2006) overtopping alone would have caused one third of the flooding that occurred. Design parameters show that there is a high probability that a hurricane Category 3 and higher could produce overtopping of the existing HPS. A design parameter not taken into consideration during the original construction of New Orleans HPS was that of overtopping scour protection (Sills 2008). Figure 4 shows the divesting effects of overtopping and scouring of the soil with no scouring protection.

Figure 4. Scour and Erosion of the Protected side of IHNC adjacent to the 9th Ward (IPET 2006)

With improvements to the soil, such as grouted riprap or concrete erosion mats along the base on the protected side, the survivability significantly increases for such a design while decreasing the potential for erosion. Both studies by Sills et al. (2008) and Vipulanandan (2006) concur with this scouring protection method. Cross sections of an I-Wall and T-Wall design are given in Figure 5.

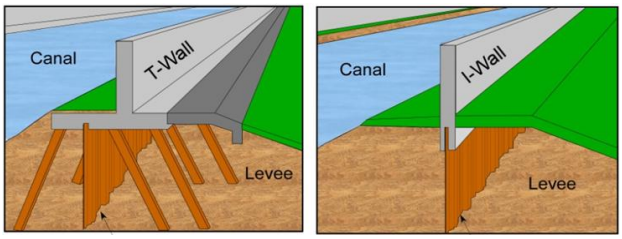

Figure 5. Cross Section of I-Wall and T-Wall (Nelson 2012)

2.2.3 *Shear Failure – Gap Formation*

Corps of Engineers E-99 Field Test: Prior to Hurricane Katrina a field test was performed testing the PZ-27 steel sheet pile I-wall. This test consisted of a 200 foot long section, and was loaded with water. This test was used to compare traditional equilibrium and soil-structure interaction to experimental results. The test very closely mimicked the conditions of the New Orleans I-walls, but the test was stopped after approximately 2 months due to a leaking seal that was allowing the water to drain uncontrollably. The formation of the gap was observed during testing but apparently not held as a high risk matter due to the wall not failing.

Breaches that occurred due to foundation issues during Hurricane Katrina had a common element, the formation of a gap between the I-wall structure and the soil, see Figure 6. According to Brandon et al. (2008) the formation of a gap directly increased the hydrostatic load on the wall and decreased the piping distance, therefore increased the potential for piping and shear failure.

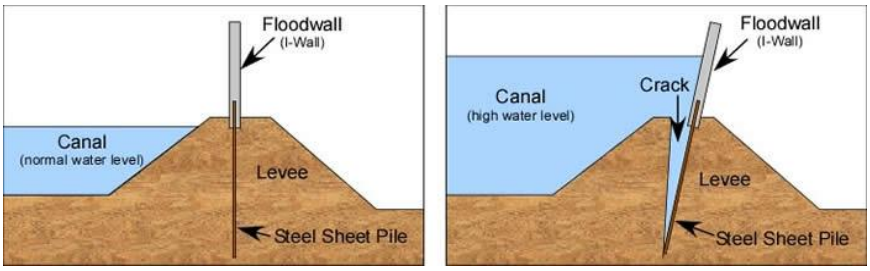

Figure 6. Diagram of Gap Formation (Nelson 2012)

Experiments conducted by ERDC concur with the logic of gap formation. The 1/64th model results yielded that where the toe of the sheet pile failed in the clayey soil layer, there was also translational failure in the clayey soil layer (IPET 2006) as shown in Figure 7.

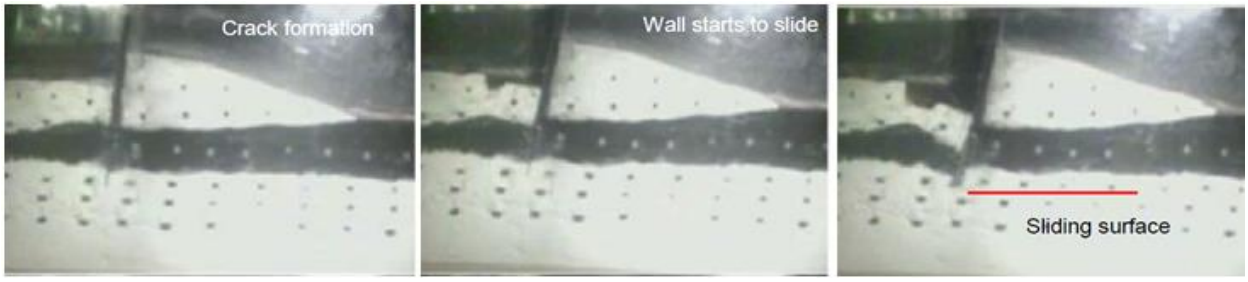

Figure 7. ERDC 1/64th HPS test model showing formation of gap. (IPET 2006)

Through the formation of the gap three critical parameters where changed; forces applied by hydrostatic pressure, circular failure path, and piping or seepage paths. With the presence of a large hydrostatic load the I-wall will deform in the direction of the protected side of the levee. In doing so the horizontal stresses on the flood side will decrease. According to Brandon et al. (2008), Rankine's active horizontal earth pressure and the total water pressures during rapid water level rise can be computed in a soil with multiple layers by the following equations and Figure 8:

Rankines Active Earth Pressure – $\sigma_{ha} = \gamma_w h_w + \sum(\gamma_i h_i) - 2c_i$

Water Pressure – $\gamma_w z_w$

Pressure Equilibrium – $(\gamma - \gamma_w)z - 2c = 0$

Equilibrium depth – $z_o = 2c/(\gamma - \gamma_w)$

Where: Cohesion ($s_u = c$); Un-drained shear strength at depth in question (c_i); Unit weight of soil (γ); Unit weight of water (γ_w); Depth of soil (z); Depth of water above ground surface (h_w); Height of the soil layer above the depth in question (h_i)

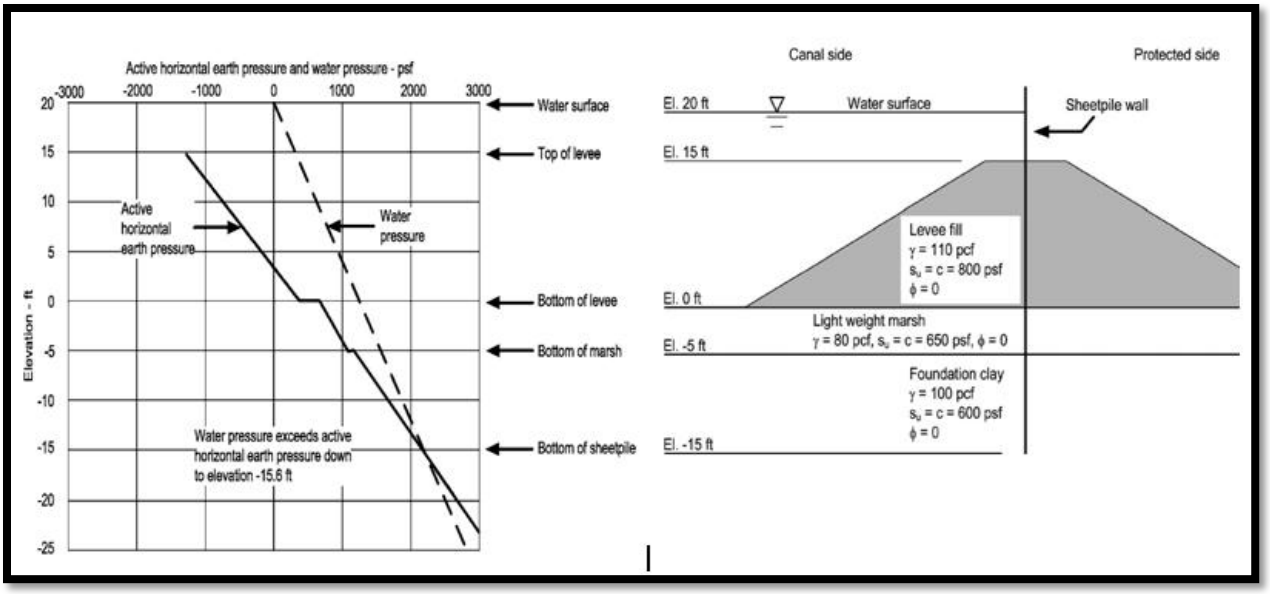

Figure 8. Pressure distribution and Layered Cohesive Soils levee example (Brandon 2008)

Also shown in Figure 8, the formation of the gap allows for hydrostatic pressure to exceed the active earth pressure above EL. -15ft. Therefore, it showed the possibility of the gap opening. Brandon et al. (2008) also conducted computational slope stability studies with Spencer's method using UTEXAS4 (Wright 1999) and SLIDE (Rocscience 2005). Both UTEXAS4 and SLIDE programs determined the same factor of safety of 1.28 for a simulated I-wall with no gap presents and 0.98 with the presents of the gap (Brandon 2008). These programs also tested for circular failure modes with and without presence of gap. With Figure 9 Brandon et al. (2008) concluded that formation of a gap has significant effect on the I-walls factor of safety and critical failure line.

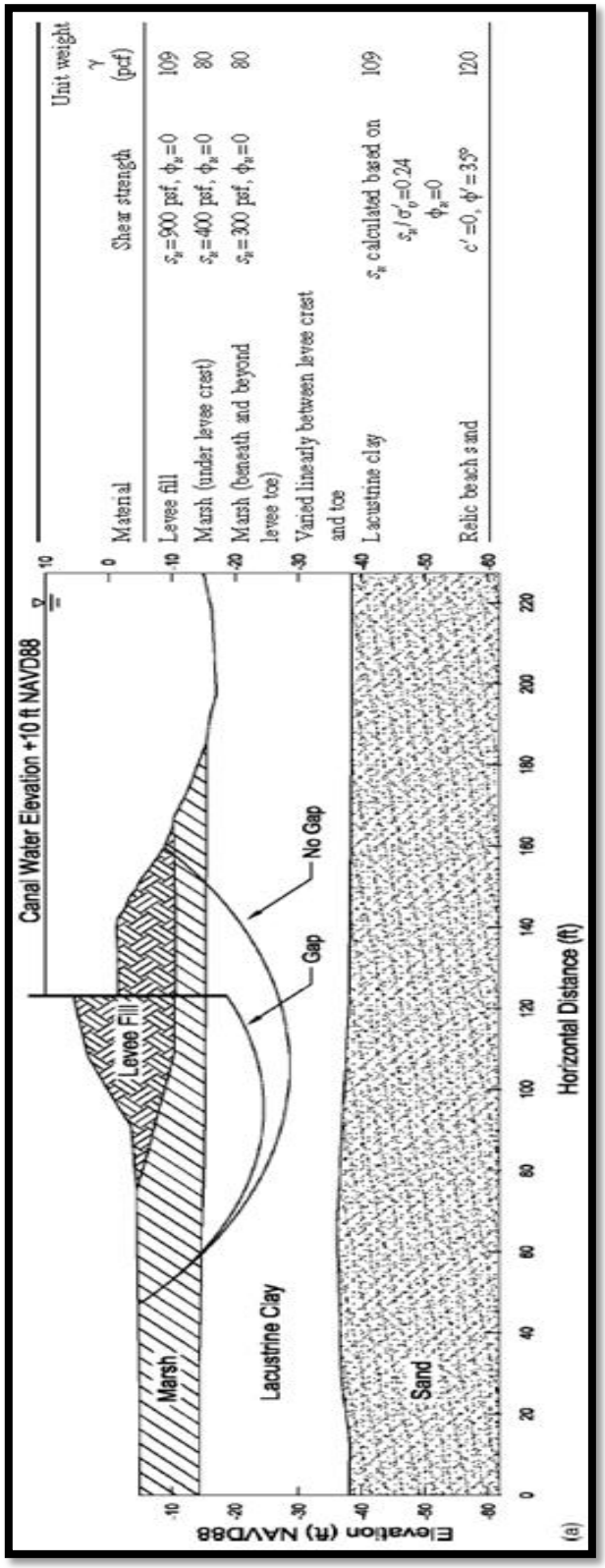

Figure 9. Cross Section of 17th Canal – Circular Failure line with and without Gap. (Brandon 2008)

2.2.5 Overview of Failure modes and Lessons Learned

The breach of the 17th Street Canal I-wall was approximately 450 feet long, while the other 26,000 feet of I-wall remained stable (Duncan 2008). The major of concerns and question that arose were why this localized failure occurred. Two main studies were conducted after Hurricane Katrina, one by IPET team (IPET 2007) and the other was by ILIT team (ILIT 2006). There were minor discrepancies between the two groups but both concurred on the four major failure mechanisms and are as follows: the formation of the gap on the river side of the floodwall; overtopping and subsequent erosion; shear failure of weaker soil layers; and piping or seepage induced failure (Adhikari 2012). It was determined that the soil types that the existing HPS was constructed with and on were inconsistent and contained a high variation of geotechnical parameters. Table 2 correlates failure mechanisms to soil conditions in localized regions. As a result to these inconsistencies, failures of the HPS were mostly local failures, and therefore, the studies to prevent the localized failures using the structural caps were conducted.

Table 2. Soil Conditions and Failure Mechanisms at Investigated I-Wall Breach Locations Duncan et al. (2008)

Location	Soil conditions	Failure mechanism
17th Street Canal	Clay levee fill/marsh/foundation clay/sand	Stability failure through foundation clay
London Avenue south breach	Clay levee fill/marsh/dense sand	Underseepage erosion of foundation sand leading to removal of support for I-wall
London Avenue north breach	Clay levee fill/marsh/loose sand	Underseepage erosion and/or foundation instability due to high uplift pressure
IHNC east bank south breach	Clay levee fill/marsh/clay/sand	Overtopping erosion of levee fill leading to removal of support for I-wall
IHNC east bank north breach	Clay levee fill/marsh/clay/sand	Stability failure through foundation clay
IHNC west bank north breach	Clay levee fill/marsh/clay/sand	Overtopping erosion of levee fill leading to removal of support for I-wall

3. University of Mississippi's Retrofitted Composite Cap System (UMRCCS)

3.1 Overview of the UMRCCS

Through the use of the UMRCCS, a new economical technique has been developed for increasing the stability and factor of safety for existing New Orleans levee walls. The following test set up shown in Figure 10 is approximately 1/7th scaled model and simulate the events that occurred at the London Ave. , Canal St., and 17th ST. Canal in New Orleans during Hurricane Katrina. But this test set up is not intended to be site dependent, this technique can be used for evaluating the behavior of a typical I-wall structure.

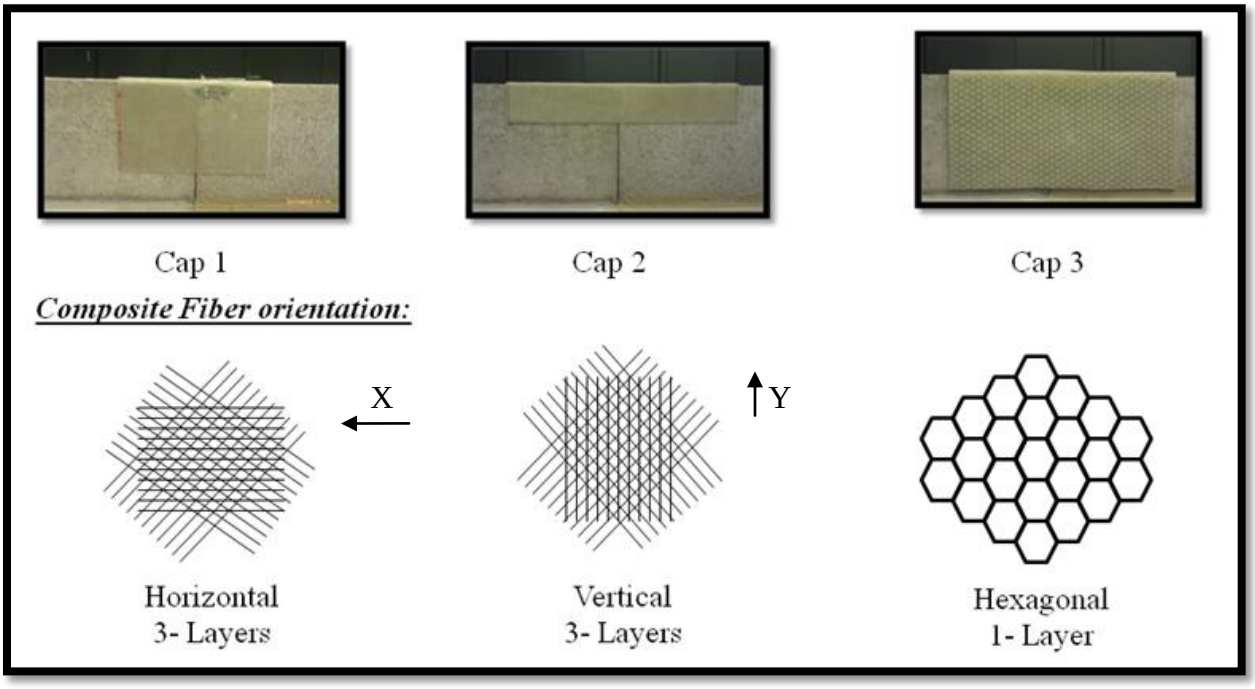

Figure 10. UM Composite Caps and Fiber orientation

Studies were conducted on three different composite caps to see which fiber orientation and what geometrical parameter would yield the optimum results. The caps could not directly be compared to one another using dimensional analysis due to different anisotropic scaling. The caps were subjected to torsion and flexural loading components due to the nature of displacement and deformation of cap. Each Cap was denoted with a caption and number to signify difference in fiber orientation. The cap denoted as Cap1 had a fiber orientation with a principle direction of X, Cap2 with a principle direction of Y, and Cap3 with a principle direction of X with the difference of Cap3 compared to Cap 1 being that Cap3 contains double the number of layered fibers and the addition of a filler. The filler divides the fibers into two groups. Therefore this study can state which cap exhibited superior structural integrity while sustaining high loading conditions with above fiber orientations.

Since it is prohibited to structurally modify the existing I-wall structure, techniques to attach the caps to the floodwalls must also be evaluated. This restriction was set to prevent potential damage or causing structural instability of the existing I-wall through cap installation by bolting or other destructive techniques. Three application methods where tested. The first method was by placing cap directly over joint, allowing surface friction between the Composite Cap and the concrete wall to keep the cap in place. Secondly was placing a rubber membrane between the cap and I-wall, increasing surface friction. Thirdly was that of adhesively bonding the cap to the I-wall with a low strength silicone compound.

3.2 Testing Apparatus & Experiment Setup

The testing apparatus composes of three concrete bricks bonded to a plywood base board using silicone calking materials and then mounted to the CEC manufactured Levee Test Fixture, as shown in Figure 11. For the wall that is expected to rotate, the silicone calking materials were cut out leaving only a quarter inch thick/wide section of silicone, so that the wall is free to rotate. The Levee Test Fixture is a steel deck equipped with four hydraulic pistons to simulate variable hydrostatic pressures, capable of testing four separated model wall sections with same load at a time, shown in Figure 11. Also shown in Figure 11 is the addition of LVDT's to measure the deflections. This apparatus is not scalable to the real New Orleans HPS but is comparable in rotational failure therefore yielding vital information in determining the viability of the University of Mississippi's RCCS.

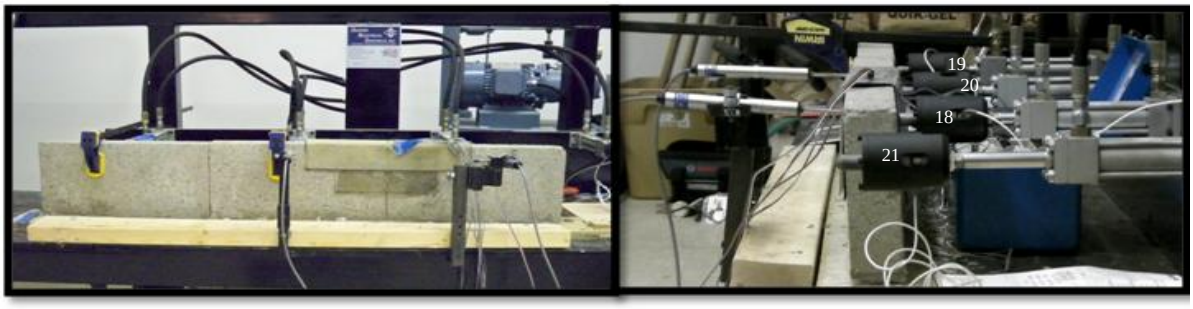

Figure 11. Floodwall Testing Set up and hydraulic piston configuration

Table 3 below shows the configuration of all strain rosette gage locations and angle orientation, LVDT's, and Load cell. For the strain rosettes, A,B, and C are denoting the angle of each gage. A and C are running +/- 45 degrees to the longitudinal direction of the cap while B is running longitudinal or parallel to the levee system, see Figure 12. The notation of top, front, and back are in relevance of the strain gage location. The front is in relation of the protected side of the levee while the back is the river side. The wall denotation is shown in Figure 13, where

Wall 2 contains the strong soil characteristics and Wall 3 the weak. The strong and weak soil properties where simulated by differing strength epoxies. Each epoxy was applied to loading deck in 1/8th inch thick sheets concrete was placed into it and epoxy was allowed to cure.

Table 3. Channel Configuration (Rosette, LVDT and Load Cell)

Cap Number	R/O Box	Rosette Location	Channels			
			Ch. 1	Ch. 2	Ch. 3	Ch. 4
1	198417	Top	C	B	A	Wall 2 LVDT1
	198418	Front	C	B	A	Wall 3 LVDT2
	199531	Back	C	B	A	Wall 3 Load Cell 2

Correction Factors:

Rosette's = 2.13; LVDT's = Full Scale of 50 mm and F.S. Mv/v =3.476; Load Cells Calibrated at 1,000 lbs, Cell # 2 = 2.009

Each LVDT is located at the center line of each wall approximately 0.5 inches from the top. The load cells are attached to the ends of each piston with a single spherical tip. The spherical tip has a contact area of 1square inch. The system is run by a 220V electric hydraulic motor that produces 1.5 hp at 1800 rpm. The systems max pressure applied load is approximately 250 psi per piston. Please see Appendix A for CEC calibration and design specifications. The Pressure Cells are located at the center of each block approximately 1 inch from the top. This location was chosen to achieve the maximum moment possible with this experimental configuration.

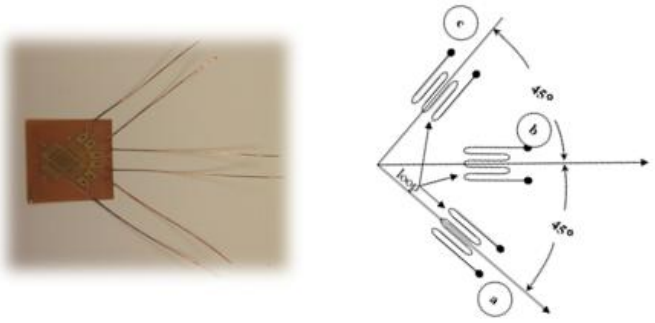

Figure 12. Micro-Measurement's (WA-06-120WR-350) Strain Gage and Strain Gage Orientation

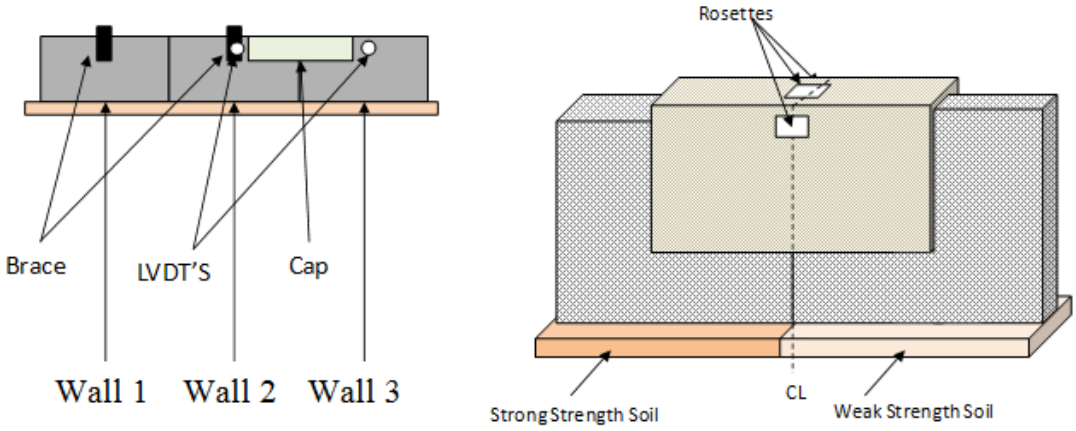

Figure 13. Wall Diagram

Pressure Cells = Orientation (Right to Left) each Calibrated at 1,000 lbs.

Cell # 4 = 1.835 Cell # 3 = 1.873 Cell # 2 = 2.009 Cell # 1 = 1.920

Micro Measurement's WA-06-120WR-350 strain rosette was chosen to be implemented onto Composite Caps. This strain rosette was chosen due to its size and strain gage orientation. Three locations were chosen to install stain rosettes; the Front, Back, and Top. The locations were selected for they are critical locations producing the highest concentrated of stresses in the material, see Figure 14. The locations of the strain gages are on the centerline of the cap directly over wall section seam (e.g. the union of two wall structures), see Figure 13.

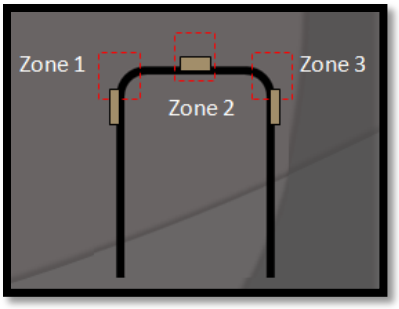

Figure 14. Cross-Section of Composite Cap with Strain Rosette locations

The load was applied in increments of 25 lbs, as shown in Figure 15, and was carried out until max load was achieved or failure of Cap occurred. The time duration during loading varied from 5 to 8 seconds between incremental loadings. During this 5-8 second time elapse the load remained constant to ensure data collection.

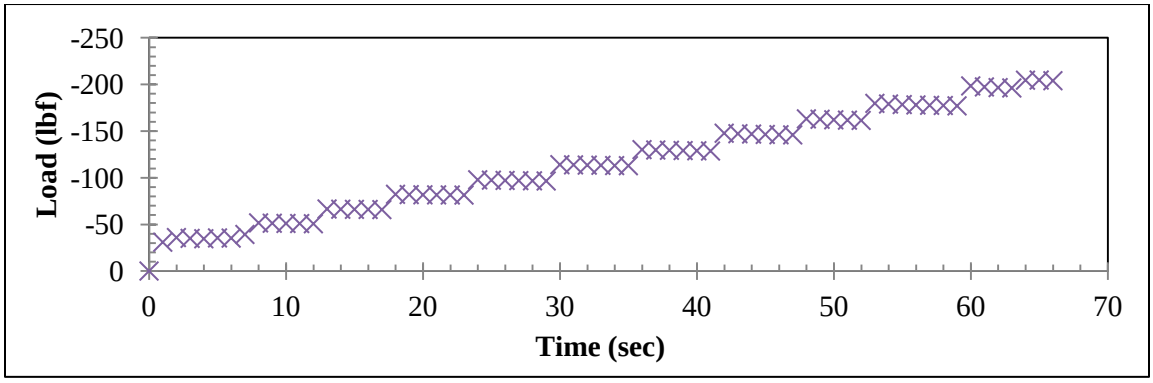

Figure 15. Incremented increase of hydrostatic pressure applied to model wall

3.2.1 Data Collection System

The P3 Vishay Strain Indicator and Recorder, shown in Figure 16, were used to monitor the taken reading and save the recorded readings from the strain rosettes, LVDT's, and load cell. See Table 3 *Channel Configuration*, for of setup instrumentation. Please see Appendix C for additional information of the Vishay P3.

Figure 16. Vishay P3 Strain Indicator and Recorder

Correction of Strain Gage Data

Each of the strain gages are attached to the cap using a two part adhesive and then each gage within the base plate of the rectangular strain rosette is connected through wire leads to its own independent recording channel on the P3. The type of bridge circuit used can be modified to best represent the function of the application. In this study the quarter bridge was utilized. Once subjected to a load, the three strain gage values are recorded at each load increment. These readings are identified as raw strain or normal strains $\hat{\varepsilon}_a$, $\hat{\varepsilon}_b$, and $\hat{\varepsilon}_c$. The "^" or hat indicates that the strain is a raw or uncorrected stain. (Bucinell, n.d.)

The data collected through rosettes require corrections, due to the bi-axial states of stress subjected on the structure about the x and y axis's. The correction of the strain gage data is

needed because as the loops of the stain gages are stretched transverse to the principal direction of the gage, causing error. Below are the transverse loading error correction equations of the gauges, thus transforming the raw strains into corrected strains. (Bucinell, n.d.)

Equations: (Bucinell, n.d.)

$$\varepsilon_a = \frac{\hat{\varepsilon}_a \cdot (1 - \nu_0 \cdot K_a) - K_a \cdot \hat{\varepsilon}_c \cdot (1 - \nu_0 \cdot K_c)}{1 - K_a \cdot K_c} \quad \textbf{(1)}$$

$$\varepsilon_b = \frac{\hat{\varepsilon}_b \cdot (1 - \nu_0 \cdot K_b)}{1 - K_b} - \frac{K_b \cdot [\hat{\varepsilon}_a \cdot (1 - \nu_0 \cdot K_a) \cdot (1 - K_c) + \hat{\varepsilon}_c \cdot (1 - \nu_0 \cdot K_c) \cdot (1 - K_a)]}{(1 - K_a \cdot K_c) \cdot (1 - K_b)} \quad \textbf{(2)}$$

$$\varepsilon_c = \frac{\hat{\varepsilon}_c \cdot (1 - \nu_0 \cdot K_c) - K_c \cdot \hat{\varepsilon}_a \cdot (1 - \nu_0 \cdot K_a)}{1 - K_a \cdot K_c} \quad \textbf{(3)}$$

Where:

ε_a, ε_b, and ε_c	Corrected Strains,
ν_0	Poisson's Ratio (.285)
K_a , K_b , K_c	Transverse Sensitivity Coeff. (.2)
G	Shear Modulus
E	Young's Modulus

Direct Calculation of Principle Strains from Corrected Strains

The corrected strains are used to calculate the principle strains. The two equations for Principle Strains are as listed: (Bucinell, n.d.)

$$\varepsilon_1 = \tfrac{1}{2}\cdot(\varepsilon_a + \varepsilon_c) + \tfrac{1}{2}\cdot\sqrt{(\varepsilon_a - \varepsilon_c)^2 + (2\cdot\varepsilon_b - \varepsilon_a - \varepsilon_c)^2} \quad \textbf{(4)}$$

$$\varepsilon_2 = \tfrac{1}{2}\cdot(\varepsilon_a + \varepsilon_c) - \tfrac{1}{2}\cdot\sqrt{(\varepsilon_a - \varepsilon_c)^2 + (2\cdot\varepsilon_b - \varepsilon_a - \varepsilon_c)^2} \quad \textbf{(5)}$$

Where, ε_1 and ε_2 are the in-plane principle strains. Equation 6 is used to calculate the principle angle ϕ, one would look to the angle between the a-axis (see Figure 12) and the maximum principle Strain ε_1 (Equation 4), (Bucinell, n.d.).

$$\tan 2\phi = \frac{2\cdot\varepsilon_b - \varepsilon_a - \varepsilon_c}{\varepsilon_a - \varepsilon_c} \quad \textbf{(6)}$$

If the material is linear, isotropic, and homogeneous the principle stresses can be computed directly from the corrected strains. For each of the case studies this assumption was taken to solve for the principle stresses directly.

Major and Minor Principle Stresses:
Where, E is denoted as Young's Modulus and ν is Poisson's ratio.

$$\sigma_1 = E\cdot\left[\frac{(\varepsilon_a + \varepsilon_c)}{2\cdot(1-\nu)} + \frac{1}{2\cdot(1+\nu)}\cdot\sqrt{(\varepsilon_a - \varepsilon_c)^2 + (2\cdot\varepsilon_b - \varepsilon_a - \varepsilon_c)^2}\right] \quad \textbf{(7)}$$

$$\sigma_2 = E\cdot\left[\frac{(\varepsilon_a + \varepsilon_c)}{2\cdot(1-\nu)} - \frac{1}{2\cdot(1+\nu)}\sqrt{(\varepsilon_a - \varepsilon_c)^2 + (2\cdot\varepsilon_b - \varepsilon_a - \varepsilon_c)^2}\right] \quad \textbf{(8)}$$

The Strong Strength and Weak Strength soil, shown in Figure 17, simulate the non-homogeneous nature of the existing soil conditions in the New Orleans area. During Hurricane Katrina certain breaches occurred not due to overtopping but due to shear failure of the weak/soft

soil. With the implementation of the UMRCC system the load subjected to the sections of I-walls that have relatively weak soil, can be distributed along its adjacent I-wall sections with relatively strong soil. Therefore the I-walls with relatively strong soil will support or distribute the load along the length of the entire I-wall system; this creates a stable global and local system in comparison to the unstable local system that exists as of now.

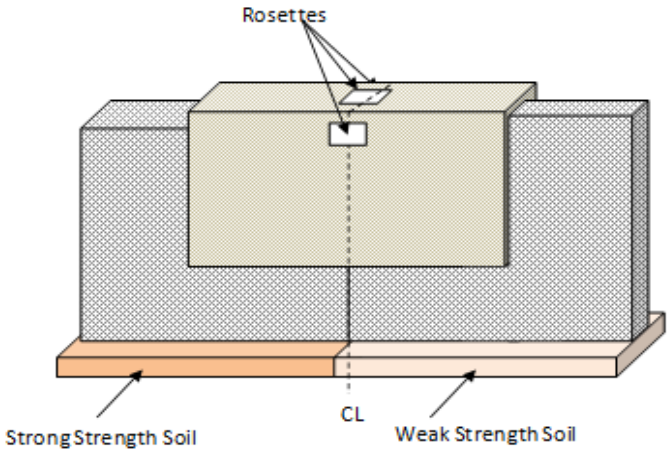

Figure 17. Strong and Weak soil Diagram

4. Material Properties

The material used in this experiment was an E-glass vinyl ester composite. When looking at Figure 18, it is notice that Cap3 is described as hexagonal. This hexagonal characteristic is in actuality the shape of the filler that assists in increasing the stiffness of the material. The fiber orientation of Cap 3 (12 layers) is the same as Cap1 (6 layers) with its principle direction the X direction or longitudinal direction.

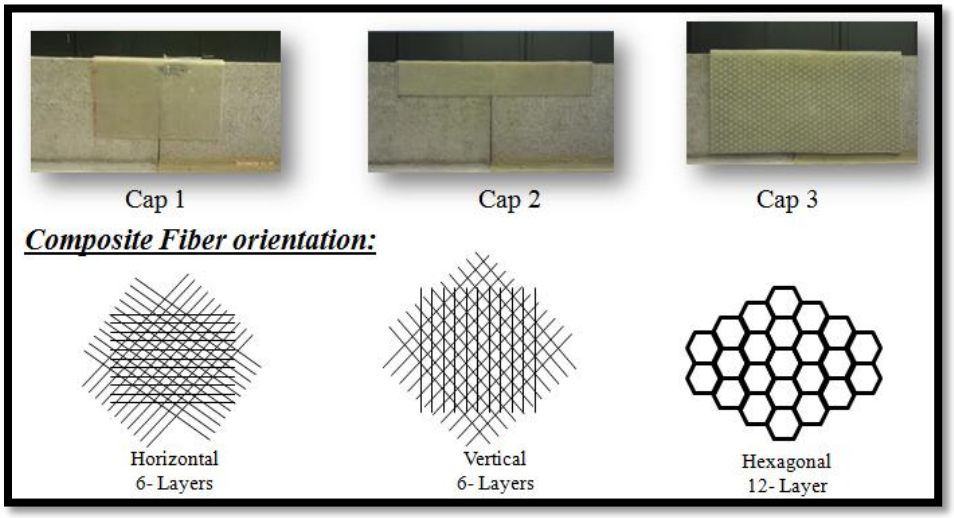

Figure 18. UM Composite Cap specimens

Table 4 represents the internal parameters of the composite materials used. ***S*** stands for small cap, tested by the University of Mississippi, in which is a set of parameter study models. ***M*** stands for mini cap, tested by ERDC, in which is an approximately 1 /64th scaled model of the true New Orleans I-wall system. Mechanical properties for UM composite caps and ERDC composite caps can be seen in Table 4. Due to the University of Mississippi's

external parameter discrepancies or inconsistency in dimensionally with ERDC's mini cap, a direct scaled relation is not possible but a parameter study for each of the University of Mississippi model caps can still yield credible data. Poisson's ratio (v) was determined in both xy and yx directions, for simplicity of computation the average was taken was taken, where x=1 and y=2, see Equation 9.

$$v = \sqrt{v_{12} v_{21}} \tag{9}$$

Table 4. Cap Comparison Chart

Comparison Chart									
Cap #	Lay up	Thickness	Ebx (Msi)	Eby (Msi)	Ex (Msi)	Ey (Msi)	vxy	vyx	Gxy (Msi)
1S	45/-45/0/0/-45/45	0.075/6	1.823	1.7	2.65	1.54	0.37	0.22	1.01
2S	(-45/45/90/90/-45/45)	0.085/6	1.79	1.91	1.57	2.71	0.22	0.38	1.04
3S	$[45/-45/0/0/45/-45]_2$	0.276/12	2.29	1.48	2.5	1.44	0.44	0.25	0.97
4M	90/-45/45	0.045/3	1.26	2.93	1.53	2.62	0.22	0.38	1
5M	90/-45/45	0.04/3	1.31	3.03	1.58	2.69	0.22	0.37	1.04

4.1 Calculation of mechanical properties of Composite

To obtain the density of the composite and the volume fraction of each cap, a burn test was conducted. Each cap was burned using ASTM D2584 before cooling down to room temperature and removed from oven. Once removed the composite was very carefully examined and separated into layers, see Figure 19. The initial mechanical properties were referenced through Dutta Technologies, Kaw 2006, and Gibson 1994.

Given: E_f = 10.5 Msi (Kaw 2006); E_m = 0.53 Msi (Dutta Technologies)

Assumed Values: ν_f = 0.2 (Kaw 2006); ν_m = 0.36 (Gibson, 1994)

Where, f denotes fiber and m denotes matrix.

With these given and assumed values one can use Equations 10 through 13 to obtain elastic moduli. When solving for shear strength of the fiber and matrix (G_f and G_m) see Equation 13 and Equation 14 with corresponding Youngs modulus of fiber and matrix (E_f and E_m) and Poisson's ratio of fiber and matrix (ν_f and ν_m).

$$E_{x'} = E_f V_f + E_m V_m \tag{10}$$

$$\frac{1}{E_{y'}} = \frac{V_f}{E_f} + \frac{V_m}{E_m} \tag{11}$$

$$\nu_{x'y'} = \nu_f V_f + \nu_m V_m \tag{12}$$

$$\frac{1}{G_{x'y'}} = \frac{V_f}{G_f} + \frac{V_m}{G_m} \tag{13}$$

$$G = \frac{E}{2(1+\nu)} \tag{14}$$

To calculate the density of the composite materials, Equation 15 is used.

$$\frac{1}{\rho_c} = \frac{W_f}{\rho_f} + \frac{W_m}{\rho_m} \quad \textbf{(15)}$$

$$\rho_c = \frac{V_f}{W_f}\rho_f \quad \textbf{(16)}$$

$$\rho_m = \frac{W_m}{\frac{1}{\rho_c} - \frac{W_f}{\rho_f}} \quad \textbf{(17)}$$

To calculate the Volume fractions of the fiber and the lamina see Equations 17 and 18 are used.

$$V_f = \frac{\rho_c}{\rho_f} W_f \quad \textbf{(18)}$$

$$V_m = \frac{\rho_c}{\rho_m} W_m = 1 - V_f \quad \textbf{(19)}$$

Sample Burn Test Data from Cap 2:

The definition of one layer is considered one layer with one set of fibers with a specific degree orientation. Where as one ply is one full sequence of layered fibers. An example of a two ply composite is that of Cap1with a fiber orientation of (45/-45/0/0/-45/45), this is considered two ply. The first ply is the sequence of fibers running 45/-45/0 then the second sequence running in the inverse 0/-45/45 is the second ply.

The following data was obtained from a sample burn test.

Length= 2.75 cm	Thickness =2.15 mm	Mass total = 1.95 g
Width=2.5 cm	Volume =1.375 cm^3	Mass final =1.22 g

Figure 19. E-Glass burn test results yielding layering system for Cap 2

Layers 1 and 7 were found to have no structural significance. As shown in Figure 19, layer 4 is comprised of two layers of vertical fibers, the first is the last layer segment of the arrangement labeled ply-1 and the other is the first layer of ply-2. From the burn test of Cap 2 the calculated weight fraction of 62.6% fiber to 37.4% matrix was determined. From the weight fraction the volume fraction can be determined, as shown below; results are shown in

Table 5.

$$\frac{1}{\rho_c}=\frac{W_f}{\rho_f}+\frac{W_m}{\rho_m}=\frac{0.626}{0.092}+\frac{0.374}{0.0366}=17.022$$

$$\Rightarrow \rho_c = 0.059(0.0512^*)lb/in^3$$

$$V_f=\frac{\rho_c}{\rho_f}W_f=\frac{0.059}{0.092}\times 0.626=0.4$$

$$V_m=1-V_f=1-0.4=0.60$$

Table 5. Volume fraction

Cap #	Thickness	V_f	V_m	$E_{x'}$ (Msi)	$E_{y'}$ (Msi)	$\nu_{x'y'}$ (Msi)	$G_{x'y'}$ (Msi)
1	0.075	0.3872	0.612	4.39	0.84	0.3	0.64
2	0.085	0.4	0.6	4.52	0.85	0.3	0.65
3	0.276	0.24	0.76	2.92	0.69	0.32	0.53

4.2 *Properties of Composite Material*

The following tests were conducted by Mantena,(n.d.) and Tadepalli, (n.d.) and associates to determine the ultimate yield parameters of composite materials. One of the samples used in these experiments is similar in composition to that of two of our three cap designs. The results of this study can be used to assist in the justification of the UMRCC results. The samples in this study denoted as PD-1 and PD-2 are similar in composition, to that of two UMRCC's. PD-1 and PD-2 are the same sample ran twice. The tensile tests performed on both PD-1 and PD-2 used the MTS 810 material testing system. The procedures are in accordance with ASTM standard D3039/D3039M-00(ASTM 2006). From these results the stress vs. strain and ultimate strength where obtained.

Table 6: Average tensile properties of laminated composite (Mantena, n.d.)

Specimen	Ultimate tensile Strength (F^{tu}) MPa (psi)	Tensile modulus (E^{chor}) GPa (psi)	Poisson's ratio (ν)	% Bending
PD-1 (2-ply) $[0/\pm 45]_2$	292 (42.4E+03)	18.6 (2.70E+06)	0.437	n/a
PD-2 (2-ply) $[0/\pm 45]_2$	318 (46.1E+03)	18.9 (2.75E+06)	0.440	3.90

The primary mode of failure for both PD-1 and PD-2 was material delimitation, other causes of apparent failure was that of gage failure. Ultimately the failure mode of the material was that of a complete material failure through the center of the specimen.

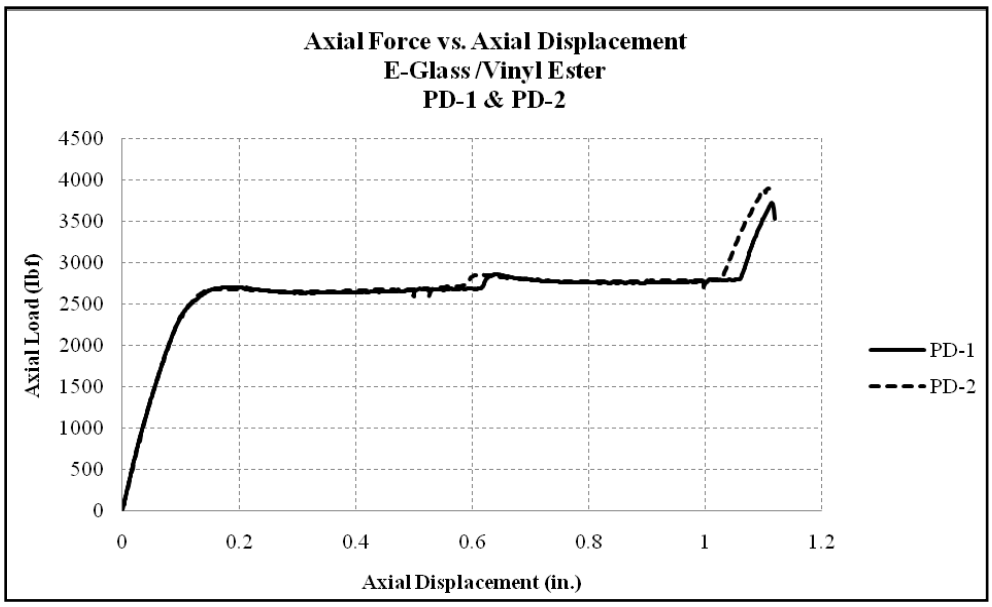

Figure 20. Axial force vs. Axial displacement for specimens PD-1 & PD-2.(Mantena, n.d.)

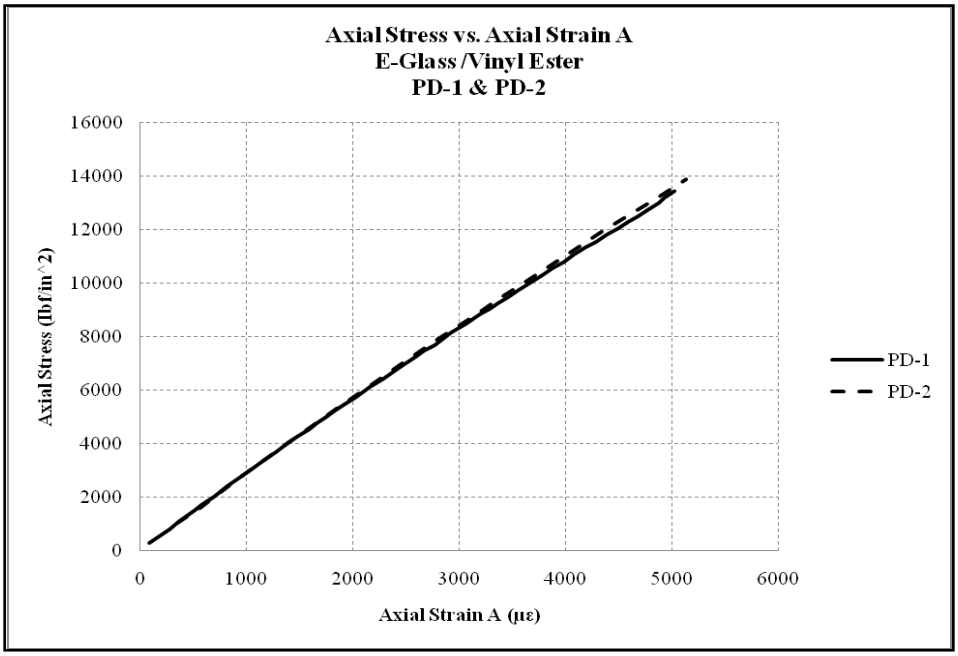

Figure 21. Axial stress vs. Axial strain for specimens PD-1 & PD-2.(Mantena, n.d.)

The above figures can be referenced to determine the fatigue and damage done to the Composite caps during testing.

Table 7. Average Shear Properties (Mantena, n.d.)

Specimen	Ultimate load (Pu) KN (lbf)	Stroke at Pu mm (in)	Ultimate Shear Strength (Fu) MPa (psi)	Shear Modulus GPa (psi)	% Twisting
PD-1 (2-ply) $[0/\pm 45]_2$	4.68 (1,053)	4.44 (0.175)	167 (24,231)	5.27 (764,349)	2.08%
PD-2 (2-ply) $[0/\pm 45]_2$	3.19 (1,043)	3.19 (0.125)	165 (24,049)	6.09 (883,280)	26.95%

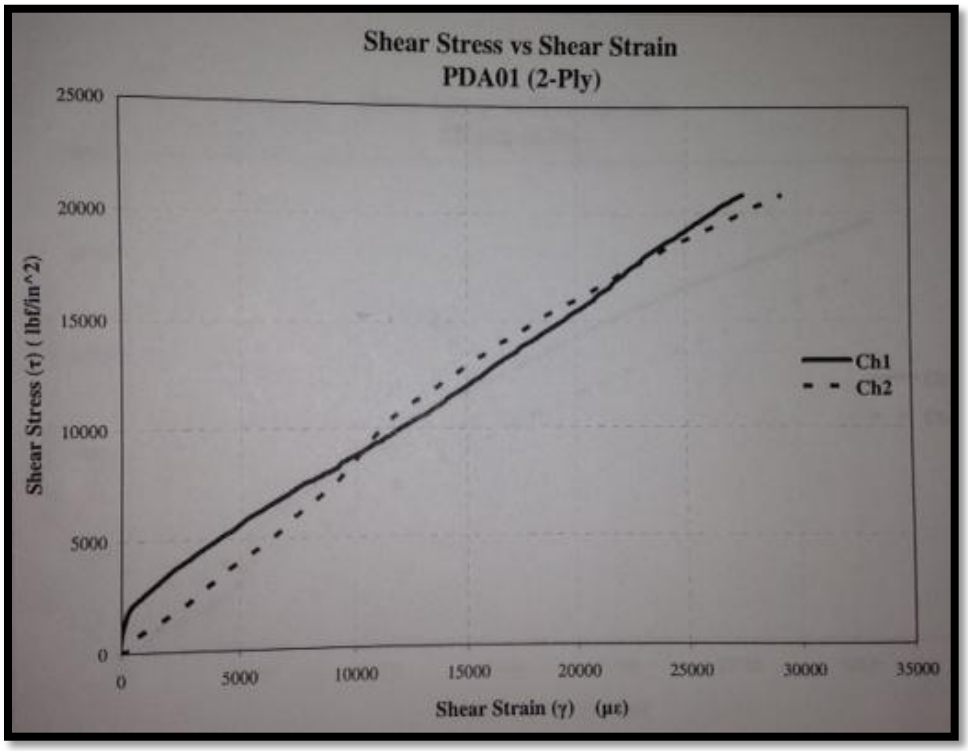

Figure 22. Shear Stress vs. Shear Strain PDA01 (Mantena, n.d.)

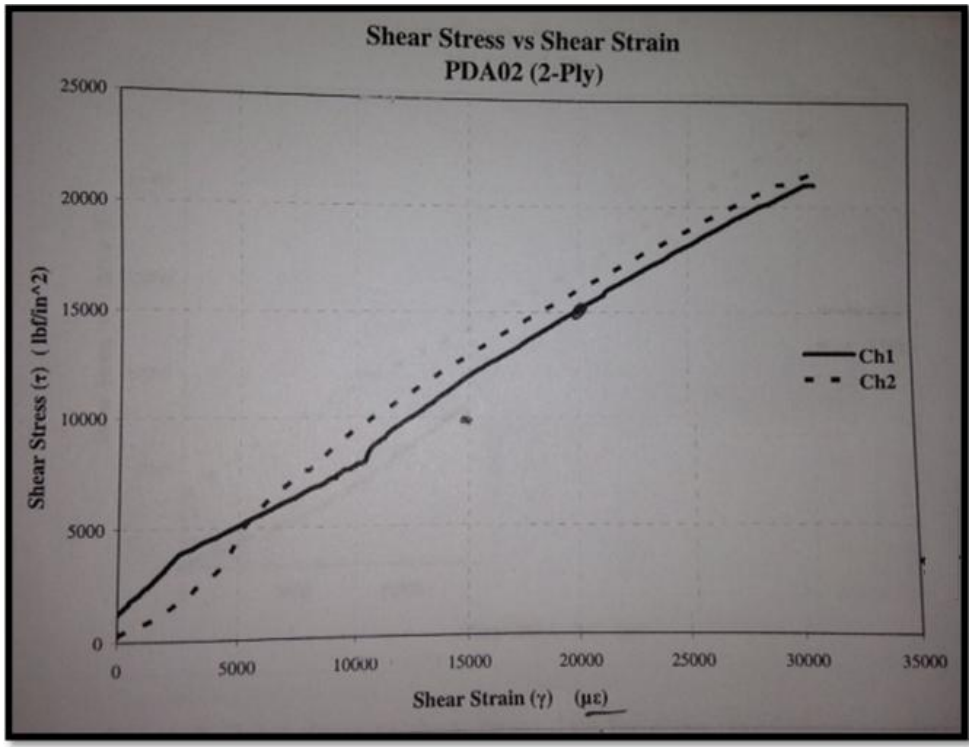

Figure 23. Shear Stress vs. Shear Strain PDAO2 (Mantena n.d.)

Both tensile and shear should be incorporated in to the results of the cap due to coupling. When a channel cross-section has a uniform web and flange thickness the shear center can be found by the following equation (Shan and Qiao, 2004).

$$e = \frac{3b_f^2}{b_w + 6b_f} \tag{20}$$

Therefore when loading, where the force is acting away from the shear center, both torsion and flexural characteristics will be present in results (Shan and Qiao, 2004).

4.3 Properties of Rubber Membrane

As a part of each study, a test was conducted by applying a rubber membrane under each of the composite caps. The rubber membrane is classified as EPDM (ethylene propylene diene monomer (M-class) rubber) and meets ASTM D4637 / D4637M – 13. To verify the mechanical properties from Table 8, a test was conducted by mounting a sample of rubber into a vice and connected a load scale on other end; results are shown in Figure 24. Figure 24 shows a modulus of 2100psi, this falls within the range given in Table 8.

Table 8. EPDM Rubber Mechanical Properties (Advanced Rubber Coatings, 2011)

Specific Gravity	0.87
Hardness, Durometer	30A to 90A
Tensile Strength, Mpa (psi)	6.9 to 20.7 (1000-3000)
Elongation, %	100-600
Useful Temperature Range	-50 to 150ºC (-60 to 300ºF)
Brittle Point	-50ºC (-60ºF) **
Tear Resistance	Fair to Good
Abrasion Resistance	Good to Excellent
Resilience	Fair to Good
Adhesion to Metal	Fair

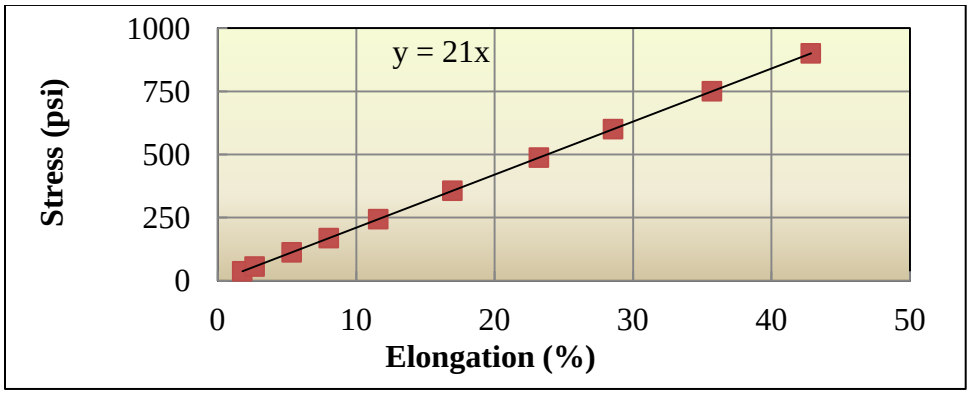

Figure 24. Stress-Strain curve of Rubber Membrane

4.4 Properties of Silicone Adhesive using DMA

The adhesive chosen for the experiment was *GE Silicone II* W/D Supreme 2X Strength.* This material meets Federal Specifications: TT-S-00230C; TT-S-001543A/ASTM C-920, Type-S, NS, Class 50, use A, G & O test requirements (GE/MPM). Using the DMA the calculated modulus of the silicone was approximately 1 Mpa, shown in Table 9. Table 10 shows the typical properties of cured GE silicone. Specimens were approximately 1/8th in x1/16th in x1in.

$$E = \sqrt{Energy\ storage^2 + Energy\ loss^2}$$

Table 9. UM DMA tests results of GE Silicone II

Storage modulus	0.959 Mpa
Loss modulus	0.114 Mpa
Stiffness	533.8 N/m
Damping	62.8 N/m
Stress	.01 Mpa
Youngs Modulus (E)	0.965 Mpa

Table 10. Typical Properties of Cured GE Silicone II* W/D Supreme 2xStrength (GE/MPM)

TYPICAL PROPERTIES – CURED

Property	Value[(1)]	Test Method
Hardness, Durometer (Type A Indenter)	20	ASTM D2240
Ultimate Tensile Strength	213 psi (1.5 Mpa)	ASTM D412
Ultimate Elongation	347 %	ASTM D412
Specific Gravity	1.02	
Joint Movement Capability	+/-25%	ASTM C719
Service Temperature Range (after cure)	-55°F to +400°F (-48°C to 204°C)	
Weathering and U.V. Resistance	Excellent	20 yr. Study
Cure Time (1/4" or 6 mm deep section) @ 75°F (24°C) 50% RH	2-3 days	
Not Paintable		
Freeze Thaw Stable		

(1) Average value. Actual value may vary.

5. Result's of UM Retrofitted Composite Cap System (UMRCCS)

In the UMRCCS experiments, three forms of composite caps were tested, each cap was tested under three scenarios with each scenario being tested three times for data consistency and repeatability. The first scenario was that of the cap by itself with no form of attachment to the model I-wall surface. This system is dependent upon the frictional coefficient between the wall and the cap to stay in place. The second scenario is the application of a rubber membrane between the cap and wall structures. This membrane is in no way bonded to either surface. Finally the third scenario is that of the cap being bonded to the concrete wall with GE Silicone II* W/D Supreme 2x Strength. The motivation of this work is to develop a new economical geotechnical technique to prevent or delay the ultimate failure of the traditionally designed I-wall in extreme conditions. The purpose of this cap is to bind all the independent I-walls to one another creating a global system. By creating a global system one I-wall does not solely rely on its own self for structural integrity. In the below sections when discussing the gages readings the terms Front, Back, and Top will be used. These references are to the location of the strain gages mounted on to the composite caps. This is also in reference to the location to the simulation of the water. The Back is referred to by ERDC as the *River-side* and the Front is referred to as the *Land-side* or *Protected-side*. Also the terms *Strong* and *Weak* will be used to refer to the strong and weak modeled soil conditions. Due to large amounts of data and to minimize error when

interpreting graphs, only the first test conducted is shown. Please see Appendix D for full data results.

5.1 Results of UMRCC 1 (Cap 1)

5.1.1 Cap 1 Scenario 1 - Bond by Friction

For the first scenario the cap was tested by solely placing the cap along the union of the two I-wall model walls. Therefore when the cap was loaded it was held in place only by the frictional coefficient between the contact points of the inner cap and wall structures. The dimensions of Cap 1 are as follows: Length of 9 inches, Height of 4.5 inches, Width of 2.3 inches, (thickness of cap perpendicular to length of wall). , Thickness of 0.085 inches. As said previously Cap 1 has a principle direction of X with additional fibers running in the 45 degree and -45 degree directions. When looking to results positive (-) is Compression and negative (+) is Tension. Cap 1, shown in Figure 25, depicts the principle fiber direction to be in the X or longitudinal direction and Table 11 shows the mechanical properties of Cap 1.

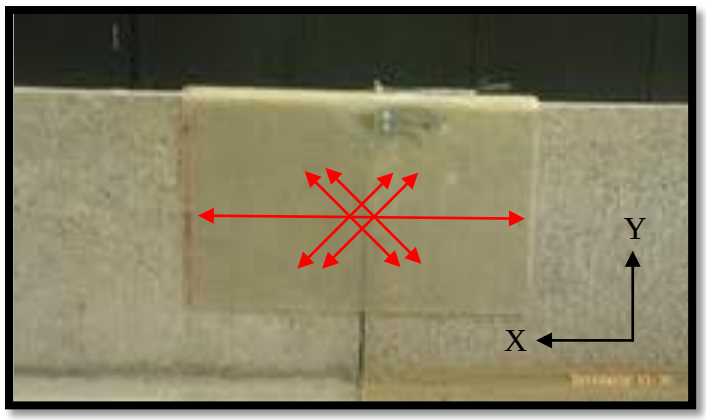

Figure 25. Cap 1

Table 11. Mechanical Properties of Cap 1

Cap #	Lay up	Thickness	E^b_x (Msi)	E^b_y (Msi)	E_x (Msi)	E_y (Msi)	ν_{xy}	ν_{yx}	G_{xy} (Msi)
1	45/-45/0/0/-45/45	0.075/6	1.823	1.70	2.65	1.54	0.37	0.22	1.01

As the test progressed a noticeable trend could be seen in the data, a natural fatigue in the material. This fatigue was due to the high loads placed on the material during testing till failure multiple times. During the experiments this fatigue was noticed at the corners of the cap, shown in Figure 27. The lamina had become frosted signifying that it had begun to crush or produce multiple micro cracks due to the repeated tests till failure. Therefore, the micro cracks allowed for weaker load results and an increased in stress and strain levels. In Figure 26 the results show that the *Front* and *Back* of the cap are in tension, while the *Top* is in compression. Please see section 5.1.4 Summary of Results for details.

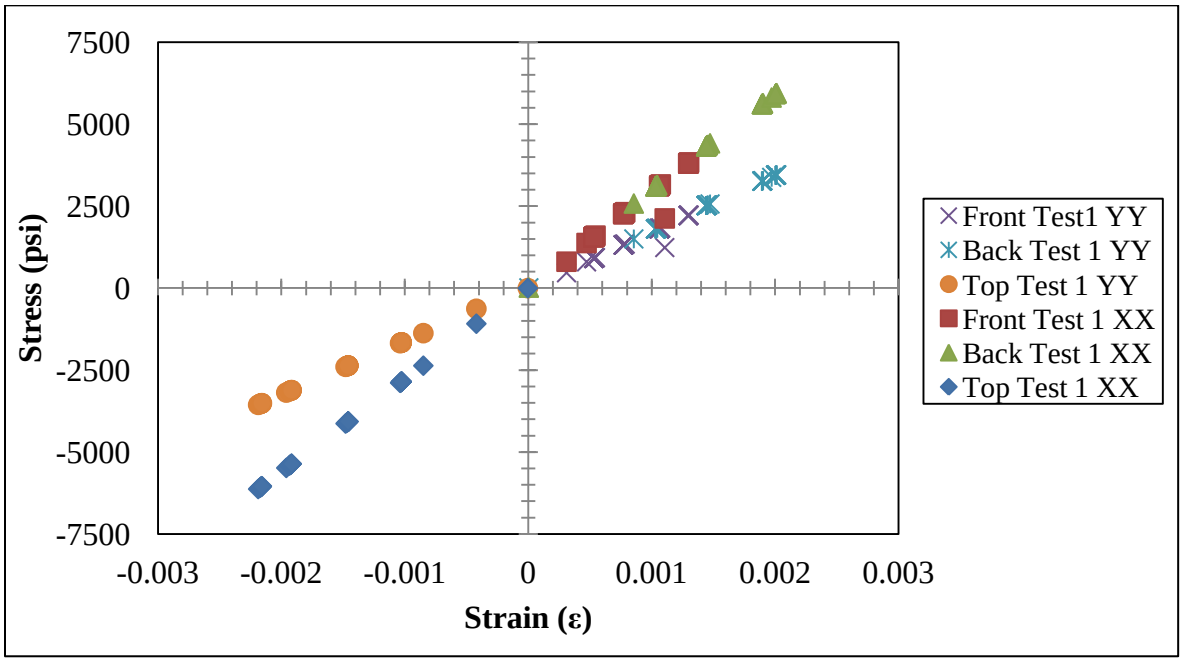

Figure 26. Stress-Strain of Cap 1

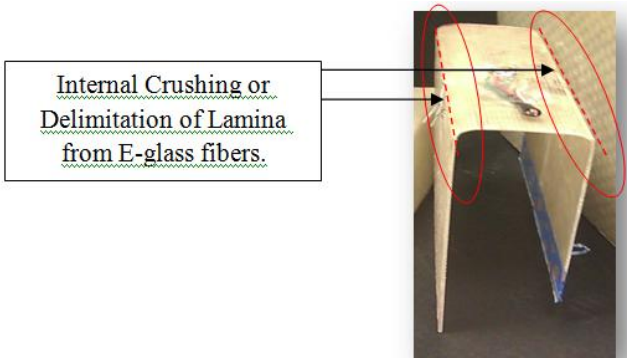

Figure 27. Fatigue zones on Cap 1.

Figure 28 shows the still shots taken from the video during the testing of Cap 1 with Scenario 1. Each frame is in increments of 25 psi until the last frame. The last frame had an average failure stress of 120 psi (Failure Range: 90psi – 130psi).

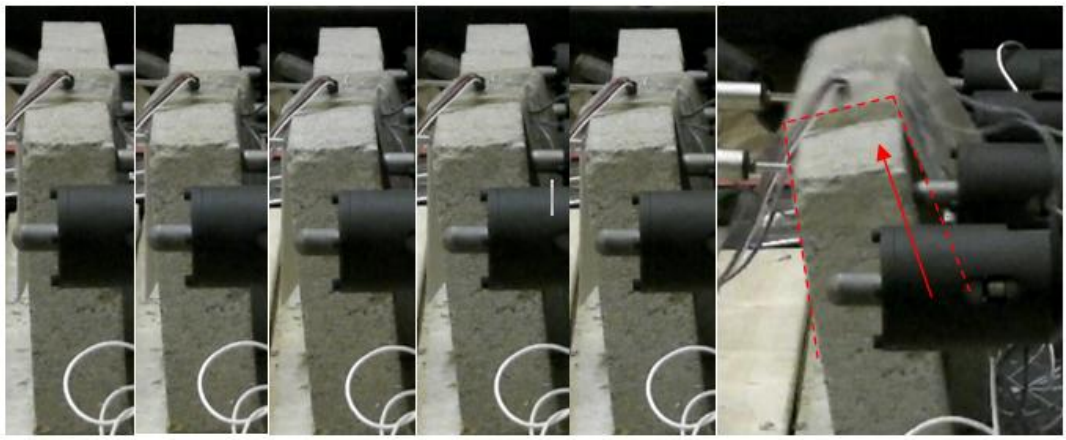

Figure 28. Still Shots Cap 1 Scenario 1

The logic behind the failure load being in a range from 90 psi to 130 psi will be discussed in this section. Cap 1 was subjected to three tests, per scenario, to verify repeatability of the results. One noticeable feature that appeared during these tests was that of fatigue of the material. This fatigue as stated was the direct result of micro cracking of the lamina. Micro-cracking was caused due to the corners being subjected to high compressions

that were surpassing the composites elastic limits. The cap failure mode of slipping was the same for each of the three tests, with the addition of the characteristic of erratic failure. The parameter that changed each time was that of the load at failure. Due to the fatigue of the material at the corners, the cap began experiencing higher stresses and strains levels at lower load levels and subsequently failed at lower load levels. Figure 29 shows the load failure point for each of the three tests conducted for Scenario 1. As shown each for each test the failure load decreased this is suspected to be due to the fatigue of material.

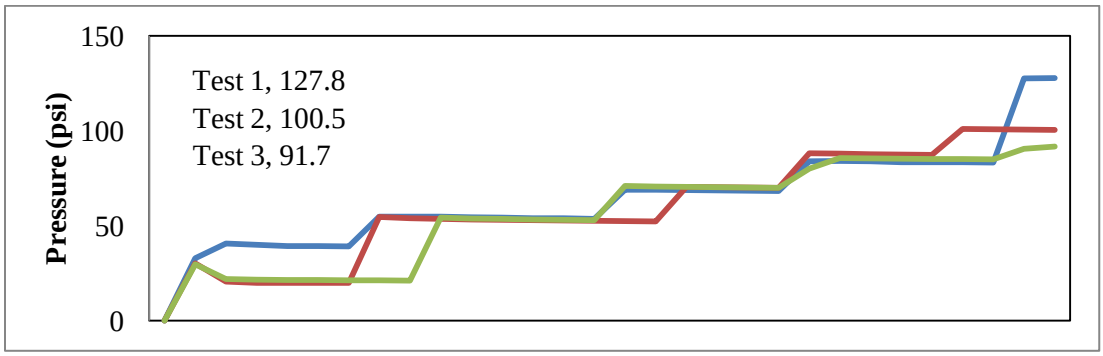

Figure 29. Load Results per test for Cap 1

5.1.2 Cap 1 Scenario 2 – Addition of Rubber Membrane

For the second scenario, the cap was tested by placing the cap along the connection point of the two model walls with the addition of an approximate 1/16th inch thick rubber membrane (EPDM rubber). This rubber membrane is cut to the same interior dimensions of the cap and placed between the cap and the wall. Therefore when the wall was loaded the cap was held in place only by the frictional coefficient between the contact points between the inner cap, rubber membrane and wall structures. In Figure 30 the results show that the *Front* and *Back* of the cap are in tension, while the *Top* is in compression. Please see section 5.1.4 for details.

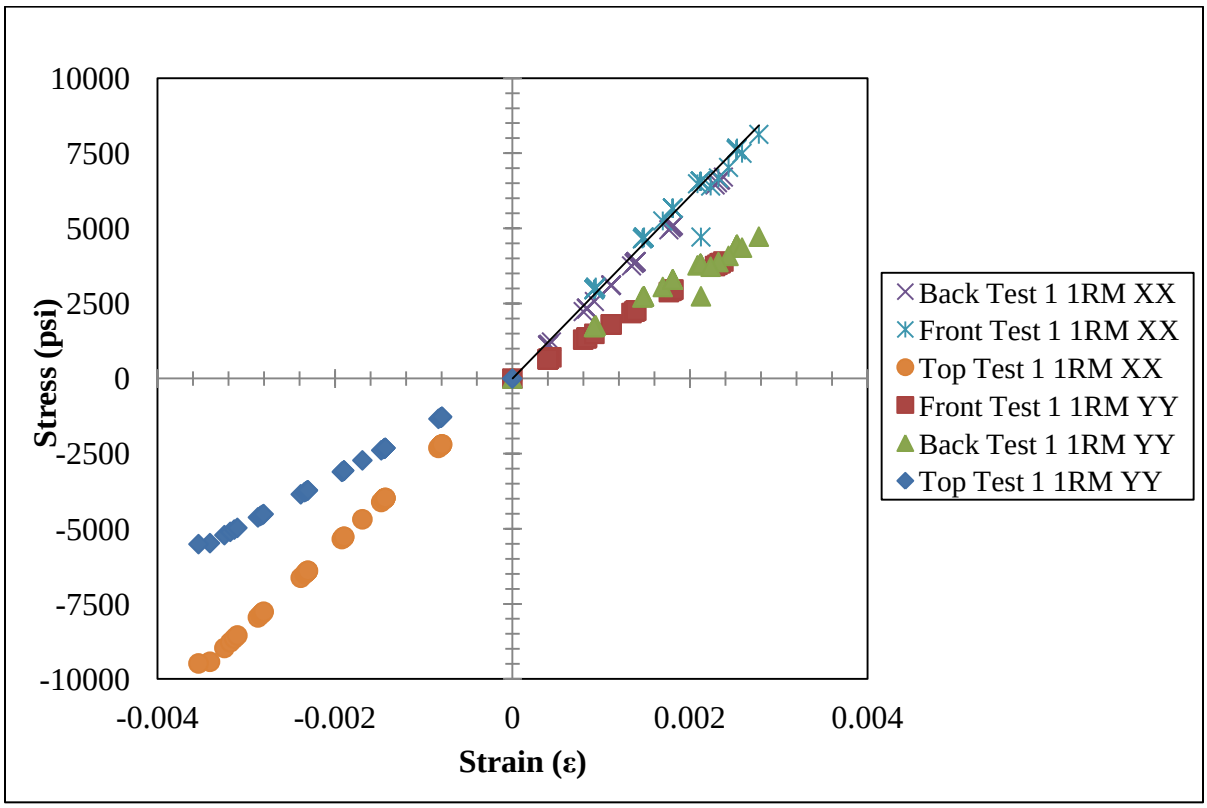

Figure 30. Stress-Strain of Cap 1 with 1 Rubber Membrane

Figure 31 shows the still shots taken from the video during the testing of Cap 1 Scenario 2. The load was applied in increments of 25 psi. The last frame had an average failure of 142 psi (Failure Range: 135psi – 150psi).

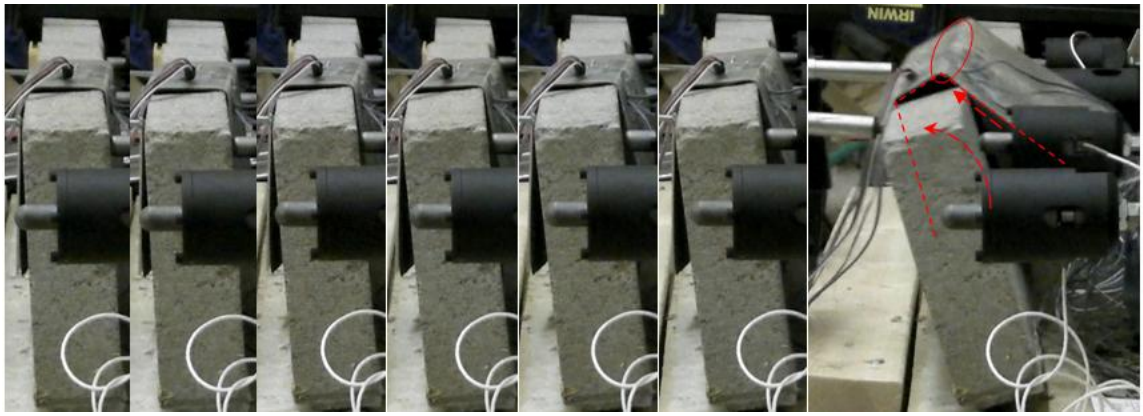

Figure 31. Still Shots Cap 1 Scenario 2

With the addition of the rubber membrane, the cap held 15% greater pressure than that of Scenario 1 and lowered the failure range by 62.5%, shown in Figure 32. As shown in Figure 31, looking to the far right image, the cap once combined with the rubber membrane resisted slipping and became a deformation failure. During these series additional test were conducted with the addition of a second layer of rubber membrane. These results yielded negligible change in results from the single layer therefore were disregarded.

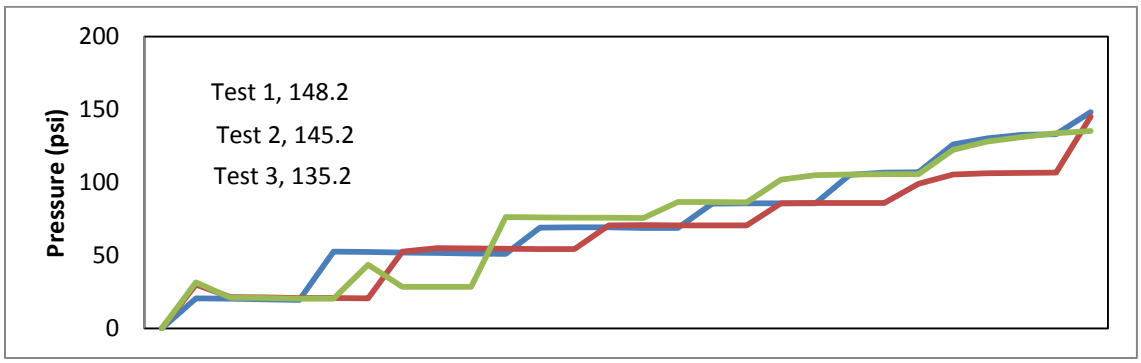

Figure 32. Load Results per test for Cap 1 with 1 layer of Rubber Membrane

5.1.3 Cap 1 Scenario 3 – Cap bonded with GE Silicone.

For the third scenario the cap was tested by bonding the cap along the union of the two I-wall model walls with GE Silicone II* W/D Supreme 2xStrength . The model wall section was coated with an approximate 1/16th inch thick layer of adhesive. Once the adhesive was applied the cap was laid on it and left to cure in 70 degree temperature for 24 hours before testing. Therefore when the cap was loaded it was held in place by the adhesive bond between the contact points of the inner cap and wall structures. In Figure 33 the results show that the *Front*, *Back*, and *Top* of the cap are in tension. Please see section 5.1.4 Summary of Results for details.

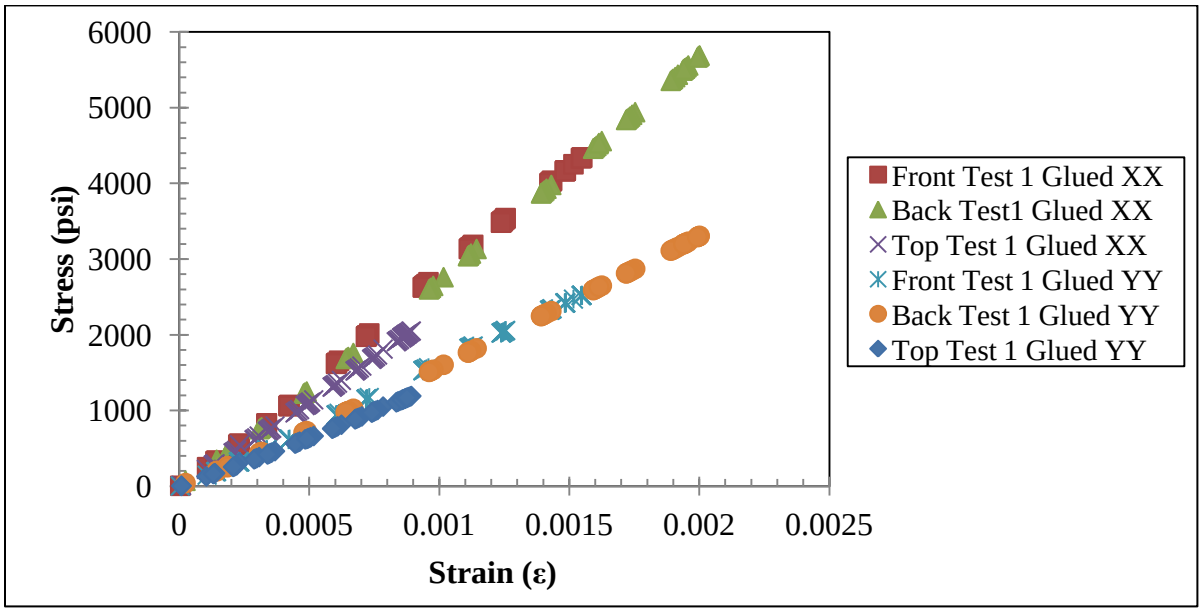

Figure 33: Stress-Strain of Cap 1

With the cap adhesively bonded to the wall there was no failure. The cap once glued reached the CEC hydraulic system's max output of 225 psi. Figure 34 show's when the cap is adhesive bonded to the wall the cap can withstand the maximum load multiple times. Section 5.1.4 will discuss the slight fatigue in silicone and tension/compression results.

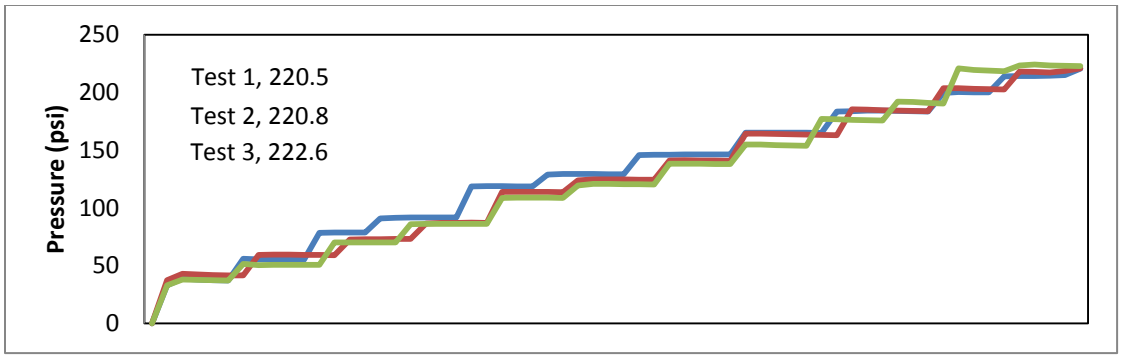

Figure 34. Load Results per test for Cap 1 with bonded with Silicone

5.1.4 Cap 1- Summary of Results

The following section will discuss the final performance results of Cap 1. Figure 24 and Figure 30 show the *Front* and *Back* strain gauges reading in tension, while the *Top* reads in compression. As shown in Figure 35, the cap and cap with rubber membrane both exhibited tensile stresses in the front and back, this is primarily due to the contact regions between the cap and the concrete. The major contact points are diagonal from one another in affect stretching the material. The top is in compression due to the flanges/legs at opposite corners of the cap being partially flexed upward. Cap 1 and Cap 1 with rubber membrane had equivalent results. The main differences in Scenario 1 and 2 was the max load capacity.

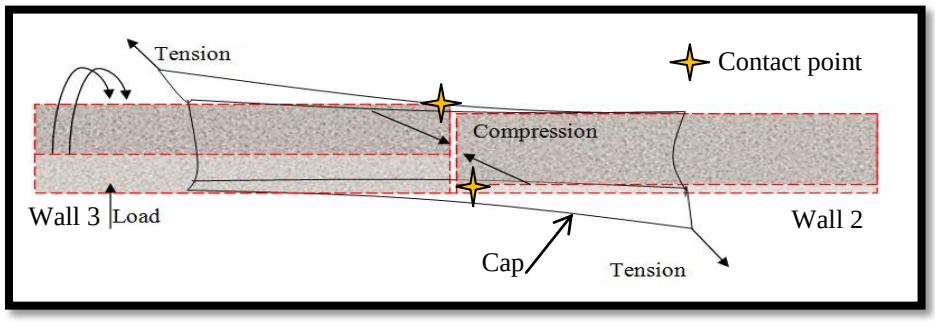

Figure 35. Diagram of Deformation of Wall and Cap

Cap 1 when glued produces tension in the top due to the cap being forced to rotate about the Y axis due to being bonded and not being allowed to bend in the Y direction as it did in Scenarios 1 and 2 see Figure 36. Figure 36 is exaggerated.

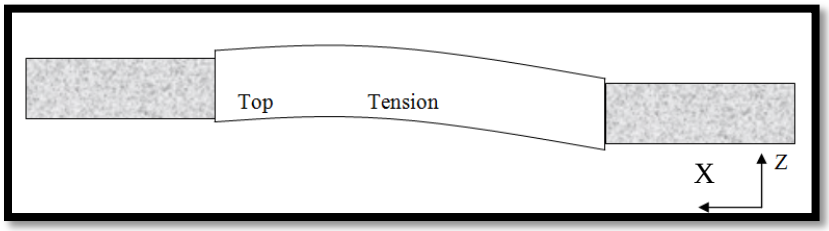

Figure 36. Diagram of Glued Cap Deforming

The displacements were taken by LVDT's at the top center of each model wall, please see Section 3.2 for setup procedures in detail. When looking to Figure 37, the Glued Cap shows the highest displacement of the Strong Wall but the lowest displacement of the Weak Wall. Cap 1 Glued did not fail during testing unlike the first two scenarios. In Figure 37, both the cap and cap with rubber membrane exhibit high relative displacements between wall sections, whereas the Glued Cap produced low relatively displacement between the wall sections. Figure 37 also shows the representation of evenly distributed load, being transferred between the walls sections. Cap 1 displays a lower displacement when compared to Cap 1RM due to Cap1 failing at a lower load. Look to Figure 38 to compare failure displacement to associated load.

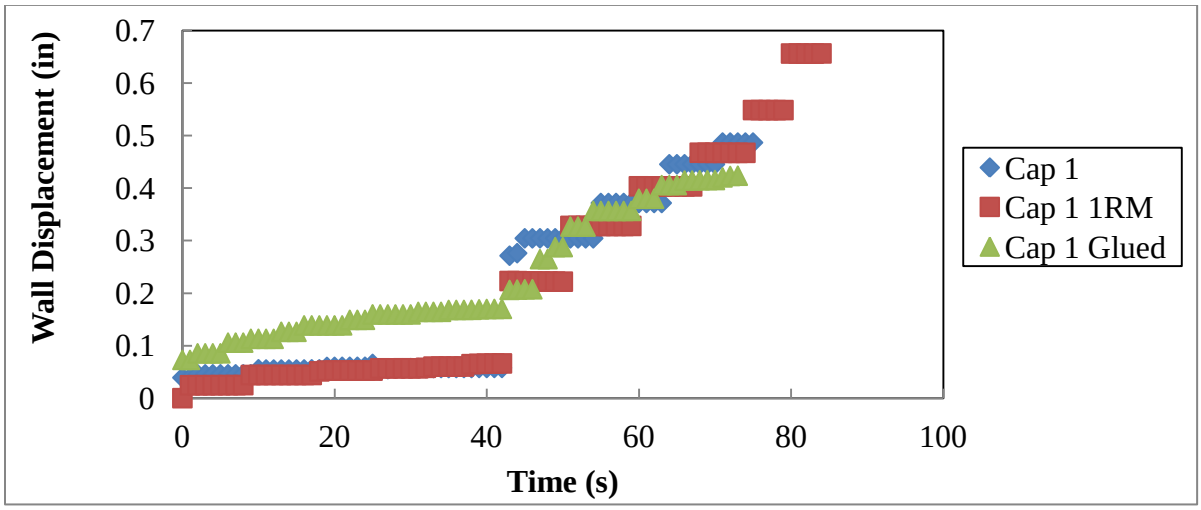

Figure 37. Wall Displacement vs. Time-Weak and Strong Walls

Figure 38 shows the wall displacement when subjected to certain load. As shown the Glued cap produces similar slopes between the weak and strong soils without failure.

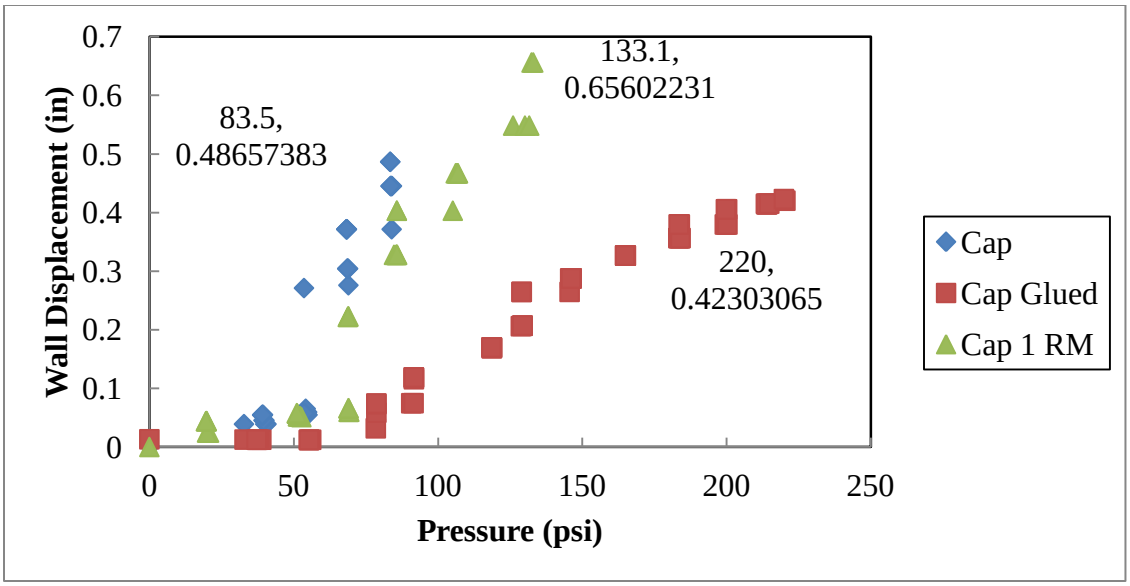

Figure 38: Load vs. Displacement – Weak and Strong Walls

Table 12 shows that the optimum Scenario for this composite structure is that of Scenario 3. Scenario 3 yielded the maximum load with the lowest relative wall displacement. The (*) next to Scenario 3's Average Max Load is due to the testing device reaching the maximum limit of output (225psi) without cap failure.

Table 12. Final Results Cap 1

Scenario	Average Max Load	Average Displacement	Max Strong Wall Displacement	Max Weak Wall Displacement
1	110 psi	0.51 in	0.06 in	0.48 in
2	142 psi	0.72 in	0.066 in	0.66 in
3	*225 psi	0.285 in	0.15 in	0.42 in

If you look to Appendix D, fatigue can be seen in results. A hypothesis behind the fatigue of the material is that of the matrix surpassing its elastic limits, and therefore producing micro-cracks in the material. Another possible source of fatigue is that of the

silicone cap. The silicone per test was slightly weakened this could be due to multiple reasons.

1. Silicone delaminating from the concrete wall.

2. Silicone delaminating from the composite

3. Air pockets within the silicone rupturing and producing weak zones.

4. Silicone surpassing its elastic limits.

5.2 Results of UMRCC 2 (Cap 2)

5.2.1 Cap 2 Scenarios 1 - Bond by Friction

The same sets of scenarios were conducted for this material as well. For the first scenario the cap was tested by solely placing the cap along the union of the two I-wall model walls. Therefore when the cap was loaded it was held in place only by the frictional coefficient between the contact points of the inner cap and wall structures. The dimensions of Cap 1 are as follows: Length of 14.25 inches, Height of 2.5 inches, Width of 2.3 inches, (thickness of cap perpendicular to length of wall). , Thickness of 0.085 inches. As said previously Cap 2 has a principle direction of Y with additional fibers running in the -45 degree and 45 degree directions. When looking to results positive (-) is Compression and negative (+) is Tension. Characteristic of Cap 2 is that the cap has a tight fit when applied were as Cap 1 easily slipped on. Cap 2, shown in Figure 39, depicts the principle fiber direction to be in the Y direction and Table 13 shows the mechanical properties of Cap 2.

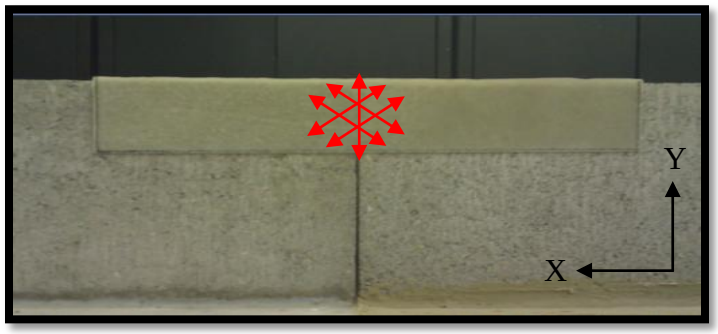

Figure 39. Cap 2 with Layup Fiber Orientation

Table 13. Mechanical Properties of Cap 2

S./N.	Cap #	Lay up	Thickness	E^b_x (Msi)	E^b_y (Msi)	E_x (Msi)	E_y (Msi)	v_{xy}	v_{yx}	G_{xy} (Msi)
1	2	45/-45/90/90/-45/45	0.085/6	1.79	1.91	1.57	2.71	0.22	0.38	1.04

The hydraulic loading system reached its maximum output capacity when testing Cap 2; therefore Cap 2's max load was 225 psi without failure. As shown in Figure 40, Cap 2 resulted in equivalent deformation characteristics as Cap 1, producing tension in the front and back of the cap and compression on the top. When comparing Scenario 1 of Cap 1 to Scenario 1 of Cap 2, Cap 2 results in lower Stress with higher load capacity. Cap 1exhibited a larger surface area of 40.5in^2 (per flange) compared to Cap 2's area of 35.625 in^2 (per flange), but Cap 2 contains a larger area of contact points therefore more evenly distributing the load resulting in lower stress to material per square inch. The results show that the *Front* and *Back* of the cap are in tension, while the *Top* is in compression. Please see section 5.2.4 Summary of Results for details.

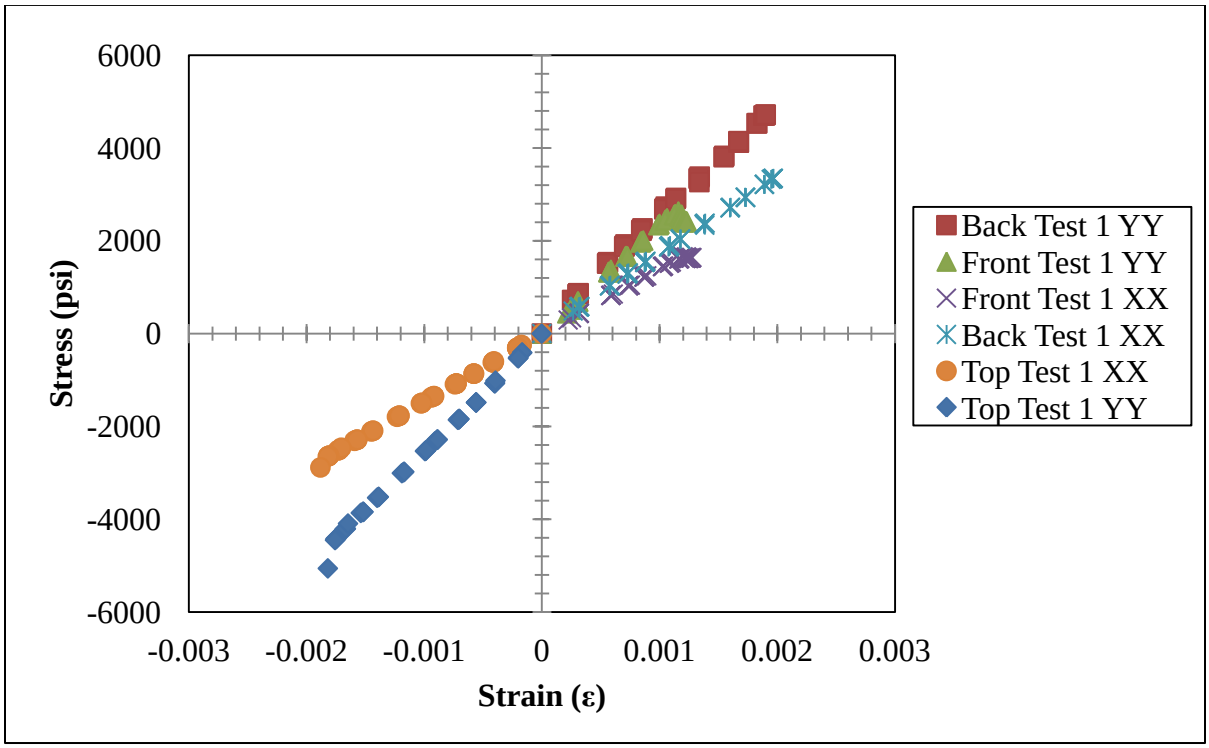

Figure 40. Stress-Strain of Cap 2

5.2.2 Cap 2 Scenario 2 – Addition of Rubber Membrane

For the second scenario the cap was tested by placing the cap along the union of the two I-wall model walls with the addition of an approximate 1/16th inch thick rubber membrane. This rubber membrane is cut to the same inter dimensions of the cap and placed between the cap and the wall. Therefore when the wall was loaded the cap was held in place only by the frictional coefficient between the contact points between the inner cap, rubber membrane and wall structures. When applying the rubber it was observed that the addition of the rubber may additional initial stress to the material due to the cap being well fitted originally without rubber membrane presences. The results show that the *Front* and *Back* of the cap are in tension, while the *Top* is in compression. Please see section 5.2.4 Summary of Results for details.

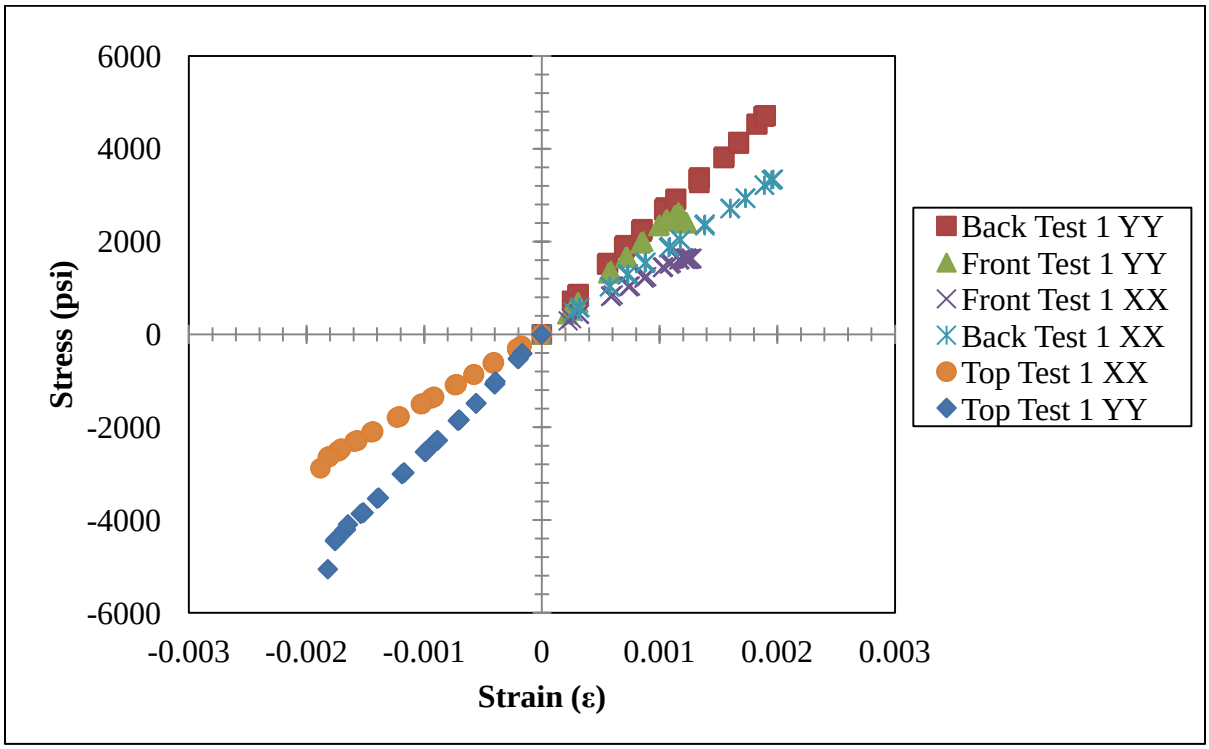

Figure 41: Stress-Strain of Cap 2 with 1 Rubber Membrane

When comparing Figure 40 and Figure 41, Scenario 2 has an average stress increase of 17% compared to Scenario 1. This increase in stress may be due to an increase in frictional coefficient between the wall and the cap with the application of the rubber membrane, or the initial stress being increased due to the cap being well fitted before the application of the rubber membrane.

5.2.3 Cap 2 Scenario 3 – Cap bonded with GE Silicone.

For the third scenario the cap was tested by bonding the cap along the union of the two I-wall model walls with GE Silicone II* W/D Supreme 2xStrength . The model wall section was coated with an approximate 1/16th inch thick layer of adhesive. Once the adhesive was applied the cap was laid on it and left to cure in 70 degree temperature for 24 hours before testing. Therefore when the wall was loaded the cap was held in place by the adhesive bond between the contact points of the inner cap and wall structures. The results show that the *Back* of the cap is in tension whereas the *Front* and *Top* are in compression. Please see section 5.2.4 Summary of Results for details.

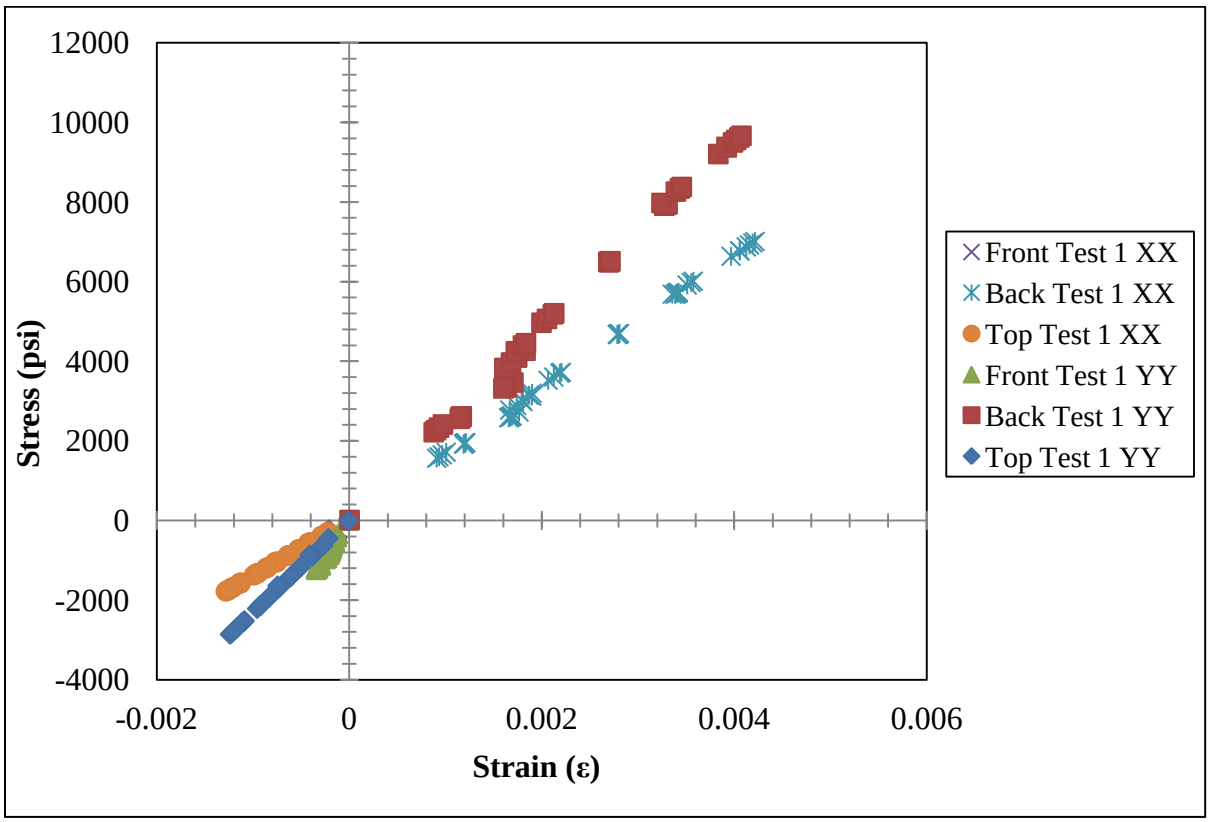

Figure 42. Stress-Strain of Cap 2 using GE Silicone

A noticeable difference in Cap 2 and Cap 1 can be seen when comparing Figure 42 and Figure 33. The results of Cap 1 suggested that when the cap was adhesively bonded to the structure all the critical locations were in tension. For Cap 2 Scenario 3 the Top and the Front are in compression, this is due to the elongated length of Cap2 when compared to Cap 1. The extra length provides additional contact points and once glued to the structure the flanges are forced upward in the YZ direction and also rotated about the Y axis. This upward motion of the front and back flanges apples compression to the top and the rotational component about the Y axis produces the compression on the front.

5.2.4 Cap 2- Summary of Results

The following section will discuss the final performance of Cap 2. Figure 40and Figure 41 show the *Front* and *Back* strain gauges reading in tension, while the *Top* reads in compression. As shown in Figure 35, the cap and cap with rubber membrane both exhibited tensile stresses in the front and back, this is primarily due to the contact regions between the cap and the concrete. The major contact points are diagonal from one another in affect stretching the material. The top is in compression due to the flanges/legs at opposite corners of the cap being partially flexed upward. Cap 2 and Cap 2 with rubber membrane had equivalent results. The main differences in Scenario 1 and 2 was the increase of stress level by 17%. Table 14 shows the final performance results of Cap 2 and Figure 43 shows the final relative displacements. Stated in the setup procedures, the displacements were taken from the top center of each model wall. When looking to Figure 43and Figure 44, all scenarios performed similarly. Again similar to Cap 1 the Cap 2 Glued performed the best in minimum relative displacement.

Table 14. Final results of Cap 2

Scenario	Average Max Load	Average Displacement	Max Strong Wall Displacement	Max Weak Wall Displacement
1	*225 psi	0.255 in	0.15 in	0.36 in
2	*225 psi	0.255 in	0.15 in	0.36 in
3	*225 psi	0.25 in	0.19 in	0.31 in

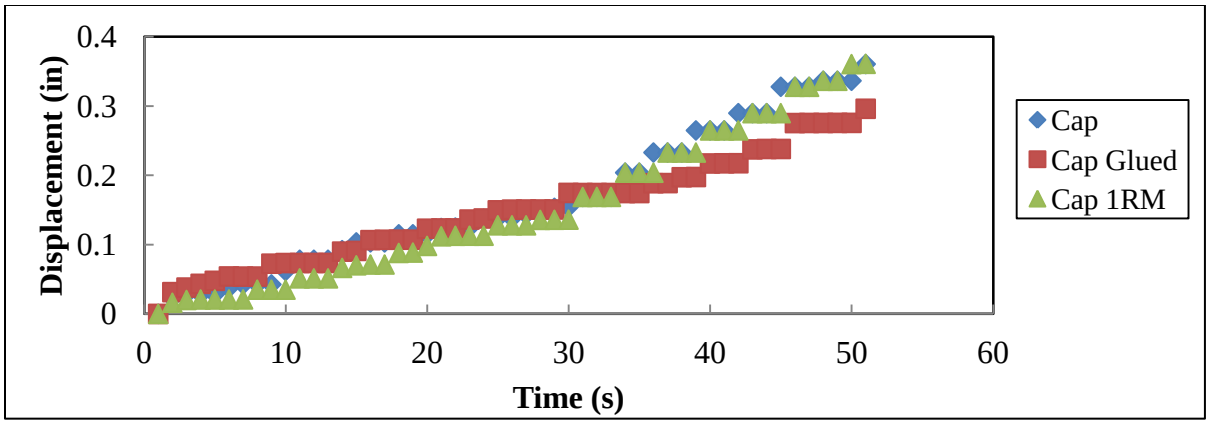

Figure 43. Displacement vs. Time - Weak and Strong Walls

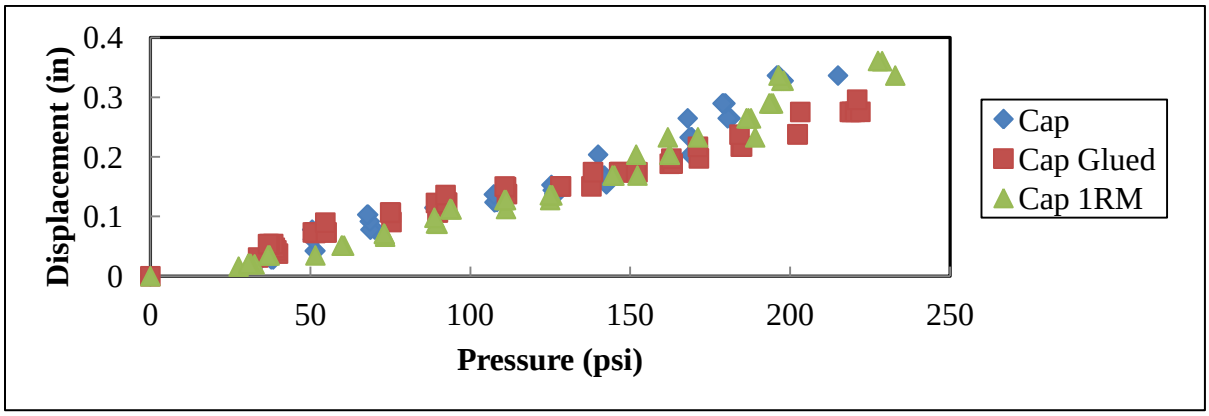

Figure 44. Pressure vs. Displacement – Weak and Strong Walls

From these results of Cap 2, the optimum scenario was undetectable due to the material resisting the hydraulic systems max load. The test for this specimen stayed within the elastic limits of the cap therefore there is no definitive evidence to lead towards a final conclusion of optimization for this specimen at this time. As the results stand the optimum chose appears to be Scenario 1 or Scenario 2 due to the even distribution of stresses throughout the cap where as the glued cap had a high concentration of stress located on the back of the cap reaching near the limits of materials elasticity.

5.3 Results of UMRCC 3 (Cap 3)

5.3.1 Cap 3 Scenarios 1 - Bond by Friction

Cap 3 shown in Figure 45. The same set of scenarios would have been conducted for this material, but due to the hydraulic systems max capacity being met during the testing of Cap 2, only the first scenario was tested to prove a major parameter of design is that of thickness to increases the moment of inertia. For the first scenario the cap was tested by solely placing the cap along the union of the two I-wall model walls. Therefore when the cap was loaded it was held in place only by the frictional coefficient between the contact points of the inner cap and wall structures. The dimensions of Cap 3 are as follows: Length of 14 inches, Height of 7.25 inches, Width of 2.3 inches, (thickness of cap perpendicular to length of wall), and a Thickness of 0.25 inches. As said previously Cap 3 has a principle direction of X or longitudinal. Cap 3 contains twice the number of ply's as of Cap 1 but contains the same sequence as Cap 1. When looking to results positive (-) is Compression and negative (+) is Tension. Characteristic of Cap 3 is that it easily slips onto model.

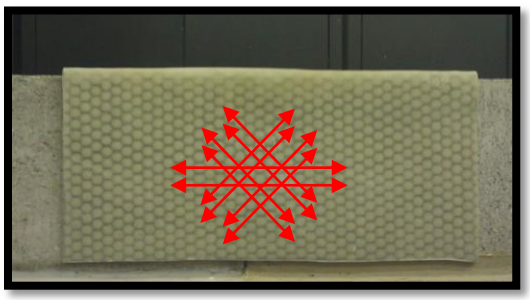

Figure 45. Cap 3 and Fiber Orientation

Table 15. Mechanical Properties of Cap 3

S./N.	Cap #	Lay up	Thickness	E^b_x (Msi)	E^b_y (Msi)	E_x (Msi)	E_y (Msi)	ν_{xy}	ν_{yx}	G_{xy} (Msi)
2	3	$[45/-45/0/0/45/-45]_2$	0.276/12	2.29	1.48	2.5	1.44	0.44	0.25	0.97

Figure 46 shows Cap 3 tested under Scenario 1, with the increase of thickness and contact surface area stress strain levels can be lowered while relative displacement of wall is lowered as well. Cap 3 is unrealistic dimensionally as a full scale solution economically when compared to Cap 1 and Cap 2.

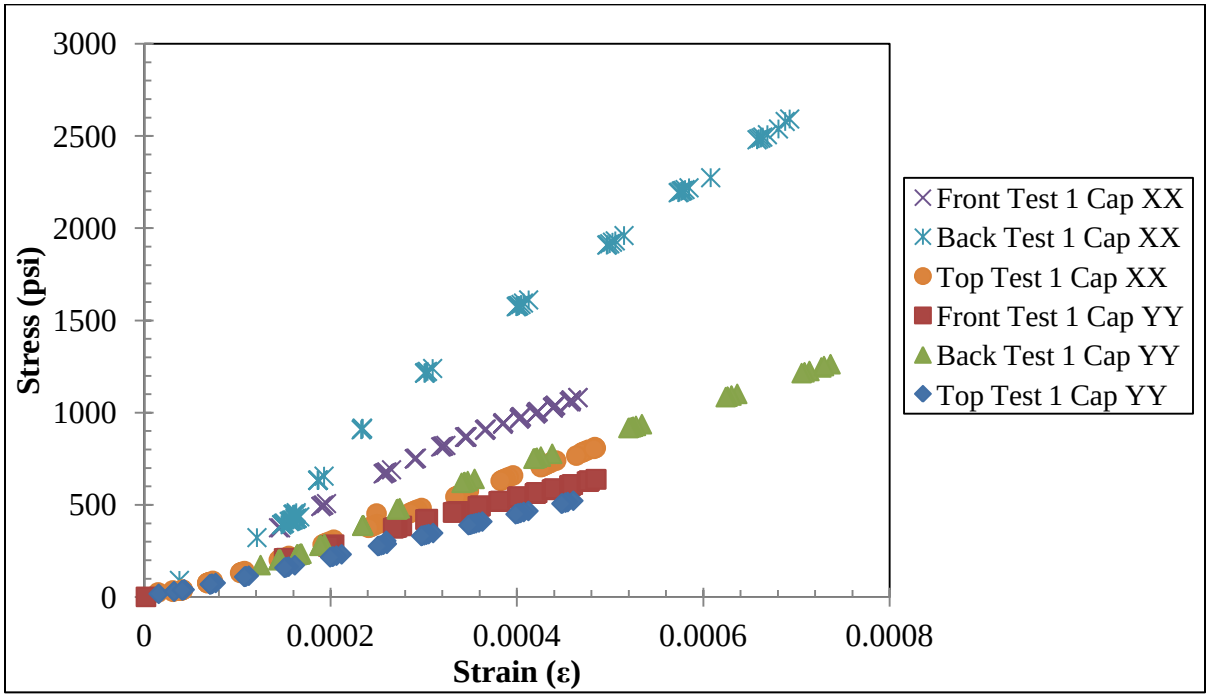

Figure 46. Stress-Strain of Cap 3

6. Numerical Analysis, Modeling, and Scalability of UMRCC's

A goal of this study was to determine if the design of a composite cap would lower the relative displacement of an I-wall and enhance the stability when subjected to loading and to also determine if there would be a scale effect with the system. There were three scaled models tested, the first being a $1/64^{th}$ model, tested by ERDC, the second an approximate $1/7^{th}$ model, test by UM, and thirdly a prediction deduced from the two sets of data, to produce a 1 to 1 scale model for application purposes. The $1/7^{th}$ model experienced discrepancies during the analysis for scalability, therefore halting any further analysis of scalability between the models. From these discrepancies the next step of action was to conduct separate parameter case studies of the $1/7^{th}$ model UMRCC's and use analytical analysis, with the understanding of dimensionless analysis and scaling laws, to evaluate the validity of a 1 to 1 model. To conduct the analytical analysis of the UMRCC's curved beam theory had to be applied to the structure.

6.1 Curved Beam Analysis

Traditional stress strain behavior cannot be analyzed through the use of beam theory for the caps used in this study. The critical locations when looking to the UMRCC's, are that of the corners. Therefore to assist in the validation of the results yielded from strain rosettes, the use of curved beam theory is required to analytically analyze these locations.

The basis behind curved beam analysis is to have the ability to determine the forces along the inner and outer surfaces of a curved material. As shown in Figure 47, the stress distribution along the cross section of the material is nonlinear in nature. This nonlinearity highly depends on the cross sectional properties of the material shown in Figure 48.

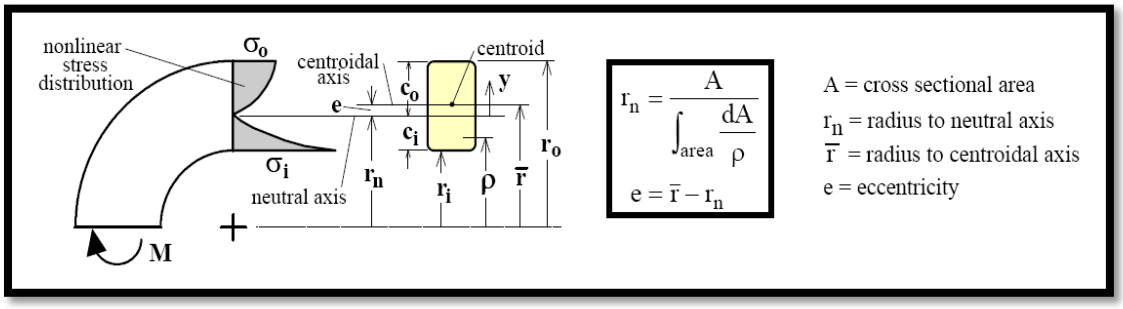

Figure 47. Curved Beam Theory Diagram (Wallace, n.d.)

Cross Section	$\bar{r}$	$\int_{area} \frac{dA}{\rho}$	A
Rectangle 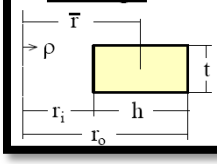	$r_i + \frac{h}{2}$	$t \cdot ln\left(\frac{r_o}{r_i}\right)$	$h \cdot t$

Figure 48. Rectangular Cross Section (Wallace n.d.)

From the cross sectional properties, Wallace (n.d.) provided three froms of stress equations; inner, outer, and any location throughout the crossection, presented in Figure 49. For the UMRCC case studies the equation σ_o was chosen. This equation was chosen due to

the location of the strain gages. Each strain gage is mounted on the outer surface as near to the curved surface as possible. Therefore the goal is to validate the experimental results with the theroretical results.

Any Position:	Inside *(maximum magnitude)*:	Outside:
$\sigma = \frac{-M \cdot y}{e \cdot A \cdot (r_n + y)}$	$\sigma_i = \frac{M \cdot c_i}{e \cdot A \cdot r_i}$	$\sigma_o = \frac{-M \cdot c_o}{e \cdot A \cdot r_o}$

Figure 49. Stress Equation for specific locations. (Wallace, n.d.)

6.1.1 Results of Curved Beam Analysis

When calculating stresses for the analytical models, the variable of moment arm length had to be estimated. The moment arm length is the length down the cap from the center of the curved beam. Due to the rotational failure mode this variable changes with load, producing a change in length, as shown in Figure 50. The range of values that were chosen, where determined by measuring the abrasion marks, made by the concrete moving down the cap, on the layer of rubber membrane during Scenario Two testing.

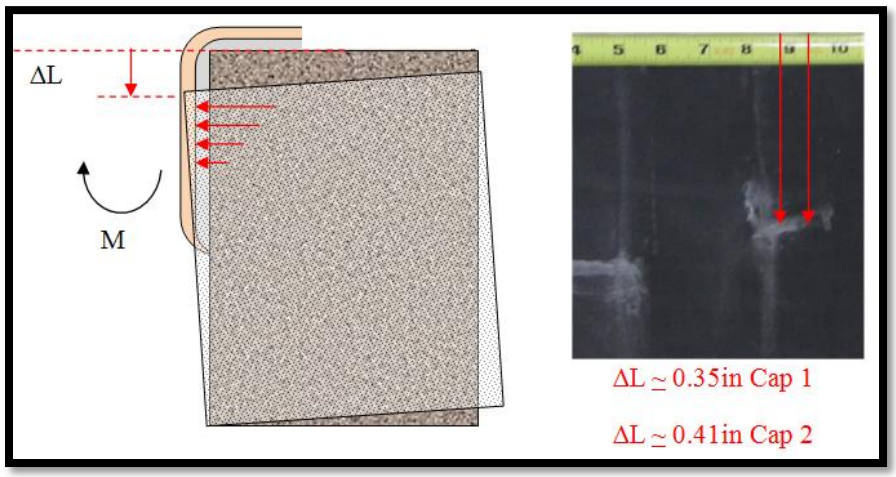

Figure 50. Change in moment arm length.

Through the use of analytical and dimensionless analysis, a prediction of the dimensions and load capacity of a scaled model can be made. Scaling laws state that stress is 1 to 1 and strain is 1 to 1 when comparing prototypes to models. Therefore when all parameters are satisfied with proper scaling, stress and strain are the same in relative to itself at different scaled levels. Scaling Laws also state that the parameter of load is a power series. Therefore when scaling load, load is denoted as N^2, where N stands of the scaled amount. For example using failure results of Cap 1 Scenario 2 averaged a failure of 142 lbs.

Using the analytical model developed for curve beam theory one can use the scaled load to predict the full scale results. Table 16 displays the results of analytical model to check its validity divide 6958 lbf by 142lbf the answer, in the case of a 1/7th scale, should be 49. Another check point is that the stress and strains carry a 1 to 1 relation relative to each other.

Table 16. Scalability of UMRCC

Predicted UM Full Scale				
Load (lbf)	**M (lb/in)**		**Strain (με)**	**Stress (psi)**
6958	17047.1		0.003539	7413.653
UM 1/7th Model				
Load (lbf)	**M (lb/in)**		**Strain (με)**	**Stress (psi)**
142	49.7		0.003539	7413.635

Figure 51 shows an example of data comparison between the analytical method and experimental method. The glued cap was selected due to clean data comparison during development of analytical model. The model can be used for all tests. There are two variables one must estimate; 1) moment arm length and 2) gap height between bottom of cap and top of wall. The moment arm length is that of the rotational displacement length of the leading edge of concrete wall down the interior of the cap.

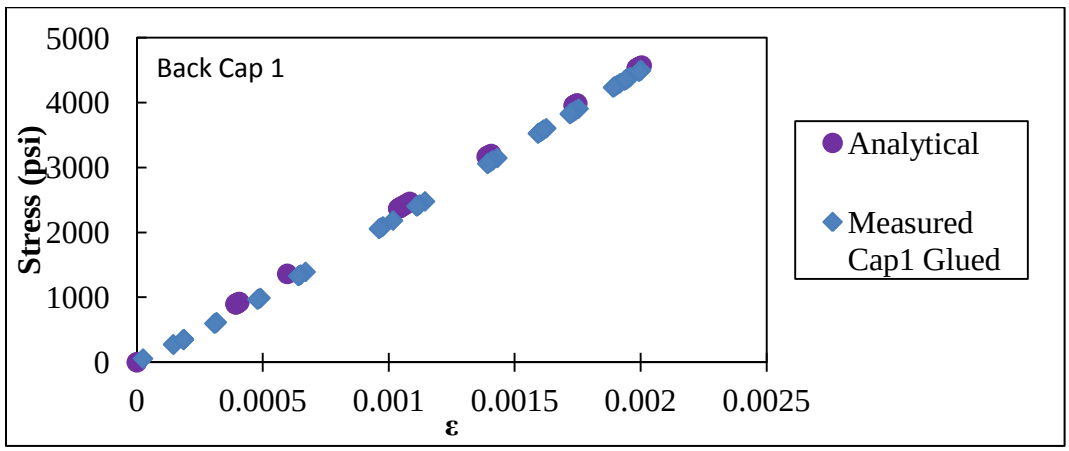

Figure 51. Analytical Model of the results of the Back of Cap 1 Glued

An example dimensional analysis:

Stress = Force / Area = ma / Lb = Mass*(Length/Time^2) / Length*Length = using Table 17.

Stress = N^3*(N/N^2) / N*N = N^4/N^4 = 1

Table 17. Scaling Laws (Balkema, 1988)

Quantity	*Prototype*	*Model*
Length	N	1
Area	N^2	1
Volume	N^3	1
Velocity	1	1
Acceleration	1	N
Mass	N^3	1
Force	N^2	1
Stress	1	1
Strain	1	1
Mass Density	1	1
Energy Density	1	1
Time (Dynamic)	N	1
Time (Diffusion)	N^2	1
Time (Creep)	1	1
Frequency	1	N

7. Final Report of Finite Element modeling conducted by UM

Researchers at the University of Mississippi conducted a multitude of experiments using Finite Element analysis and centrifugal (1/64th model) tests, to determine the results and possibilities of dimensional optimization of applied full scaled composite cap prototypes. Experimental systems were setup to mimic Hurricane Katrina conditions as similarly as possible. The dimensions of each I-wall in the London Avenue canal area are as follows: Length = 24ft, Base/Width of Top of Wall= 1ft, Height=13.8ft (Song 2012). The cross section of the prototype and typical I-wall design is shown in Figure 52.

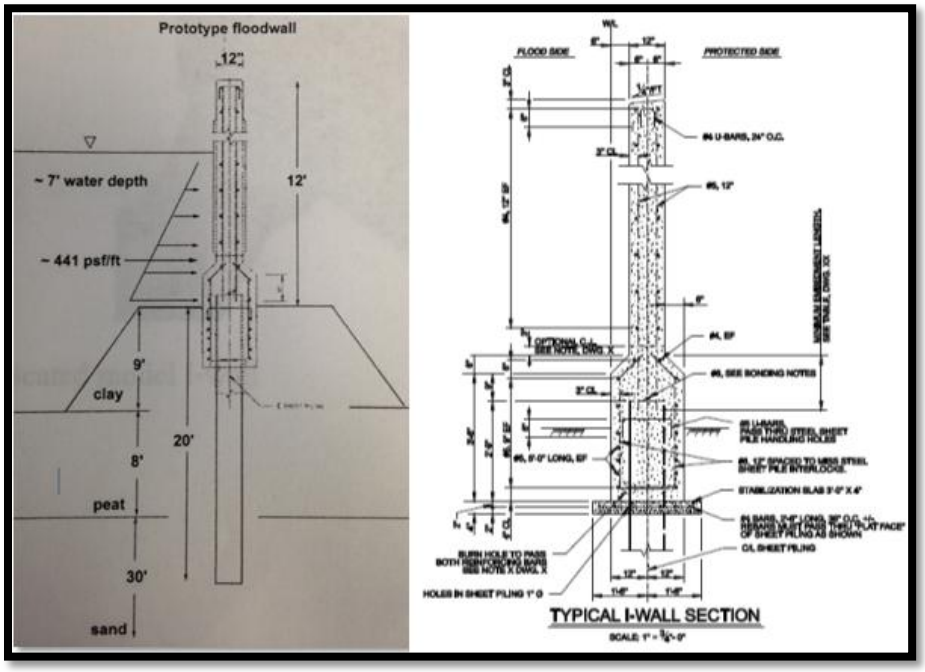

Figure 52. Typical I-wall design and Prototype design. (Song 2012)

7.1 ERDC – 1/64th Tests

ERDC's centrifuge shown Figure 54 is has the capability of reaching 150g's. For the following experiments the max load applied was 100g's. The logic behind centrifugal data is that when model is scaled properly, for example 1/64th and experimental apparatus is placed in the centrifuge and accelerated to 64g's the model should experience similar properties of that of a full scale prototype. Though many times when moving from model to prototype a scale effect is notice. The data recorded during test was smoothed and displayed using D-Plot. D-Plot is specialized engineering software that can handle massive amounts of data in 2D and 3D.

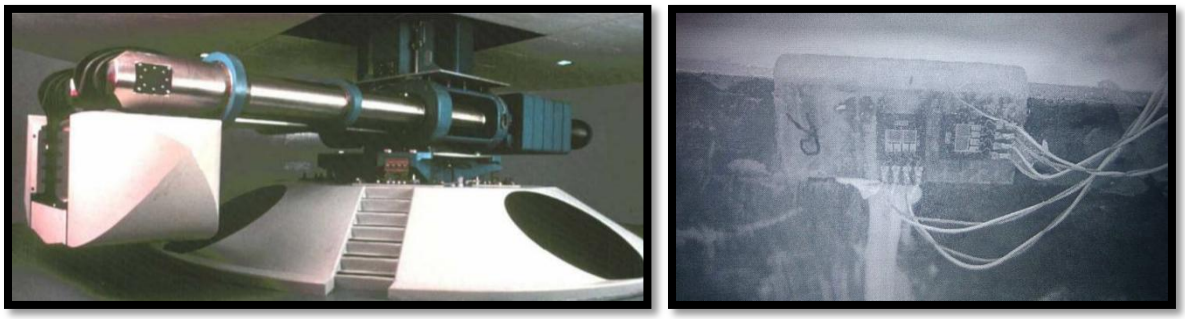

Figure 53. ERDC Centrifuge and 1/64th model Cap

Data reduction is shown in Figure 54. Each rectangular strain gauge was labeled in reference to wall connection point (S) and each side of wall (D and R). D stands for *Dry/Protected Side* and R stands for *River Side*. The connection points were labeled S(1-3) and walls were labeled D(5-8) and R(1-4). The recorded data was plotted as strain vs. time, the test reached 64g's at approximately 1150 seconds. The test was run up to 100g's with no failure. The total relative wall displacement of the right and left sides were approximately 7.5 mm. Please see Table 4 for mechanical properties of ERDC caps.

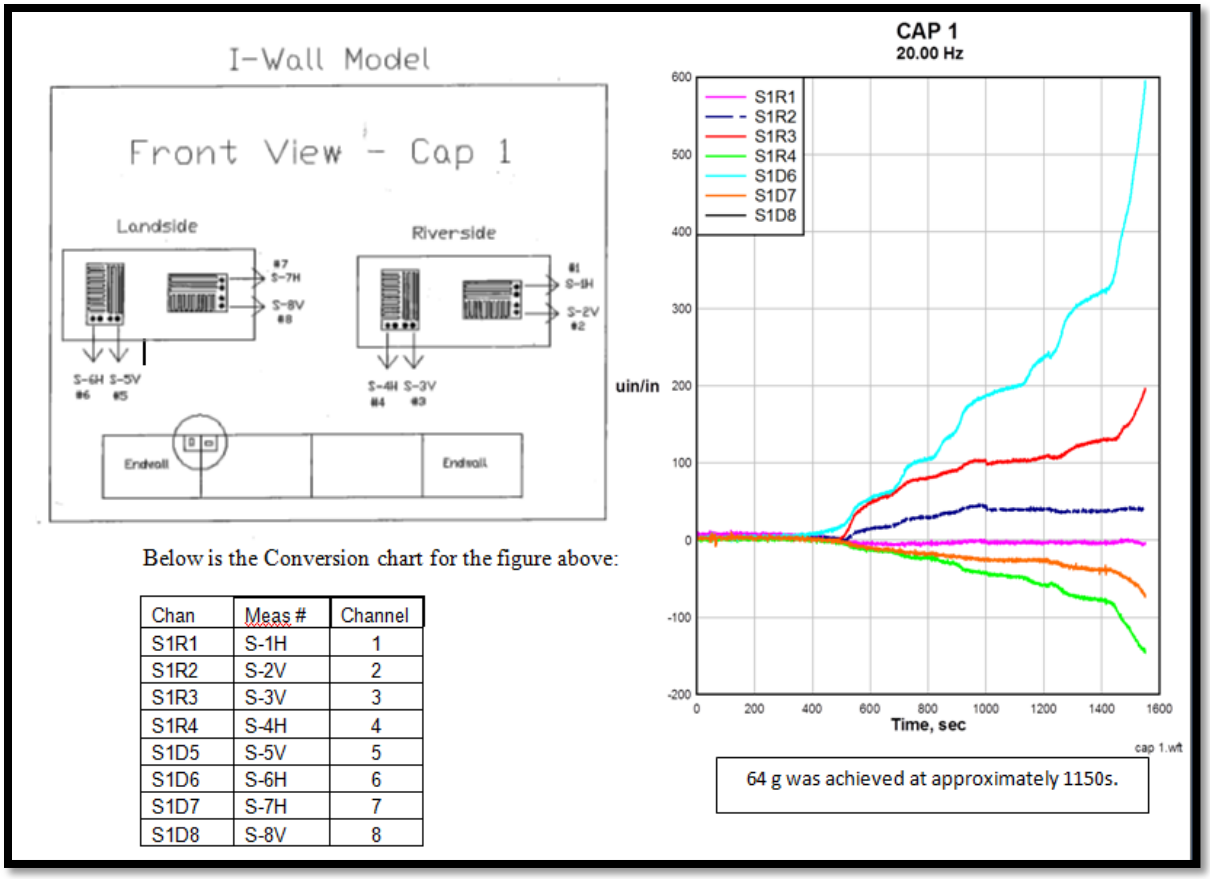

Chan	Meas #	Channel
S1R1	S-1H	1
S1R2	S-2V	2
S1R3	S-3V	3
S1R4	S-4H	4
S1D5	S-5V	5
S1D6	S-6H	6
S1D7	S-7H	7
S1D8	S-8V	8

Figure 54. ERDC Result of Cap at location 1.

7.2 Scale Effect

The question at hand is that do material properties change with scale? For the case of elastic modulus the answer is for the most part no. When looking to a very small scale a variance in modulus will be apparent but when multiple readings have been taken over a respectable grid the average of the modulus's will be equivalent to the full scale modulus.

However scale effects are apparent in the strength of a composite and rely heavily on the quality of manufacturing. Wisnom (1999) stated that defects exist in the microstructure of the material, for example; flaws in the fibres and matrix. Multiple publications have concurred that scale effect has been noticed in tensile and flexural test, and produces a larger strength in bending rather than tension Wisnom (1999). Wisnom (1999) also states that there are indications that tension diminishes with the increase in scale. Tests results yielded a decrease in strength when specimen was scaled up when manufacturing process and test configurations wee identical Wisnom (1999). Sutherland et al. (1998) agrees that size effect in respect to strength is a main priority of understanding scaled modeling, but an accurate understanding of such size effects, such as defects in the fibre and/or matrix have proven to be a complex task to quantify. To quantify size effect one must conduct multiple scaled test and derive an equation from the corresponding results. The yielded equations will allow for better understanding of material behavior to assist in a prediction of full scale prototype behaviors.

7.3 UM Model Results

The following section will discuss results yielded form finite element simulations, conducted by the University of Mississippi. To simplify boundary conditions UM Researchers did not take the steel pile and soil into consideration. Springs were added to the system to control the boundary conditions of interactions between the wall, soil, and pile. Details can be found in Song et al. (2012).

Shown in Figure 55 is the flow chart used in the optimization of the composite cap. By varying the material and geometry parameters and comparing those parameters to the maximum allowed relative displacement one can conduct a parametric investigation that will determine the optimum cap. These models where tested similarly to Scenario 1 where the cap is being held by friction between the cap and concrete I-wall. Song et al. (2012) also agree that the addition of rubber may assist in the reduction of the cap failing due slipping off.

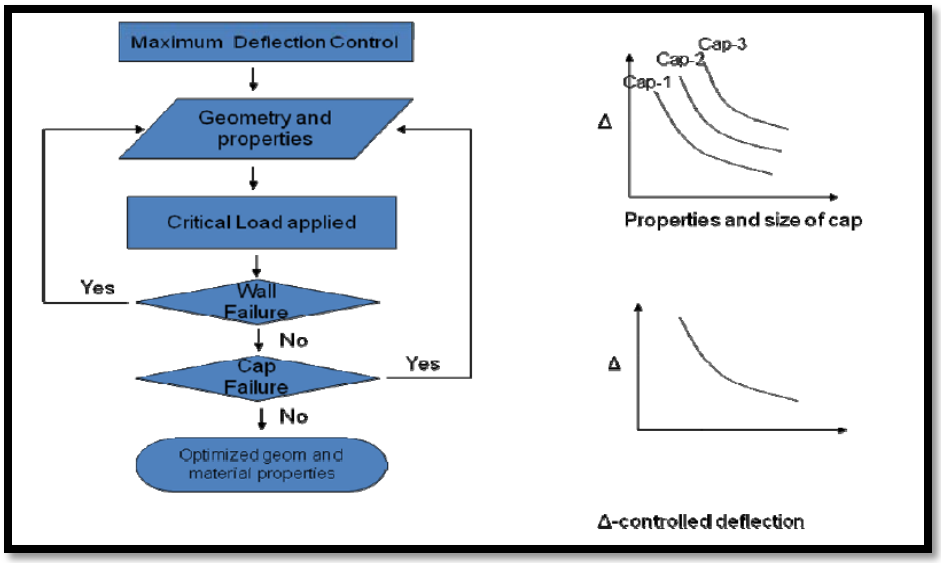

Figure 55. Cap Optimization Flow Chart (Song 2012)

Song et al. (2012) determined the maximum magnitude of hydrostatic pressure to occur at 9.8ft, at a pressure of 611.79 lbf/ft^2. The composite lay-up tested is shown in Figure 56. Multiple test of modified test specimens were conducted with two thicknesses 20 ply and 40 ply. Variables modified were as follows: Length, Height, Thickness, Material properties (PVC, E-glass, and Graphite), and soil stiffness. The objective of this particular study was to determine the deformation on the top of the floodwall and the relative displacement between adjacent floodwalls Song et al. (2012).

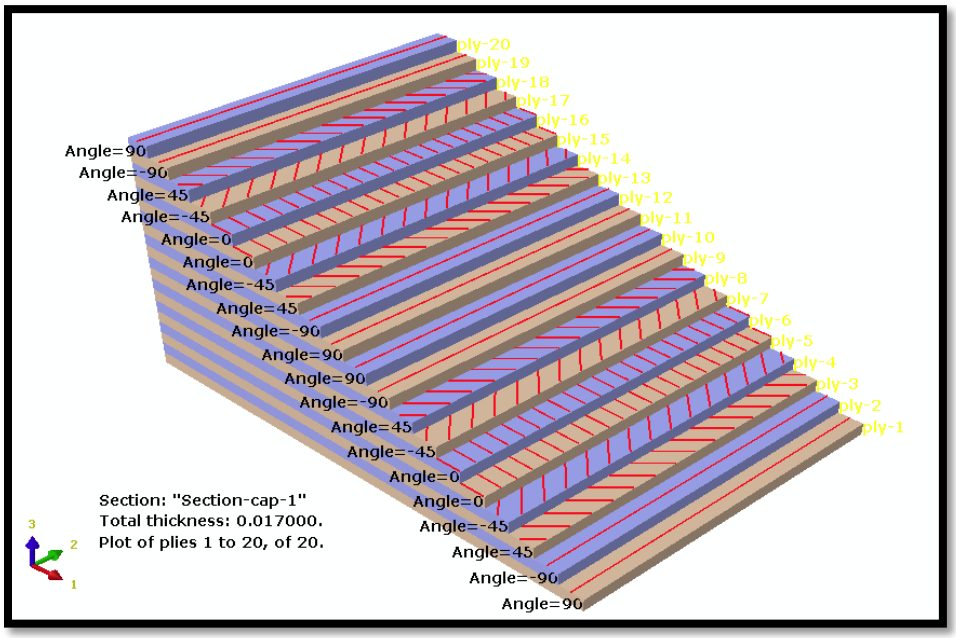

Figure 56. Composite Cap Fiber Orientations 20-ply. (Song 2012)

Looking to the results of the E-glass polymer test, shown in Figure 57, the simulation results yield a range from (0.15 ft-0.195 ft) when loaded at 611.79 lbf/ft^2. When comparing results separating the data into two separate groups due to soil stiffness. It appears that in both groups the 2L-2t-H prevailed with the lowest displacements.

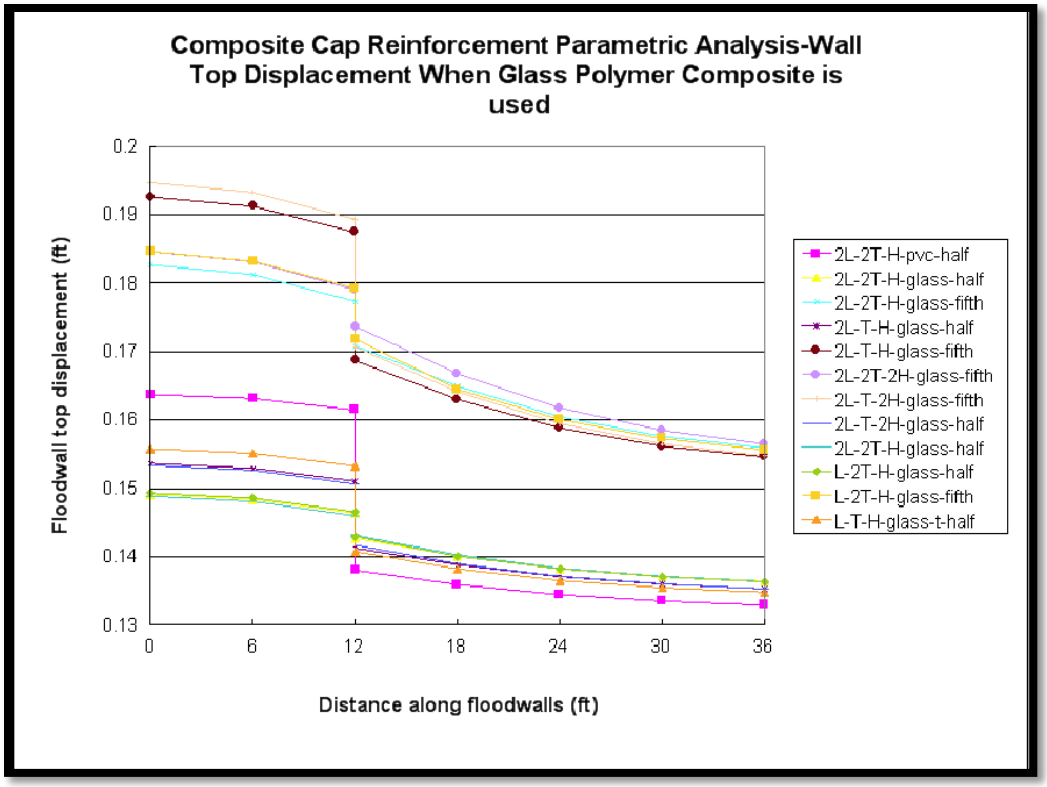

Figure 57. Displacement of top of wall with E-glass polymer Song et al. (2012)

8. Conclusion

The motivation of these studies was to ultimately determine if the introduction of retrofitted composite caps would lower the overall relative displacement of I-walls without the consideration of additional displacement due to the formation of the gap when subjected to extreme conditions.

The results yield that when an optimum cap is designed so that the cap is strong enough to resist movement yet large enough to contain the proper contact surface area to not damage the concrete wall, then this technique is a viable and economic solution.

Some of the major findings during this study are as follows:

- Fiber orientation, length and thickness play major roles in governing the strength of the material and floodwall displacement. Where thickness holds the most importance followed by orientation and length.
- The height of the cap is relatively insignificant, due to the effective contact area.
- The cap experienced both flexural and torsional components.
- When scaling one must use proper scaling techniques such that all parameters are scaled homogenously. If comparing to dissimilar objects scaling becomes not viable or an improbable method prone to error.

- Application method, friction and rubber with no mount points to composite are not recommended, an adhesive bond bonding cap to wall is recommended to keep the cap in place from flying off during extreme loading.
- Application of the cap can reduce relative displacement by 70%+
- When the composite cap is bonded to the wall with GE Silicone, fatigue and damage of silicone was apparent in the results. Cap 1 was not damaged between test one and two but was damaged by 6% between test two and three. Cap 2 was damaged by 17% between test one and two and was damaged by 22% between test two and three. Therefore Cap 2 had a 36% loss in strength in three tests.
- The relative displacement of the walls with Cap 2 matched up well with the Finite Element full scale model. Cap 2 averaged .145ft at full scale while the FE model predicted and average of 0.17ft.
- Modeling with FE software is very complicated when signifying contact parameters for this application due to the interactions between surfaces.

In the future, know that there is a better understanding of fiber orientation and geometrical properties a proper scaled model should be constructed with steel or aluminum plate similarly to that of ERDC's $1/64^{th}$ model study to verify results. This model should be constructed with springs to simulate soil properties and multi sized caps with same property configuration to validate an optimum geometry. Also the hydraulic system should have the ability to rotate freely in the Z direction on both ends so that the resultant force will imitate that of a falling wall with changing resultant force angle. Aluminum or steel would be preferred due to the scale. Scaling concretes aggregates so that one can achieve similar

moduli and strength parameters can be difficult. Therefore steel or aluminum would provide the ease and accuracy of scaling and application of gauges. Simulations can be conducted similarly to the ones conducted in Song et al. (2012) to determine the proper geometrical contact area and stiffness of cap needed to not structurally damage the concrete. Once geometry and stiffness are concluded on one can use this steel/aluminum setup to determine the optimum fiber matrix combination.

List of References

- ASTM D3039/D 3039M-00 (2006),” Standard Test Method for Tensile Properties of Polymer Matrix Composite Materials”, ASTM International.
- Brandon, T. L., Wright, S. G., and Duncan, J. M. _2008_. “Analysis of the stability of I-walls with gaps between the I-wall and levee fill.” J. Geotech. Engrg., 134_5_, 692–700.
- Dally, J.W., & William, F.R., “Chapter 9: Strain-Analysis Methods,” Experimental Stress Analysis, 3rd ed., McGraw-Hill, Boston, 1993, p.313-315.
- Duncan, J. M., Brandon, T. L., Wright, S. G., and Vroman, N. _2008_. “Stability of I-walls in New Orleans during Hurricane Katrina.” J. Geotech. Engrg., 134_5_, 681–691.
- G. L. Sills, P.E., M.ASCE; N. D. Vroman, P.E.; R. E. Wahl, P.E., M.ASCE; and N. T. Schwanz, P.E.(2008) “Overview of New Orleans Levee Failures: Lessons Learned and Their Impact on National Levee Design and Assessment”.
- GE Window & Door Supreme Silicone. Momentive Performance Materials Inc.,2006-2009, http://www.caulkyourhome.com/ge-silicone-II-window-and-door-supreme.php,
- Graumann, Axel, et al. Hurricane Katrina: a climatological perspective: preliminary report. US Department of Commerece, National Ocanic and Atmospheric Administration, National Environmental Satellite Data and Information Service, National Climatic Data Center, 2006.
- Graumann, A., Houston, T., Lawrimore, J., Levinson, D., Lott, N., McCown, S., Stephens, S., Wuertz, D., 2005. Hurricane Katrina: a climatological perspective,

preliminary report. Technical Report 2005-01. U.S. Department of Commerce, National Oceanic and Atmospheric Administration, Washington, DC.

- Interagency Performance Evaluation Task Force IPET. 2007. “Performance evaluation of the New Orleans and southeast Louisiana hurricane protection system.”
- Interagency Performance Evaluation Task Force IPET. 2007, Final Rep. of the Interagency Performance Evaluation Task Force, U.S. Army Corps of Engineers, https://ipet.wes.army.mil.
- Jackson, R. B. _1988_. “E-99 sheet pile wall, field load test report.” Technical Rep. No. 1, U.S. Army Engineer Division, Lower Mississippi Valley, Vicksburg, Miss.
- Mantena, P. Raju, Tadepalli, Tezeswi. “Shear Properties of Laminated Composite Specimens by ARCAN Test Method.” University of Mississippi, Dept. Mechanical Engr. Pg(6,9)
- Mantena, P. Raju., Tadepalli, Tezeswi., Stoddard, Damian., “Tensile Properties of Laminated Composite Specimens.” University of Mississippi, Dept. Mechanical Engr. Pg(6,8-11)
- MicroMeasurements Group Technical Note TN-509, “Transverse Sensitivity Errors,” Measurements Group, Inc., 1993.
- MTS Systems Corporation (2007), “MTS User manual, Load Unit 318.10” 14000 Technology Drive Eden Prairie, Minnesota 55344-2290 USA
- Nelson, S.A., 2012, Why New Orleans is Vulnerable to Hurricanes Geologic and Historical Factors, http://www.tulane.edu/~sanelson/New_Orleans_and_Hurricanes/New_Orleans_Vulnerability.htm,Tulane University , (January 15, 2013)

- Rocscience, Inc. _2005_. “Slide v5.0–2D limit equilibrium slope stability analysis.” Toronto.
- Ronald B. Bucinell, Ph.D., P.E., “Calculating Principal Strains using a Rectangular Strain Gage Rosette”, Union College, Department of Mechanical Engineering Schenectady, NY 12308
- Shan, L., & Qiao, P. (2005). Flexural–torsional buckling of fiber-reinforced plastic composite open channel beams. *Composite structures*, *68*(2), 211-224.
- Song, Chung R., Cheng, Alexander., Al-Ostaz., Ahmed, Mantena, Raju. 2012. “Structural, Material, and Geotechnical Solutions to Levee and Floodwall Construction and Retrofitting.” SERRI Report 70023,. School of Engineering University of Mississippi., 34-50.
- The Louisiana Department of Transportation and Development , 2006, Hurricane Katrina and Ser Surge, Chapter 2, http://www.dotd.louisiana.gov/administration/teamlouisiana/team%20louisiana%20-%20part%20i,%20chap%202.pdf , (November,2012)
- Vipulanandan,C.,Ph.D., P.E.(2006), “Lessons Learned From Failures Due To Hurricanes Katrina And Rita”. Department of Civil and Environmental Engineering, University of Houston, Houston, TX
- Wikipidia contributors, 2013, New Orleans Outfall Canals, http://en.wikipedia.org/w/index.php?title=New_Orleans_Outfall_Canals&oldid=551325431 , (2013)
- Wright, S. G. _1999_. “UTEXAS4 - A computer program for slope stability calculations.” Shinoak Software, Austin, Tex.

Appendix A

University of Mississippi Levee Test Fixture

Manufactured by CEC

UNIVERSITY OF MISSISSIPPI

LEVEE TEST FIXTURE
CEC PROJECT #2010_3801

REFERENCE MANUAL

a division of
Cooper Electrical Controls, Inc.

Electrical Controls & Automation | Production Metal Processing | Machine Design & Build | Custom Security Solutions

928 Sam T. Barkley Drive PO Box 338 New Albany, MS 38652 Office: 662.534.4457 Fax: 662.534.4498 www.cecontrols.com

Honeywell

2080 Arlingate Lane
Columbus, Ohio 43228 U.S.A.
Phone: 614-850-5000
Toll free: 800-848-6564
Fax: 614-850-1111
www.honeywell.com/sensotec
sensotec.service@honeywell.com

CERTIFICATE OF CALIBRATION

Product Identification

Product Type:	LOAD	Part No.:	060-0238-07
Model:	53	Order Code:	AL131CV,1A,2U,6E,15C
Serial No.*:	1315419	Instrument Serial No.:	N/A

* A letter at the end of the serial number indicates the associated bridge.

Product Specifications

Capacity:	1000lbs	Excitation:	10.0 Vdc
Calibrated At:	1000.00lbs	Amplifier Output:	N/A
Direction / Type:	Compression	Electrical Leakage:	∞ MegΩ

Calibration Data

Shunt Cal Factor:	1.4950 mV/V	Input Resistance:	380 Ω	Calibration Factor:	1.8349mV/V
Shunt Cal Resistor:	59K Ω	Output Resistance:	354 Ω	Calibration Date:	09/14/2010

Calibration Procedure: 072-LC75-10, Rev -, Date 02/19/2008

Wiring Code

UNAMP#1,4-COND,CBL

COLOR	DESIGNATION
RED	(+)EXCITATION
BLACK	(-)EXCITATION
GREEN	(-)OUTPUT
WHITE	(+)OUTPUT

001-0333-01

Calibration Data

% Capacity	Load (lbs)	Raw (mV/V)	Normalized (mV/V)
0	0.00	-0.0154	0.0000
50	500.00	0.9017	0.9171
100	1000.00	1.8192	1.8346
50	500.00	0.9032	0.9186
0	0.00	-0.0153	0.0001

Environmental Data

Temperature: 74 °F Humidity: 43 %RH Pressure: 14.18 psiA

This unit has been calibrated using standards whose accuracies are traceable to the National Institute of Standards and Technology (NIST). Units are calibrated based upon ANSI/NCSL Z540 on equipment whose accuracies are within a 4:1 ratio unless otherwise indicated. Reported values may be scaled due to limitations st equipment such as dead weight increments or local barometric pressure. This certificate of calibration shall not be reproduced in any form, except in full, without the expressed written consent of Honeywell. If you have any questions concerning this certificate of calibration, please call our service department at (614) 850-5000.

Certificate No

Esztr Gozon

Esztr Gozon, Quality Manager

1315419-001

PRINT DATE: 9/14/2010

Document No. 086-1000-01

Honeywell

2080 Arlingate Lane
Columbus, Ohio 43228 U.S.A.
Phone: 614-850-5000
Toll free: 800-848-6564
Fax: 614-850-1111
www.honeywell.com/sensotec
sensotec.service@honeywell.com

CERTIFICATE OF CALIBRATION

Product Identification

Product Type:	LOAD	Part No.:	060-0238-07
Model:	53	Order Code:	AL131CV,1A,2U,6E,15C
Serial No.*:	1315418	Instrument Serial No.:	N/A

* A letter at the end of the serial number indicates the associated bridge.

Product Specifications

Capacity:	1000lbs	Excitation:	10.0 Vdc
Calibrated At:	1000.00lbs	Amplifier Output:	N/A
Direction / Type:	Compression	Electrical Leakage:	∞ MegΩ

Calibration Data

Shunt Cal Factor:	1.4876 mV/V	Input Resistance:	379 Ω	Calibration Factor:	2.0086mV/V
Shunt Cal Resistor:	59K Ω	Output Resistance:	354 Ω	Calibration Date:	09/14/2010

Calibration Procedure: 072-LC75-10, Rev -, Date 02/19/2008

Wiring Code

UNAMP#1,4-COND,CBL

COLOR	DESIGNATION
RED	(+)EXCITATION
BLACK	(-)EXCITATION
GREEN	(-)OUTPUT
WHITE	(+)OUTPUT

001-0333-01

Calibration Data

% Capacity	Load (lbs)	Raw (mV/V)	Normalized (mV/V)
0	0.00	0.0118	0.0000
50	500.00	1.0173	1.0055
100	1000.00	2.0195	2.0077
50	500.00	1.0175	1.0057
0	0.00	0.0119	0.0001

Environmental Data

Temperature: 74 °F Humidity: 43 %RH Pressure: 14.18 psiA

This unit has been calibrated using standards whose accuracies are traceable to the National Institute of Standards and Technology (NIST). Units are calibrated based upon ANSI/NCSL Z540 on equipment whose accuracies are within a 4:1 ratio unless otherwise indicated. Reported values may be scaled due to limitations ist equipment such as dead weight increments or local barometric pressure. This certificate of calibration shall not be reproduced in any form, except in full, without the expressed written consent of Honeywell. If you have any questions concerning this certificate of calibration, please call our service department at (614) 850-5000.

Eszter Gozon, Quality Manager

Certificate No

1315418-001

PRINT DATE: 9/14/2010

Document No. 086-1000-01

Honeywell

2080 Arlingate Lane
Columbus, Ohio 43228 U.S.A.
Phone: 614-850-5000
Toll free: 800-848-6564
Fax: 614-850-1111
www.honeywell.com/sensotec
sensotec.service@honeywell.com

CERTIFICATE OF CALIBRATION

Product Identification

Product Type:	LOAD	Part No.:	060-0238-07
Model:	53	Order Code:	AL131CV,1A,2U,6E,15C
Serial No.*:	1315420	Instrument Serial No.:	N/A

* A letter at the end of the serial number indicates the associated bridge.

Product Specifications

Capacity:	1000lbs	Excitation:	10.0 Vdc
Calibrated At:	1000.00lbs	Amplifier Output:	N/A
Direction / Type:	Compression	Electrical Leakage:	∞ MegΩ

Calibration Data

Shunt Cal Factor:	1.4961 mV/V	Input Resistance:	379 Ω	Calibration Factor:	1.8728mV/V
Shunt Cal Resistor:	59K Ω	Output Resistance:	354 Ω	Calibration Date:	09/14/2010

Calibration Procedure: 072-LC75-10, Rev -, Date 02/19/2008

Wiring Code

UNAMP#1,4-COND,CBL

COLOR	DESIGNATION
RED	(+)EXCITATION
BLACK	(-)EXCITATION
GREEN	(-)OUTPUT
WHITE	(+)OUTPUT

001-0333-01

Calibration Data

% Capacity	Load (lbs)	Raw (mV/V)	Normalized (mV/V)
0	0.00	-0.0255	0.0000
50	500.00	0.9095	0.9350
100	1000.00	1.8477	1.8732
50	500.00	0.9114	0.9369
0	0.00	-0.0254	0.0001

Environmental Data

Temperature: 74 °F Humidity: 43 %RH Pressure: 14.18 psiA

This unit has been calibrated using standards whose accuracies are traceable to the National Institute of Standards and Technology (NIST). Units are calibrated based upon ANSI/NCSL Z540 on equipment whose accuracies are within a 4:1 ratio unless otherwise indicated. Reported values may be scaled due to limitations of test equipment such as dead weight increments or local barometric pressure. This certificate of calibration shall not be reproduced in any form, except in full, without the expressed written consent of Honeywell. If you have any questions concerning this certificate of calibration, please call our service department at (614) 850-5000.

Esther Gocon

Esther Gocon, Quality Manager

Certificate No.

1315420-001

PRINT DATE: 9/14/2010

Document No. 086-1000-01

Honeywell

2080 Arlingate Lane
Columbus, Ohio 43228 U.S.A.
Phone: 614-850-5000
Toll free: 800-848-6564
Fax: 614-850-1111
www.honeywell.com/sensotec
sensotec.service@honeywell.com

CERTIFICATE OF CALIBRATION

Product Identification

Product Type:	LOAD	Part No.:	060-0238-07
Model:	53	Order Code:	AL131CV,1A,2U,6E,15C
Serial No.*:	1315421	Instrument Serial No.:	N/A

* A letter at the end of the serial number indicates the associated bridge.

Product Specifications

Capacity:	1000lbs	Excitation:	10.0 Vdc
Calibrated At:	1000.00lbs	Amplifier Output:	N/A
Direction / Type:	Compression	Electrical Leakage:	∞ MegΩ

Calibration Data

Shunt Cal Factor:	1.4927 mV/V	Input Resistance:	379 Ω	Calibration Factor:	1.9201mV/V
Shunt Cal Resistor:	59K Ω	Output Resistance:	354 Ω	Calibration Date:	09/14/2010

Calibration Procedure: 072-LC75-10, Rev -, Date 02/19/2008

Wiring Code

UNAMP#1,4-COND,CBL

COLOR	DESIGNATION
RED	(+)EXCITATION
BLACK	(-)EXCITATION
GREEN	(-)OUTPUT
WHITE	(+)OUTPUT

001-0333-01

Calibration Data

% Capacity	Load (lbs)	Raw (mV/V)	Normalized (mV/V)
0	0.00	-0.0120	0.0000
50	500.00	0.9473	0.9593
100	1000.00	1.9089	1.9209
50	500.00	0.9472	0.9592
0	0.00	-0.0119	0.0001

Environmental Data

Temperature: 74 °F Humidity: 43 %RH Pressure: 14.18 psiA

This unit has been calibrated using standards whose accuracies are traceable to the National Institute of Standards and Technology (NIST). Units are calibrated based upon ANSI/NCSL Z540 on equipment whose accuracies are within a 4:1 ratio unless otherwise indicated. Reported values may be scaled due to limitations ...st equipment such as dead weight increments or local barometric pressure. This certificate of calibration shall not be reproduced in any form, except in full, ...thout the expressed written consent of Honeywell. If you have any questions concerning this certificate of calibration, please call our service department at (614) 850-5000.

Ezster Gozon, Quality Manager

Certificate No
1315421-001

PRINT DATE: 9/14/2010

Document No. 086-1000-01

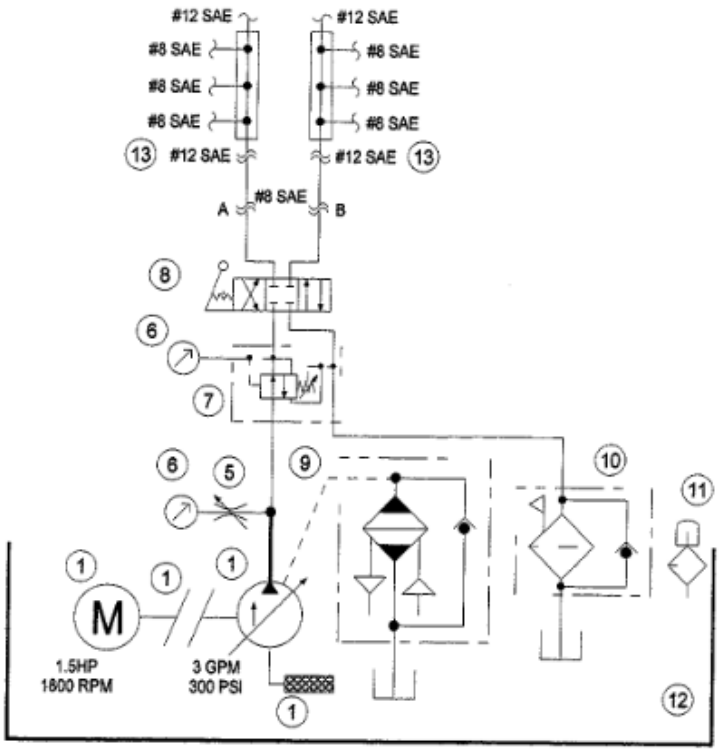

ITEM	QUAN	PART NUMBER	DESCRIPTION
1	1	TM1.5-18-145TC	TORQUEMASTER 1PHZ ELECTRIC MOTOR
2	1	M056422A	MAGNALOY PUMP/MOTOR ADAPTER
2A	1	M100-20806	MAGNALOY FLEXIBLE DRIVE COUPLING
2B	1	M100-01604	MAGNALOY FLEXIBLE DRIVE COUPLING
2C	1	M170-N6	MAGNALOY COUPLING INSERT
3	1	PVER-3B05-RF-0-1N	CONTINENTAL VARIABLE VANE PUMP
4	1	PSS5	VESCOR SUCTION STRAINER
5	1	NSAB-KXV-BA	SUN GAUGE CUT-OFF VALVE
6	2	25.300-0-600	NOSHOK PRESSURE GAUGE
7	1	PPDB-KDN-EBP	SUN D03 SAND REDUCING/REL VALVE
8	1	VMD03M-4A-G-10	CONTINENTAL D03 DIRECTIONAL VALVE
8A	1	AD03-SP-S-8S	DAMAN D03 SUBPLATE
9	1	AO-1-61231	THERMAL TRANSFER A/O COOLER
10	1	MTA-3TAZ10-S8-Y2C	SCHROEDER HYD RETURN FILTER
11	1	ABF3/10-S	SCHROEDER FILLER/BREATHER ASSY
12	1	10010	VESCOR 10GAL JIC RESERVOIR
*13	2	AH-000-03-08S	DAMAN HEADER BLOCK

* INDICATES ITEM SHIPPED LOOSE FOR CUSTOMER INSTALLATION

ranklin Electrofluid Co., Inc.

Memphis TN 1-800-238-7500
Little Rock AR Harahan LA
Fort Smith AR Shreveport LA
Jackson MS

DESIGNED FOR
COOPER ELECTRICAL CONTROLS

DATE	SERIAL NUMBER
09/15/10	7-610RF1-Z

DRAWING
7610RF1Z/CIR-DIRS

REVISION

Performance Data:

HP	RPM	Frame Size	Full Load Current At 230V (A)	Full Load Current At 460V (A)	Full Load Torque (Lb. Ft.)	Locked Rotor Torque (%)	Breakdown Torque (%)	Efficiency			Power Factor			Service Factor	Approximate Weight (Lb.)
								100	75	50	100	75	50		
1	1800	143TC	3.0	1.5	3.00	260%	350%	84.0%	83.0%	79.4%	0.71	0.63	0.44	1.15	58
1.5	1800	145TC	4.2	2.1	4.41	240%	320%	85.5%	85.6%	83.5%	0.74	0.66	0.54	1.15	60
2	1800	145TC	5.4	2.7	6.05	240%	260%	85.5%	86.0%	85.0%	0.77	0.70	0.58	1.15	70
3	1800	182TC	7.7	3.9	9.07	280%	330%	88.5%	88.1%	86.3%	0.81	0.75	0.63	1.15	90
5	1800	184TC	11.8	5.9	15.10	240%	310%	88.5%	89.0%	88.6%	0.83	0.78	0.66	1.15	110
7.5	1800	213TC	18.6	9.3	22.00	200%	330%	90.2%	90.6%	89.1%	0.81	0.75	0.64	1.15	160
10	1800	215TC	24.8	12.4	30.10	200%	300%	90.2%	90.6%	90.0%	0.83	0.76	0.66	1.15	180
15	1800	254TC	35.4	17.7	43.70	170%	270%	91.7%	90.5%	89.5%	0.84	0.81	0.72	1.15	325
20	1800	256TC	47.6	23.8	59.70	170%	240%	91.7%	91.5%	91.2%	0.84	0.82	0.75	1.15	370
25	1800	284TC	56.4	28.2	73.60	170%	290%	93.0%	93.5%	93.0%	0.87	0.86	0.79	1.15	420
30	1800	286TC	67.2	33.6	87.40	170%	270%	93.0%	93.2%	92.0%	0.88	0.86	0.80	1.15	470
40	1800	324TC	93.0	46.5	119.00	190%	300%	93.6%	94.0%	93.3%	0.86	0.83	0.75	1.15	590
50	1800	326TC	114.6	57.3	147.00	180%	290%	93.6%	93.8%	93.4%	0.86	0.83	0.75	1.15	650
60	1800	364TC	139.4	69.7	179.00	180%	260%	94.1%	94.3%	93.7%	0.85	0.83	0.77	1.15	780
75	1800	365TC	172.8	86.4	221.00	180%	250%	94.5%	94.7%	94.0%	0.84	0.83	0.76	1.15	870
100	1800	405TC	230.0	115.0	296.00	180%	260%	95.0%	95.3%	93.4%	0.87	0.86	0.80	1.15	1350

Appendix B

Micro-Measurements P3 Strain Indicator and Recorder

P3

Micro-Measurements

StrainIndicatorandRecorder

FEATURES

- Four input channels
- Direct reading LCD display
- On-board data storage
- 0 to 2.5 VDC analog output
- Quarter-, half-, and full-bridge circuits
- Built-in bridge completion
- 120-, 350-, and 1000-ohm dummy gages
- Automatic zero-balancing and calibration
- Intuitive, menu-driven operations
- USB data link
- Operation from keypad or PC
- Portable, lightweight, and rugged
- Battery, USB, or line-voltage power
- Optional 10-pin transducer connectors

DESCRIPTION

The Model P3 Strain Indicator and Recorder is a portable, battery-operated instrument capable of simultaneously accepting four inputs from quarter-, half-, and full-bridge strain-gage circuits, including strain-gage-based transducers. Water-resistant grommets in the hinged cover allow the lid to be closed with leadwires attached. Designed for use in a wide variety of physical test and measurement applications, the P3 functions as bridge amplifier, static strain indicator, and digital data logger.

The Model P3 Strain Indicator and Recorder, utilizing a large LCD display for readout of setup information and acquired data, incorporates many unique operating features that make it the most advanced instrument of its kind. An extensive, easy-to-use menu-driven user interface operates through a front-panel keypad to readily configure the P3 to meet your particular measurement requirements. Selections include active input and output channels, bridge configuration, measurement units, bridge balance, calibration method, and recording options, among others.

Standard sensor input connection is via eccentric-lever-release terminal blocks. Optional transducer connection is available via side-mounted bayonet locking circular connectors.

Data, recorded at a user-selectable rate of up to 1 reading per channel per second, is stored on a removable flash card and is transferred by USB to a host computer for subsequent storage, reduction and presentation with the supplied software.

The P3 can also be configured and operated directly from your PC with a separate software application included with each instrument. Additionally, a full set of ActiveX components is provided for creating custom applications in any language supporting ActiveX.

A highly stable measurement circuit, regulated bridge excitation supply, and precisely settable gage factor enable measurements of ±0.1% accuracy and 1 microstrain resolution. Bridge completion resistors of 120, 350 and 1000 ohms are built in for quarter-bridge operation. Also, input connections and switches are provided for remote shunt calibration of transducers and full-bridge circuits.

The P3 operates from two readily available D cells. Battery life depends upon mode of operation but ranges up to 600 hours of continuous use for a single channel. It can also be powered by connection to an external battery or power supply, a USB port on a PC or with an optional external line-voltage adapter, the Model P3-A105.

Strain Indicator and Recorder

HARDWARE SPECIFICATIONS

All specifications nominal or typical at +23°C unless noted.

Inputs

Eccentric-lever-release terminal blocks accept up to four independent bridge inputs. Accommodates 16-28 AWG (1.3 to 0.35 mm diameter) wire.

The Transducer Option includes four 10-pin bayonet locking circular connectors mounted on the side of the case and wired in parallel to the lever-release terminal blocks. The supplied mating connector has a 0.046 inch (1.17 mm) diameter solder well.

BridgeConfigurations

Quarter-, half-, and full-bridge circuits. Internal bridge completion provided for 120Ω, 350Ω and 1000Ω quarter bridges, 60 to 2000Ω half or full bridge.

Display

Full dot-matrix structure with 128 dots x 64 dots FSTN positive, gray transflective LCD with backlight. Display update is twice a second.

DataConversion

High-resolution sigma-delta converter. 60 Hz or 50 Hz noise rejection. User selectable.

BasicRange

±31,000 microstrain (±1 microstrain resolution) at Gage Factor = 2.000

Accuracy

±0.1% of reading ±3 counts. (Normal mode operation at
Gage Factor = 2.000)

GageFactorSettings

Range 0.500 to 9.900

Balance

Single key operation to initiate automatic software balance

BridgeExcitation

1.5 VDC nominal. Readings are fully ratiometric, and not degraded by variation in excitation voltage

CommunicationInterface

Universal Serial Bus with type B connector. Used for transferring stored data and firmware.

DataStorage

Media: Removable Secure Digital or Multimedia Card (2GB max).

Data Recording Rate: 1 reading per second maximum.

Calibration

Shunt calibration across each dummy resistor to simulate 5000 microstrain (±0.1%). Remote calibration supported via accessible switch contacts at input terminal block.

AnalogOutput

BNC connector. 0 to 2.5V maximum output. Device impedance of 2000Ω or greater. 480 samples/second DAC output update rate.

Power

Internal battery pack using two "D" cells. Battery life up to 600 hours (single channel, normal mode.) Can also be powered from USB or by external battery or other power source of 6 to 15 VDC. AC adapter optional (Model P3-A105).

OperationalEnvironment

Temperature 0 to + 50°C. Humidity up to 90% RH, noncondensing

Strain Indicator and Recorder

FIRMWARE FEATURES

DisplayUpdateRate

2 readings per second

RecordingRates Up to 64 data files

Automatic recording

1 reading every 1 to 3600 seconds

Individually selectable per channel

Manual recording

Automatic date/time stamping

Scaling

Automatic scaling for microstrain, based upon gage factor, with nonlinearity correction based upon bridge type

Automatic calculation of mV/V

Linear scaling for other engineering units

Units

με	g	rpm	hp
mV/V	lbf	m	deg
psi	lb	s	rad
ksi	kg	A	oz
GPa	in	N	mV
MPa	mm	V	m/s^2
Pa	mil	Ohms	ton

BridgeTypes

Quarter bridge

Half bridge, adjacent arms, equal and opposite strains

Half bridge opposite arms equal strains

Shear bridge, 2 active arms

Poisson half bridge

Full bridge 4 fully active arms

Shear bridge, 4 active arms

Full bridge, Poisson gages in opposite arms

Full bridge, Poisson gages in adjacent arms

Undefined full bridge

Undefined half bridge/quarter bridge

BridgeBalance

Automatic

Manual offset adjust

Disabled (Raw offset)

BacklightControl

Programmable on time while in run mode

5, 15 or 60 seconds

Manual off/on

If illuminated, backlight will remain illuminated while operating menus

SoftwareAdjustableContrast

OperatingModes

Normal mode

Analog output (any one of four channels)

DataLink

USB interface

Windows-based P3 software provided for control and data storage

No device driver required (treated as an HID device)

Real-timeClock

SystemCalibration/Verification

Requires Model 1550A Strain Indicator calibrator or other compatible calibrator

Calibration date stored in flash memory

FirmwareUpgradeable

View Showing Optional Transducer Input Connectors

Appendix C

Stress Strain Graphs

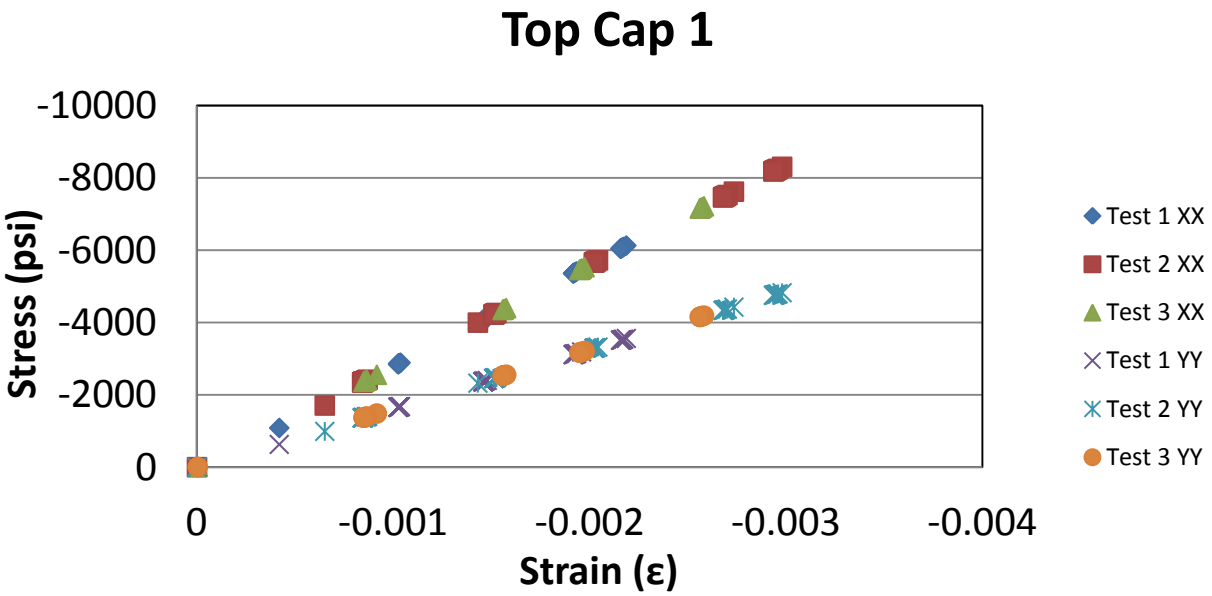
Top Cap 1
-10000
-8000
-6000
-4000
-2000
0
Stress (psi)
0
-0.001
-0.002
-0.003
-0.004
Strain (ε)
Test 1 XX
Test 2 XX
Test 3 XX
Test 1 YY
Test 2 YY
Test 3 YY

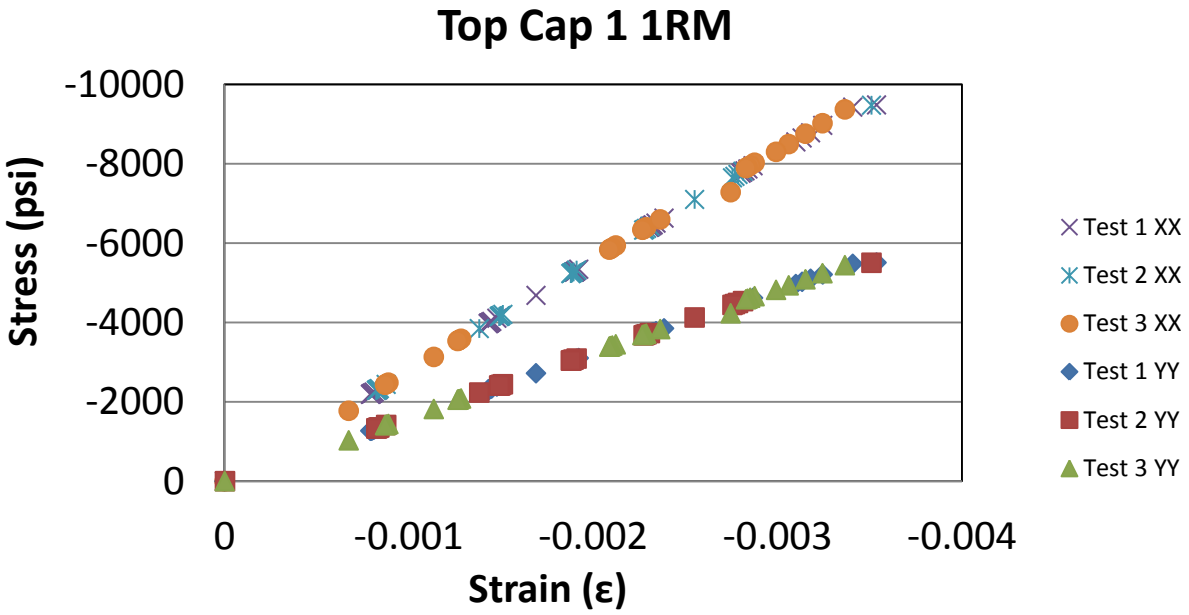
Top Cap 1 1RM
-10000
-8000
-6000
-4000
-2000
0
Stress (psi)
0
-0.001
-0.002
-0.003
-0.004
Strain (ε)
Test 1 XX
Test 2 XX
Test 3 XX
Test 1 YY
Test 2 YY
Test 3 YY

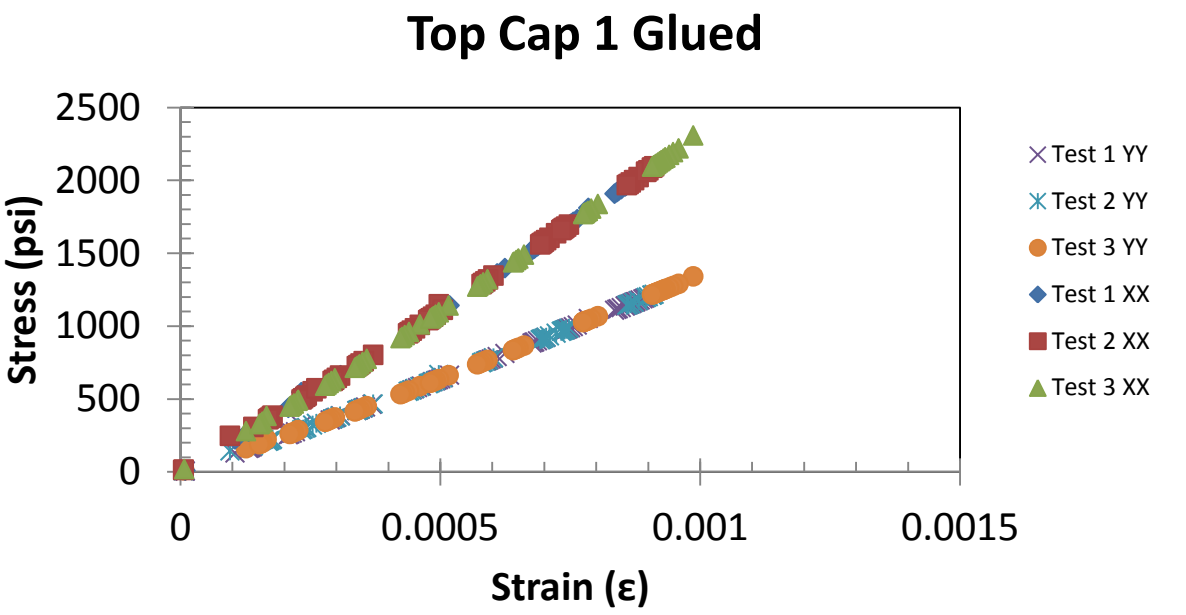
Top Cap 1 Glued
Stress (psi)
2500
2000
1500
1000
500
0
0
0.0005
0.001
0.0015
Strain (ε)
Test 1 YY
Test 2 YY
Test 3 YY
Test 1 XX
Test 2 XX
Test 3 XX

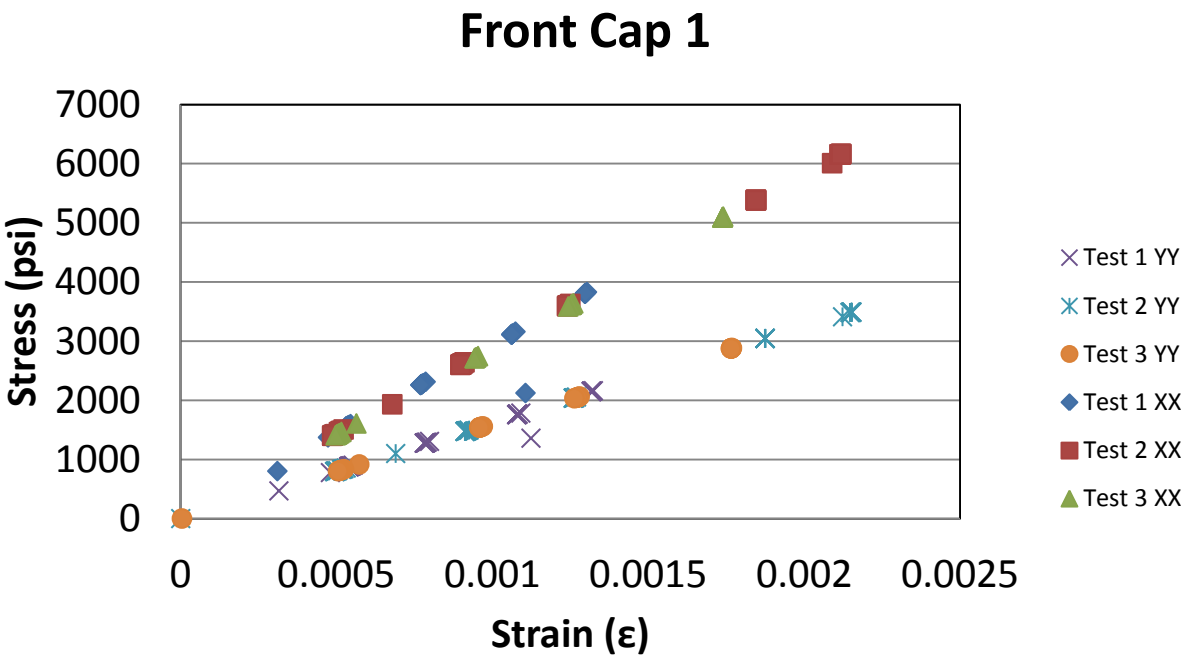
Front Cap 1
Stress (psi)
7000
6000
5000
4000
3000
2000
1000
0
0
0.0005
0.001
0.0015
0.002
0.0025
Strain (ε)
Test 1 YY
Test 2 YY
Test 3 YY
Test 1 XX
Test 2 XX
Test 3 XX

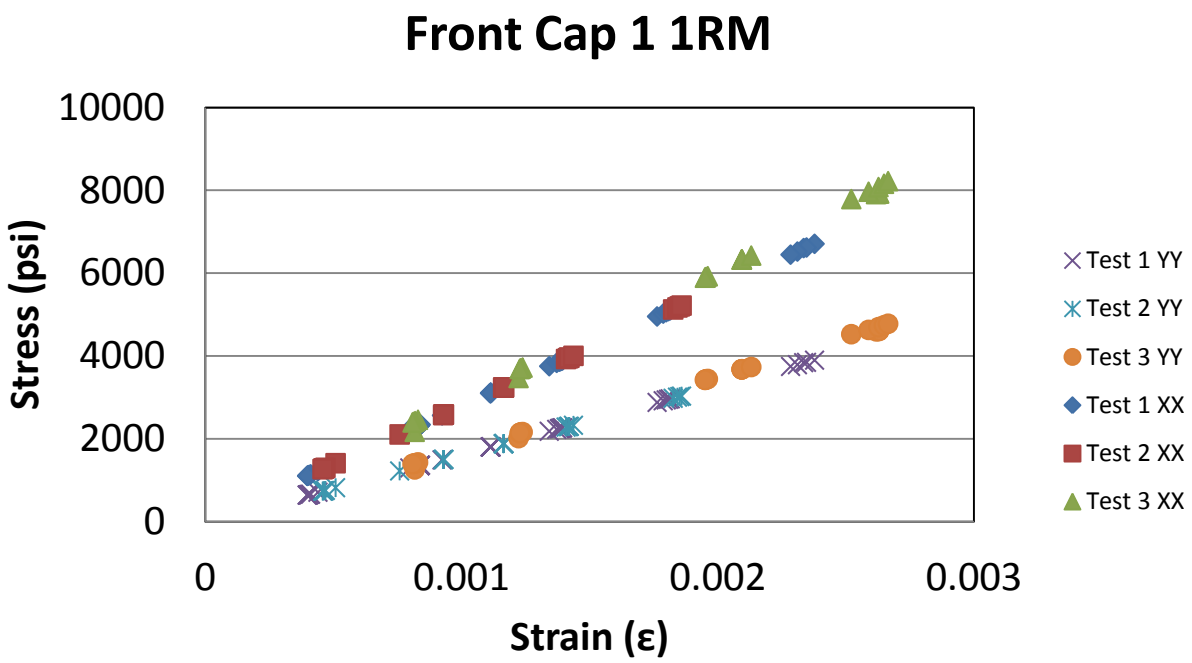
Front Cap 1 1RM
10000
8000
6000
4000
2000
0
Stress (psi)
0
0.001
0.002
0.003
Strain (ε)
Test 1 YY
Test 2 YY
Test 3 YY
Test 1 XX
Test 2 XX
Test 3 XX

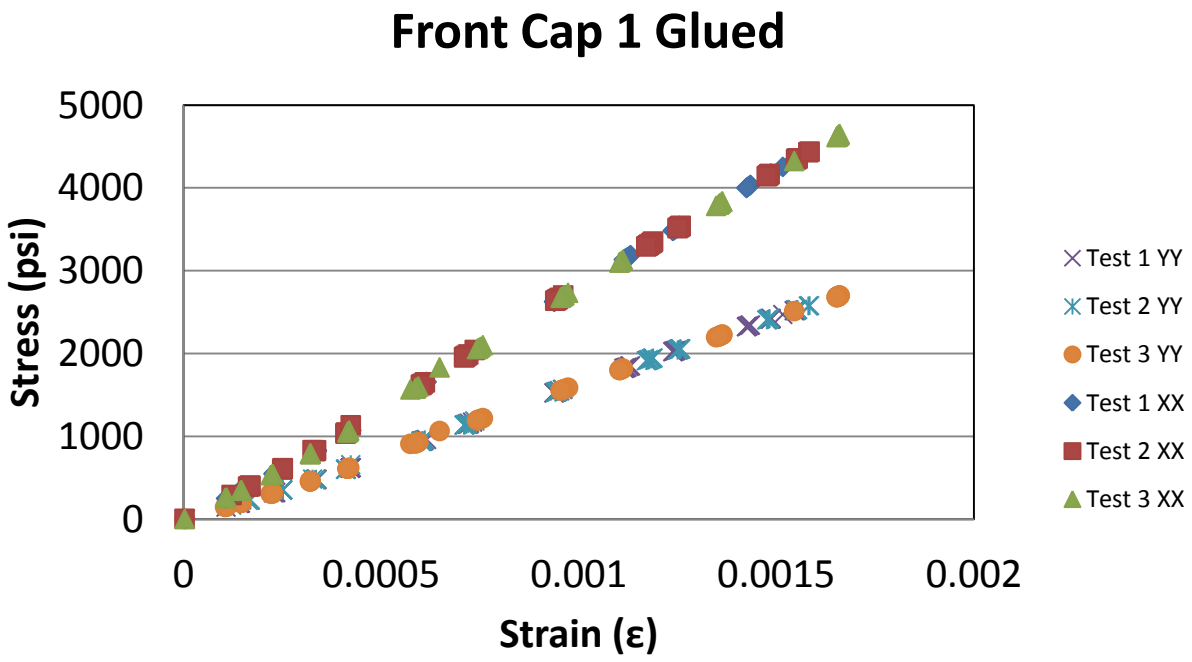
Front Cap 1 Glued
5000
4000
3000
2000
1000
0
Stress (psi)
0
0.0005
0.001
0.0015
0.002
Strain (ε)
Test 1 YY
Test 2 YY
Test 3 YY
Test 1 XX
Test 2 XX
Test 3 XX

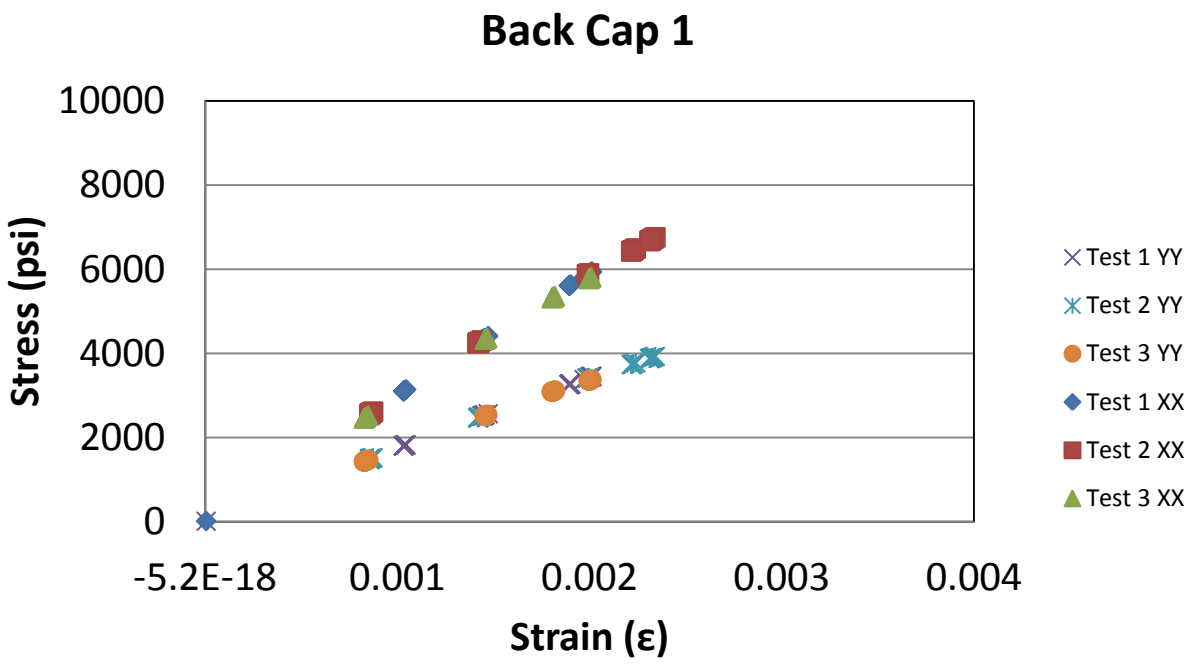
Back Cap 1
10000
8000
6000
4000
2000
0
Stress (psi)
-5.2E-18
0.001
0.002
0.003
0.004
Strain (ε)
Test 1 YY
Test 2 YY
Test 3 YY
Test 1 XX
Test 2 XX
Test 3 XX

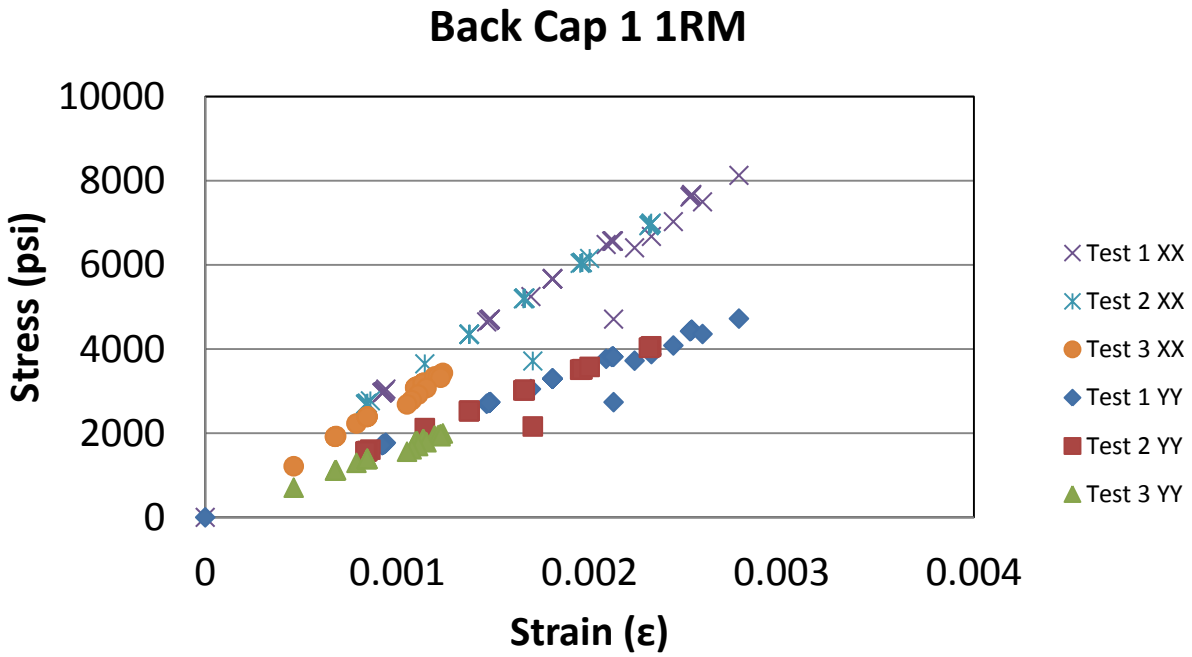
Back Cap 1 1RM
10000
8000
6000
4000
2000
0
Stress (psi)
0
0.001
0.002
0.003
0.004
Strain (ε)
Test 1 XX
Test 2 XX
Test 3 XX
Test 1 YY
Test 2 YY
Test 3 YY

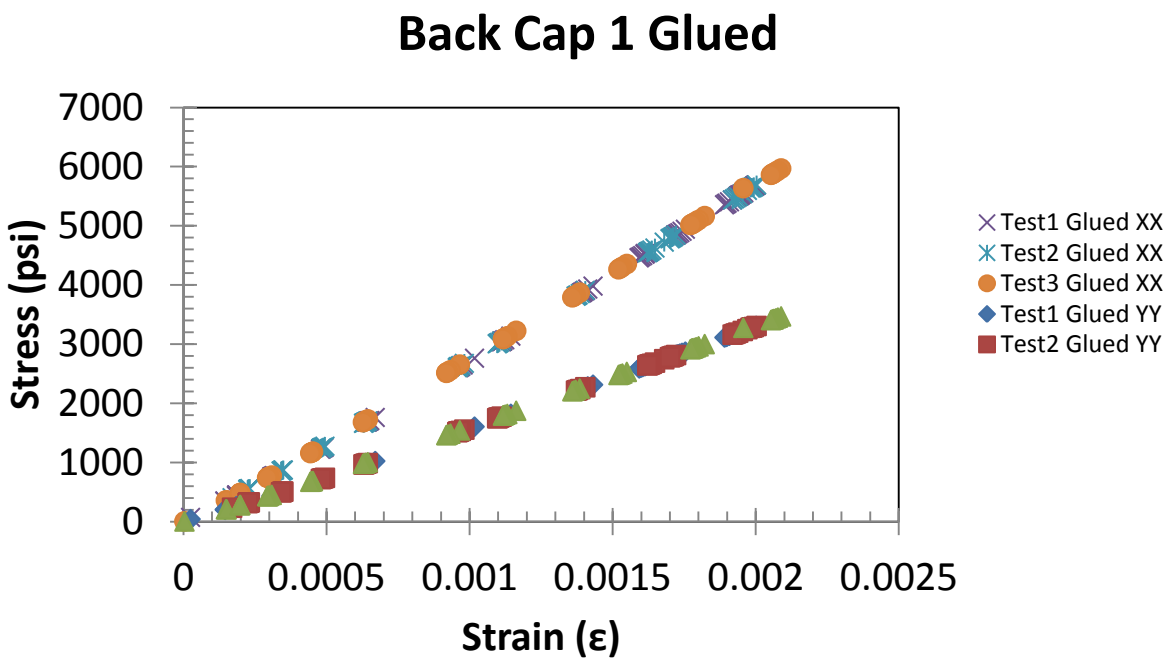
Back Cap 1 Glued
Stress (psi)
7000
6000
5000
4000
3000
2000
1000
0
0
0.0005
0.001
0.0015
0.002
0.0025
Strain (ε)
Test1 Glued XX
Test2 Glued XX
Test3 Glued XX
Test1 Glued YY
Test2 Glued YY

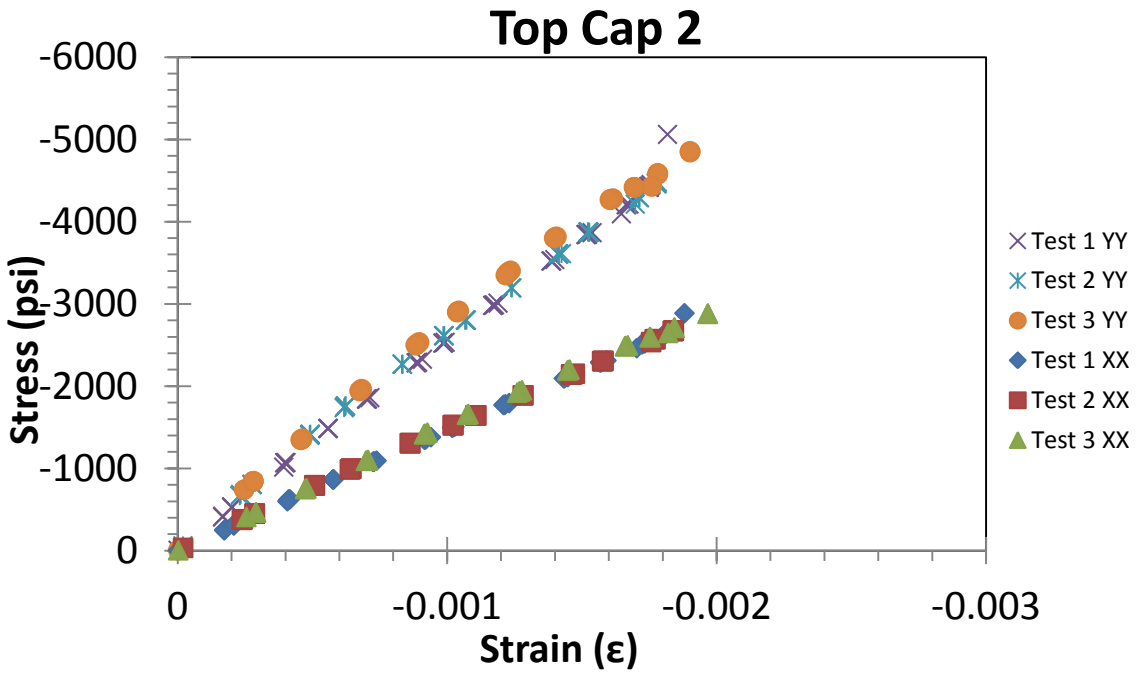
Top Cap 2
Stress (psi)
-6000
-5000
-4000
-3000
-2000
-1000
0
0
-0.001
-0.002
-0.003
Strain (ε)
Test 1 YY
Test 2 YY
Test 3 YY
Test 1 XX
Test 2 XX
Test 3 XX

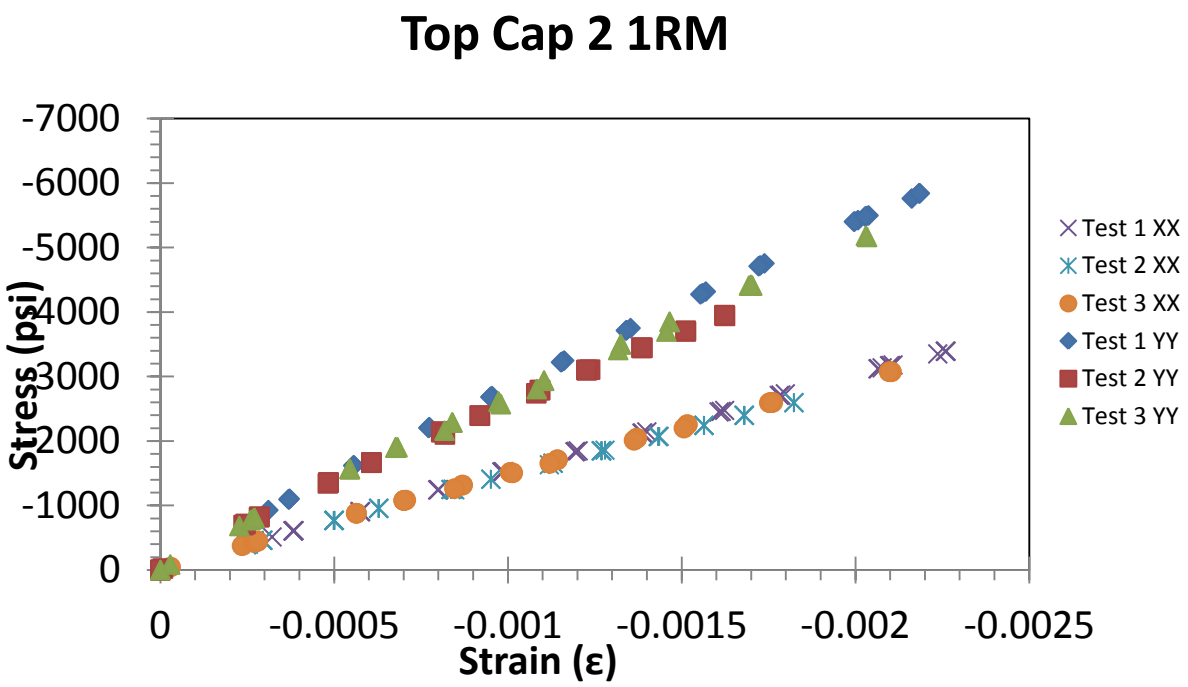
Top Cap 2 1RM
-7000
-6000
-5000
-4000
-3000
-2000
-1000
0
Stress (psi)
0
-0.0005
-0.001
-0.0015
-0.002
-0.0025
Strain (ε)
Test 1 XX
Test 2 XX
Test 3 XX
Test 1 YY
Test 2 YY
Test 3 YY

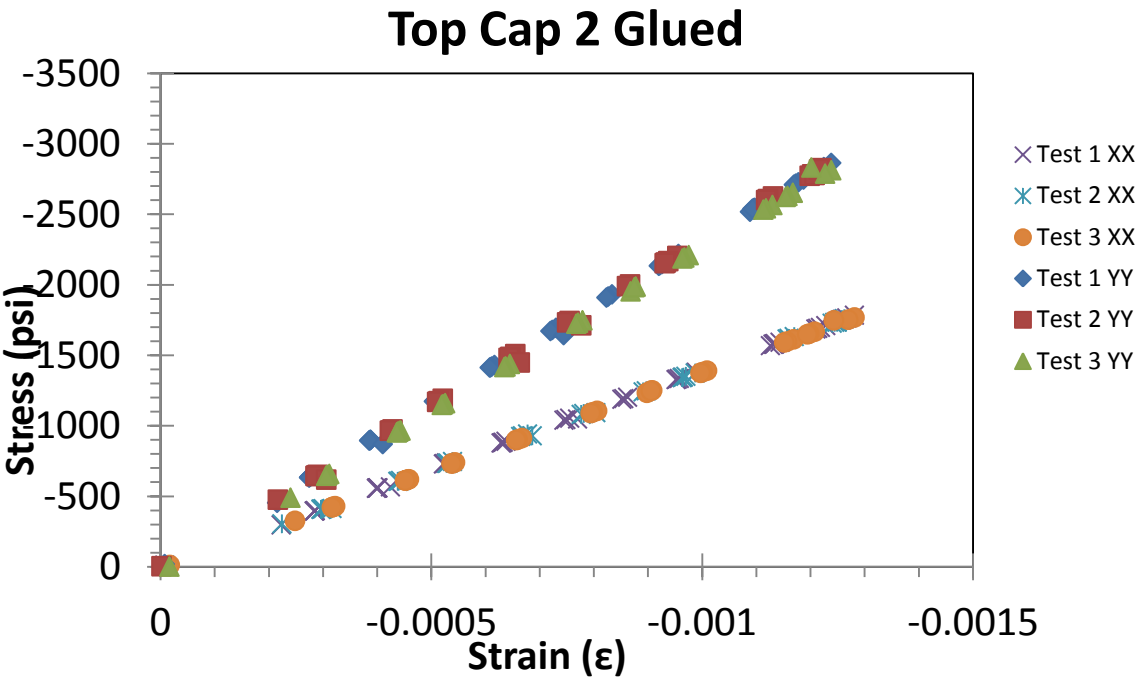
Top Cap 2 Glued
-3500
-3000
-2500
-2000
-1500
-1000
-500
0
Stress (psi)
0
-0.0005
-0.001
-0.0015
Strain (ε)
Test 1 XX
Test 2 XX
Test 3 XX
Test 1 YY
Test 2 YY
Test 3 YY

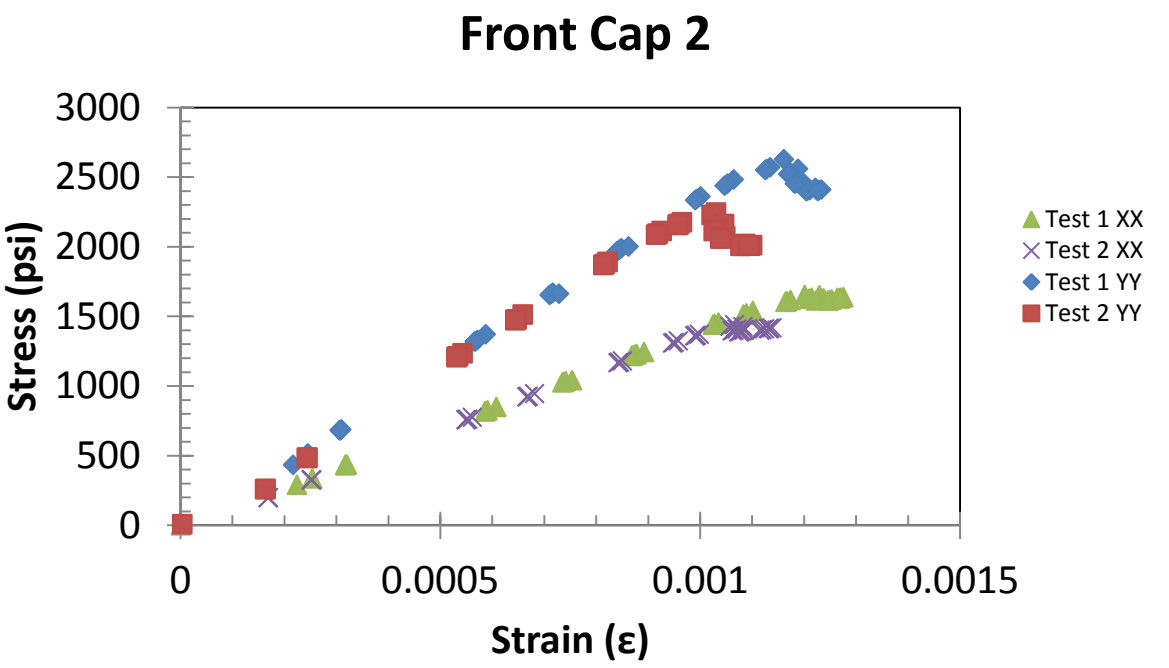
Front Cap 2
Stress (psi)
3000
2500
2000
1500
1000
500
0
0
0.0005
0.001
0.0015
Strain (ε)
Test 1 XX
Test 2 XX
Test 1 YY
Test 2 YY

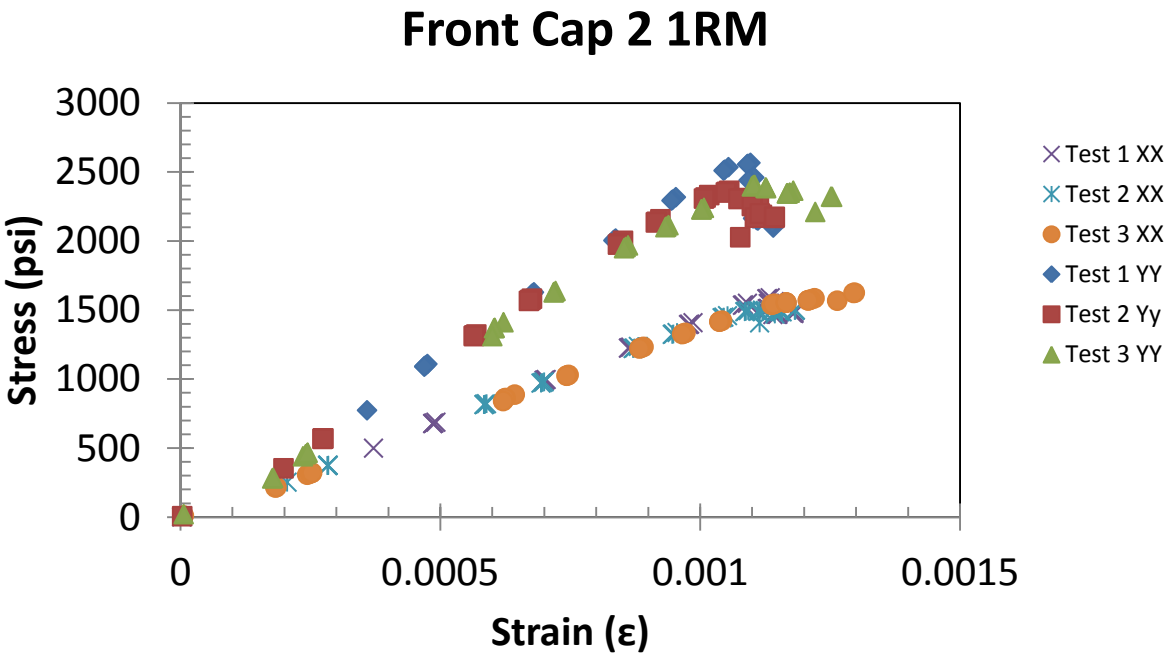
Front Cap 2 1RM
Stress (psi)
3000
2500
2000
1500
1000
500
0
0
0.0005
0.001
0.0015
Strain (ε)
Test 1 XX
Test 2 XX
Test 3 XX
Test 1 YY
Test 2 Yy
Test 3 YY

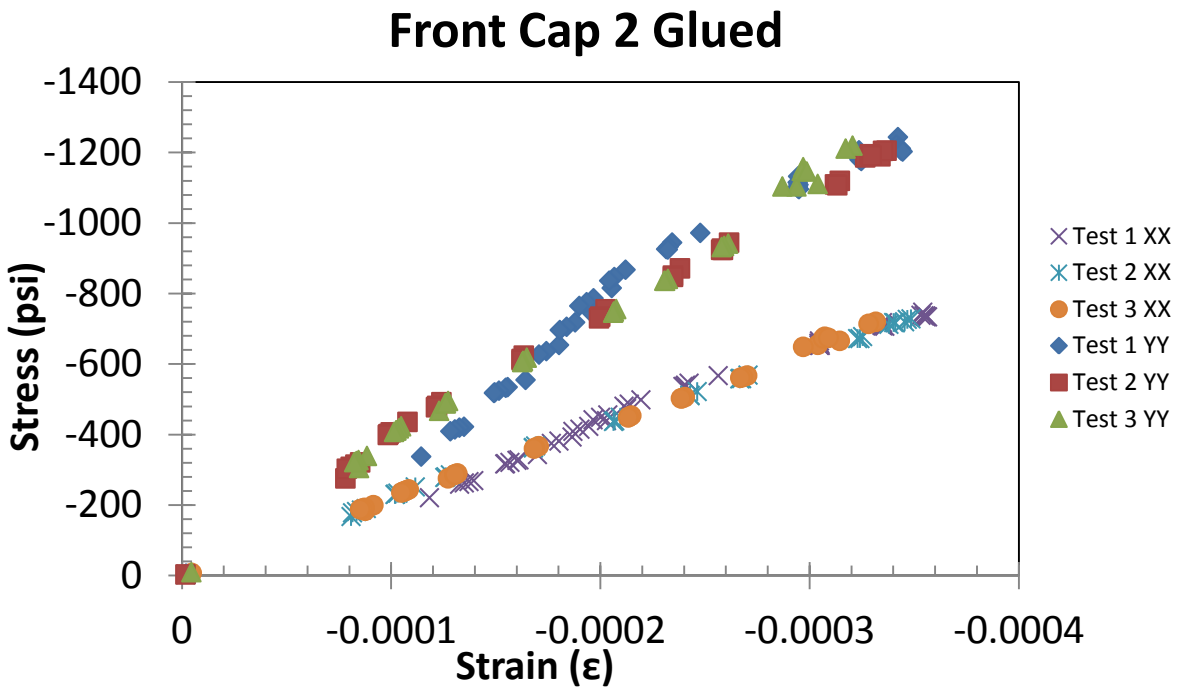
Front Cap 2 Glued
-1400
-1200
-1000
-800
-600
-400
-200
0
Stress (psi)
0
-0.0001
-0.0002
-0.0003
-0.0004
Strain (ε)
Test 1 XX
Test 2 XX
Test 3 XX
Test 1 YY
Test 2 YY
Test 3 YY

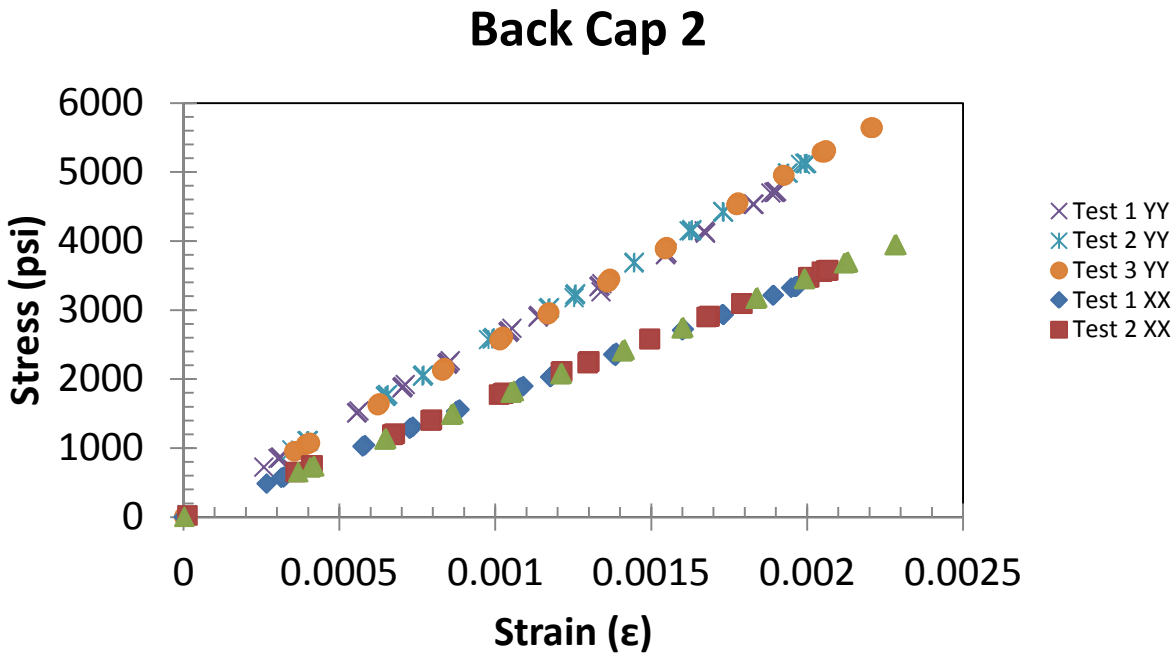
Back Cap 2
6000
5000
4000
3000
2000
1000
0
Stress (psi)
0
0.0005
0.001
0.0015
0.002
0.0025
Strain (ε)
Test 1 YY
Test 2 YY
Test 3 YY
Test 1 XX
Test 2 XX

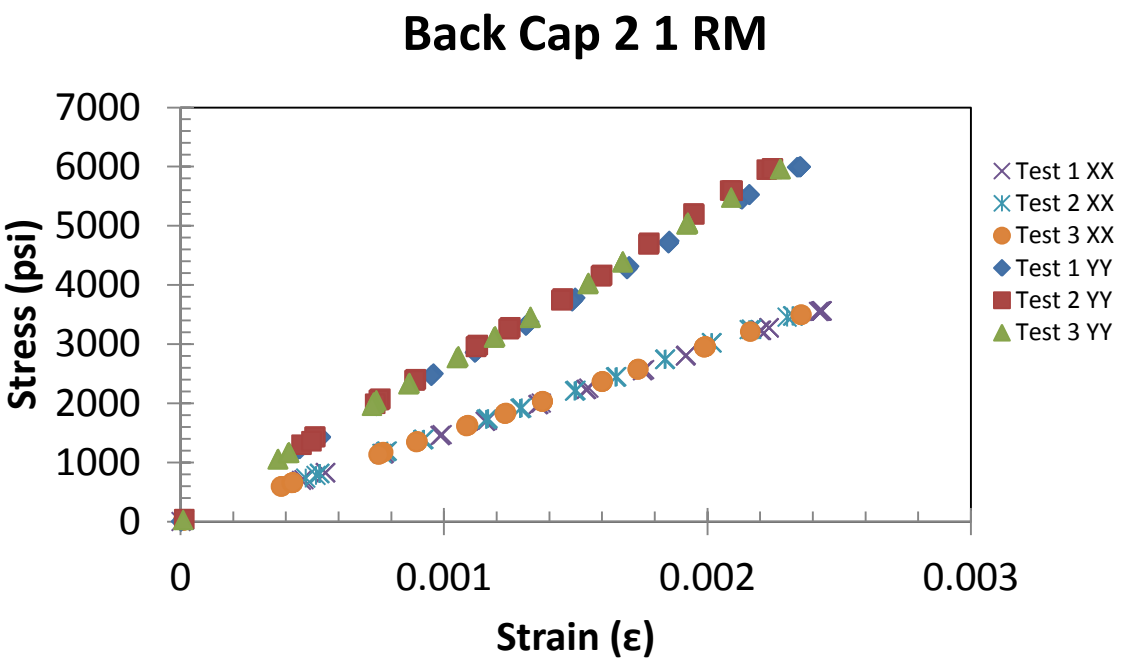
Back Cap 2 1 RM
Stress (psi)
7000
6000
5000
4000
3000
2000
1000
0
0
0.001
0.002
0.003
Strain (ε)
Test 1 XX
Test 2 XX
Test 3 XX
Test 1 YY
Test 2 YY
Test 3 YY

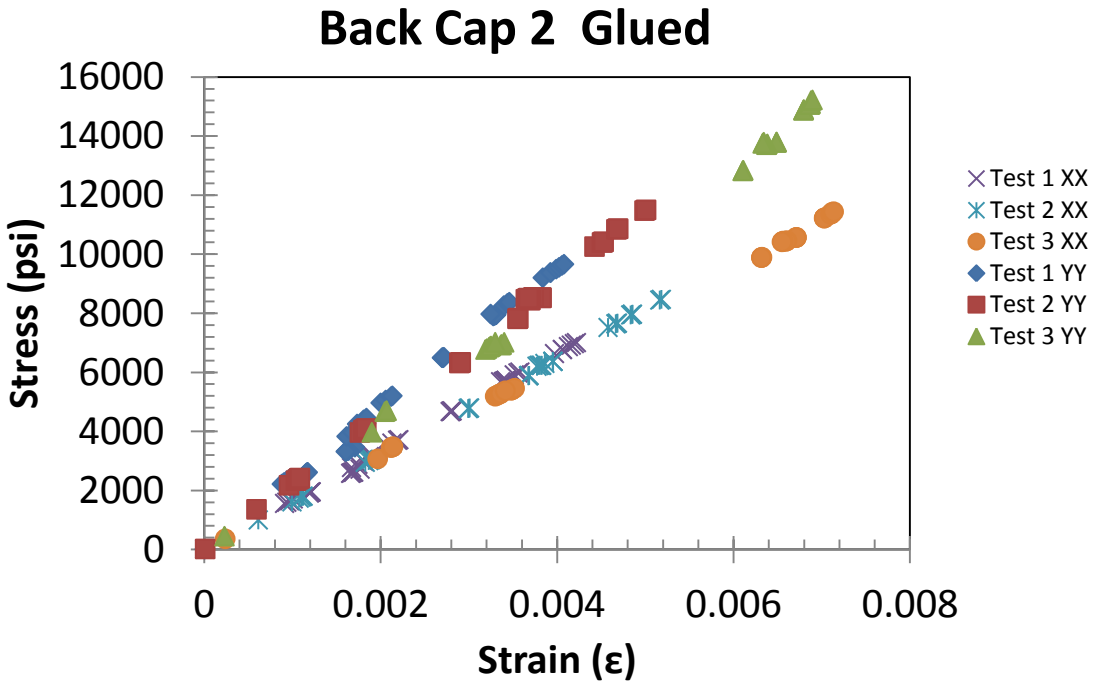
Back Cap 2 Glued
Stress (psi)
16000
14000
12000
10000
8000
6000
4000
2000
0
0
0.002
0.004
0.006
0.008
Strain (ε)
Test 1 XX
Test 2 XX
Test 3 XX
Test 1 YY
Test 2 YY
Test 3 YY

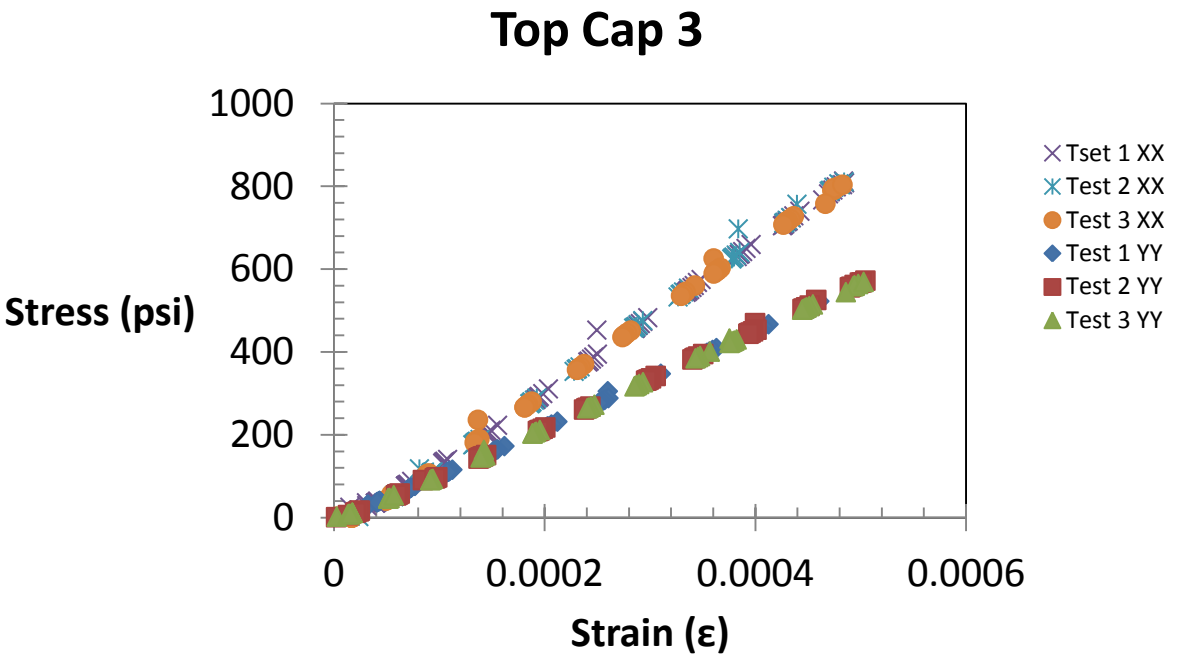
Top Cap 3
Stress (psi)
1000
800
600
400
200
0
0
0.0002
0.0004
0.0006
Strain (ε)
Tset 1 XX
Test 2 XX
Test 3 XX
Test 1 YY
Test 2 YY
Test 3 YY

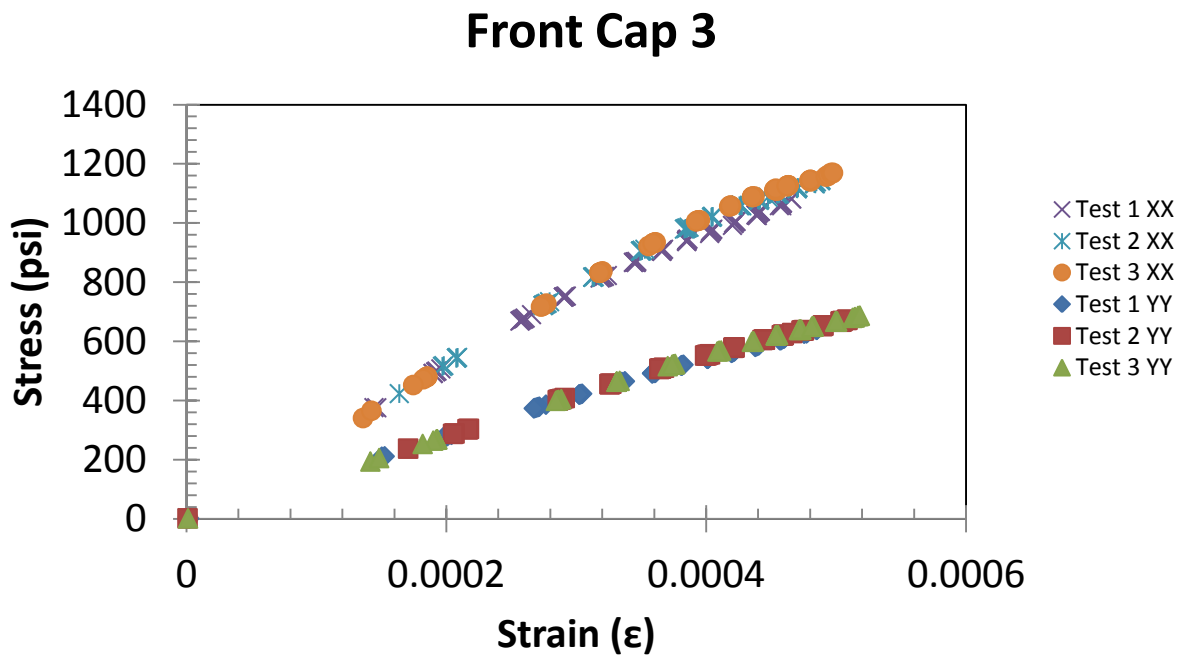
Front Cap 3
Stress (psi)
1400
1200
1000
800
600
400
200
0
0
0.0002
0.0004
0.0006
Strain (ε)
Test 1 XX
Test 2 XX
Test 3 XX
Test 1 YY
Test 2 YY
Test 3 YY

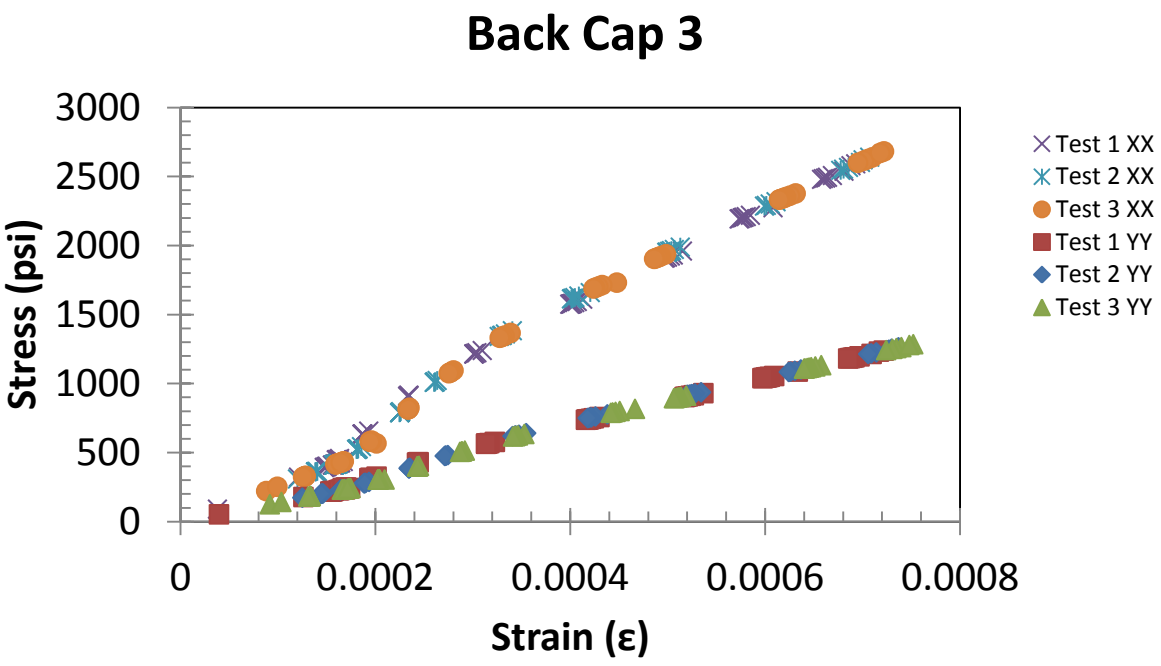
Back Cap 3
Stress (psi)
3000
2500
2000
1500
1000
500
0
0
0.0002
0.0004
0.0006
0.0008
Strain (ε)
Test 1 XX
Test 2 XX
Test 3 XX
Test 1 YY
Test 2 YY
Test 3 YY

VITA

Jimmy Irby Jackson II was born on the 8th of October 1987. He was born in Greenville Mississippi. He completed his first two years of his undergraduate degree at Mississippi Delta Community College before transferring in 2009 to the University of Mississippi where he achieved his bachelor's in Civil Engineering in 2011. During his time at MDCC he was the vice president of Phi Theta Kappa, and received achievement awards in Calculus 1-4, Differential Equations, and Physics 1 and 2. During his time at UM he held positions such as Senator of the Civil Engineering Graduate School Council**,** President of Chi Epsilon, Vice President of (ITE) Institute of Transportation Engineers at Ole Miss**,** Represented the Under Graduate Civil Engineering Dept., and represent the student body on the Engineering Advisory Board. He decided to stay on and earn his Masters Degree in Engineering Science with an emphasis in Civil Engineering with Dr. Chung Rak Song. His research interest was in the structural aspect of geotechnical engineering. He is currently pursuing a career in cementing for the petroleum industries.